NASA TECHNICAL MEMORANDUM

NASA TM X-1426

NASA TM X-1426

FEASIBILITY STUDY OF A TUNGSTEN WATER-MODERATED NUCLEAR ROCKET

VII. System Dynamics and Control Analysis

by James R. Mihaloew

Lewis Research Center
Cleveland, Ohio

NATIONAL AERONAUTICS AND SPACE ADMINISTRATION • WASHINGTON, D. C. • MARCH 1968

NASA TM X-1426

FEASIBILITY STUDY OF A TUNGSTEN WATER-MODERATED NUCLEAR ROCKET

VII. SYSTEM DYNAMICS AND CONTROL ANALYSIS

By James R. Mihaloew

Lewis Research Center
Cleveland, Ohio

NATIONAL AERONAUTICS AND SPACE ADMINISTRATION

For sale by the Clearinghouse for Federal Scientific and Technical Information
Springfield, Virginia 22151 - CFSTI price $3.00

PREFACE

The concept of a nuclear rocket system based on the use of a tungsten water-moderated reactor (TWMR) was originated at the Lewis Research Center. The TWMR is a thermal reactor that uses water as the moderator, uranium dioxide as the fuel, and tungsten enriched in tungsten 184 as the fuel element structural material. As is common to all nuclear rocket systems, hydrogen is used as the propellant to maximize specific impulse. The reactor (see illustration) consists of a tank containing a number of pressure tubes that are attached to tube sheets at the inlet and outlet ends of the reactor. The pressure tubes contain the fuel elements. The space inside the tank between the tubes is filled with water, which serves both as the neutron moderator and as a coolant for the structure. Heat is generated in the water by neutrons and gamma rays and is also transferred to the water by heat leakage from the hot fuel elements, each of which is located in a pressure tube. The removal of heat is provided by pumping the water through the core and a heat exchanger in a closed loop. The water is regeneratively cooled in the heat exchanger by the hydrogen propellant, which flows from a supply tank through the nozzle and heat exchanger into the core. As the hydrogen flows through the core pressure tubes and through the fuel elements, it is heated to a high temperature and is expanded out the nozzle to produce thrust.

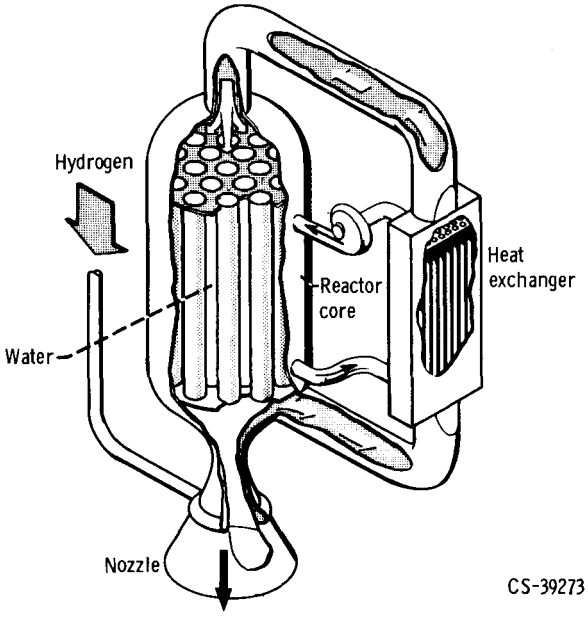

The potential advantages of the concept lie in the following areas: The use of tungsten provides a high-temperature material with good thermal shock resistance, tensile and compressive strength, thermal conductivity, and resistance to corrosion by the hydrogen propellant. The properties of tungsten also permit the fabrication of fuel elements with very thin cross sections for good heat transfer. The use of water as the moderator provides a good coolant for the pressure vessel and structural members and reduces core size and weight over that obtained for most moderator materials. In this concept, the fuel element assemblies are structurally independent of each other and thus permit individual development of these assemblies.

A program was undertaken at Lewis to investigate the engineering feasibility and performance of the TWMR nuclear rocket system. The results of these investigations, which are summarized in part I (NASA Technical Memorandum X-1420) of this series of reports, are presented in detail in the other six parts of the series as follows: II. Fueled Materials (NASA Technical Memorandum X-1421); III. Fuel Elements (NASA Technical Memorandum X-1422); IV. Neutronics (NASA Technical Memorandum X-1423); V. Engine System (NASA Technical Memorandum X-1424); VI. Feed System and Rotating Machinery (NASA Technical Memorandum X-1425); VII. System Dynamics (NASA Technical Memorandum X-1426).

CONTENTS

FEASIBILITY STUDY OF A TUNGSTEN WATER-MODERATED NUCLEAR ROCKET

VII. SYSTEM DYNAMICS AND CONTROL ANALYSIS

by James R. Mihaloew

Lewis Research Center

SUMMARY

A system dynamics and control analysis was performed on several versions of a tungsten water-moderated (TWMR) nuclear rocket system, which used a combination bleed-topping (split-feed) cycle concept. Analog and digital simulation models were developed and used in the analysis. The purpose of the study was to determine the overall feasibility and control requirements of the system over the range from chilldown to start-up and power range operation.

Results of steady-state mapping of the TWMR showed that heat exchanger hydrogen bypass was required to prevent icing in the water-moderator cooling heat exchanger. Without heat exchanger bypass, steady-state operation below 36 percent total hydrogen flow and 32 percent reactor power was impossible because of intersecting pump stall and heat exchanger icing limits. The icing limit restricted operation to a narrow corridor above approximately 90 percent of maximum chamber temperature. Transient analysis indicated that preheating the water prevented icing during chilldown but that pump stall was aggravated. Operation with heat exchanger bypass eliminated icing and expanded the operating region considerably. Heat exchanger bypass was also found to be an effective means for reactor power control.

A comparative system analysis of the several TWMR versions showed that the all-topping cycle version with heat exchanger bypass was substantially superior with respect to system simplicity and flexibility at the design chamber pressure of 600 psia (414 N/cm^2 abs) used in this study. However, a split-feed cycle version with heat exchanger bypass represented the most promising system because of its superior chamber pressure uprating potential.

The control analysis of this version showed that chamber temperature control with a poison insertion-extraction (on-off) scheme was extremely fast in response, but necessarily discontinuous. Chamber temperature control with heat exchanger bypass was, on the other hand, comparatively slow but inherently continuous. A control system based on heat exchanger bypass for primary chamber temperature control and poison reactivity for augmentation was conceptually designed. The performance of the TWMR with this control system was demonstrated satisfactorily over a typical operating cycle.

INTRODUCTION

The capability of producing high specific impulse is a main feature of nuclear rockets. For this reason, research is being conducted to develop reactor concepts with will permit high specific impulse.

TUNGSTEN WATER-MODERATED REACTOR CONCEPT

The type of reactor which has been under development for the nuclear rocket program is a homogeneous thermal type in which the fuel is intimately mixed with the moderator material. As a result the highest temperatures in the reactor occur in the moderator and are limited by its maximum temperature. A heterogeneous thermal reactor avoids this limitation by geometric separation of fuel and moderator materials. The moderator can then be cooled separately and maintained at a lower temperature. The fuel would then be allowed to operate nearer to its maximum temperature. From this type of reactor concept, the tungsten-fuel-element water-moderated-reactor system (TWMR) has evolved. It has the advantage of negative fuel and water temperature reactivity coefficients. Thus, independent control of water temperature provides an inherent control prospect. The concept does, however, involve the complication of a moderator cooling system; also, the moderator must be thermally insulated from the fuel element. The TWMR does seem to have a potential for producing high specific impulse.

FEED SYSTEM CONCEPT

The fact that energy is available from the moderator cooling process suggests the use of a topping cycle. The topping cycle, as applied to a nuclear rocket, is characterized by series flow of the working fluid through a topping turbopump and the major components of the engine. The distinguishing feature of this cycle is that the flow of all the working fluid passes through the exhaust nozzle at maximum specific impulse thus yielding an optimum performance engine for any given reactor outlet temperature. However, this cycle is limited to chamber pressure levels lower than those obtainable with the bleed cycle. In the bleed cycle, a portion of the working fluid is bled from the thrust chamber, mixed to an appropriate temperature, passed through the turbine, and finally exhausted. The prime disadvantage of this scheme is its degradation of specific impulse; however, it has a high chamber pressure growth potential.

To achieve some of the advantages of each cycle, a combination bleed and topping cycle, referred to as the split cycle, was innovated. In this cycle, a bleed driven turbo-

pump is put in series with a topping turbopump. Some of the working fluid is bled and heated to supply the bleed turbine and then exhausted. A small loss in specific impulse results; however, the growth potential of a system using this cycle is enhanced.

RESEARCH PROGRAM

A part of the nuclear rocket program at Lewis has been directed toward a rocket propulsion system using the TWMR and split-feed-system concepts. The bulk of the effort was expended on the analysis, design, and experimental evaluation of components within the system. Supporting research in the materials area has yielded a considerable amount of technical advancement.

As a result of these studies, a preliminary reference-design system evolved which formed the basis for investigating system operating feasibility, system dynamics, and control requirements. To fulfill this requirement, in-house and contractual programs were formulated and executed independently. The in-house program was designed to provide long-range information on the preliminary reference-design system in the power range of operation. It utilized a detailed nonlinear analog-simulation model for both steady-state and transient studies. The results of a study using this model are reported in reference 1.

In support of the overall TWMR program, a study contract was awarded to Rocketdyne Division of North American Aviation to perform a complete system and control analysis of the preliminary reference-design system. Its primary objective was to investigate analytically the reactor and feed system over the range from chilldown to startup and power range operation with regard to system feasibility and control-system requirements.

The contractual study was divided into four tasks:

Task I - the development of analytical and simulated models

Task II - the execution of a system analysis program aimed primarily at preliminary reference-design-system feasibility with respect to steady-state, dynamic, and control operation

Task III - a comparative system analysis of several design modifications designed to improve the preliminary reference-design-system performance

Based on this study, a design was chosen and redesignated the reference-design system.

Task IV - a control analysis study of the final reference-design system to determine a suitable startup program and power range control system

The detailed results of these studies are reported in references 2 to 5.

This report presents a summary of all system dynamics and control work done for the TWMR system. It contains primarily the contractual study with only appropriate ref-

erences to the in-house studies. The analytical and simulation models are described. A research procedure is presented and applied to a preliminary reference-design system and four modified configurations. Each configuration is evaluated for steady-state and transient performance. A comparison is made which results in a final or reference-design configuration. A control analysis is performed on this design and a control system designed and evaluated.

Members of the Rocketdyne staff who contributed substantially to the study program by assisting the author in their specialized areas include R. D. Marcy, L. Bulgier, and W. Cannon.

ANALYTICAL MODELS

From preliminary reference-design-system geometry and detailed component characteristics, a physical model was developed using simplifications and assumptions. General equations were derived and applied to the physical model to form a mathematical model from which two simulation models were developed. A digital-simulation model was developed to study detailed transient performance particularly in the chilldown and bootstrap ranges, and an analog-simulation model to study general dynamic behavior in the startup and power range.

DESCRIPTION OF PRELIMINARY REFERENCE DESIGN

A brief description of the preliminary reference-design system that evolved during the TWMR study is presented in the following sections. The system is shown schematically in figure 1. A detailed description is given in references 2 and 6.

Hydrogen Flow

Liquid hydrogen flows from the propellant tank through a main propellant shutoff valve (MPV) to the series bleed and topping turbopumps. At the design point, the total hydrogen flow is 92.7 pounds per second (42.05 kg/sec). It is then pumped through the feedline and into the nozzle coolant passages where it receives convected heat from the hot exhaust gas and radiation from the core exit face. As the hydrogen changes to a gas, it flows into the parallel-flow heat-exchanger tubes to cool the water. The gaseous hydrogen from the heat exchanger is ducted in parallel paths through the series topping-turbine throttle valve (TTTV) and topping turbine and to the topping-turbine bypass valve

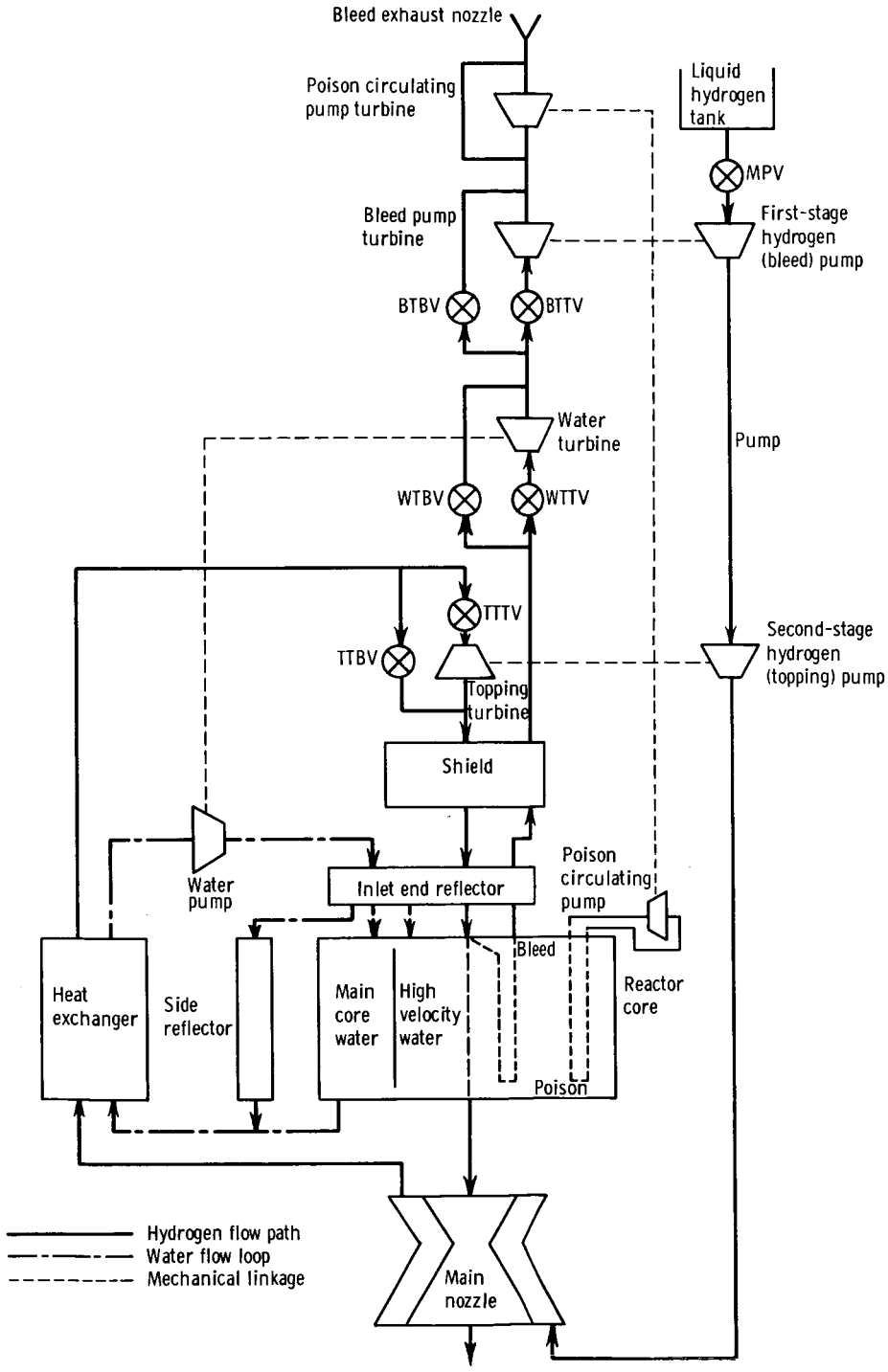

Figure 1. - Schematic flow diagram of tungsten water-moderated reactor preliminary reference-design system.

(TTBV). The flow paths are rejoined and pass through the shield and reactor dome area. The fluid then flows through the inlet end reflector inserts and into the core fuel assemblies.

The core consists of fuel assemblies made up of a series of concentric multicylinder fueled stages with center plugs. The stages are supported by a continuous cylindrical tungsten support tube. Each fuel assembly is enclosed in an aluminum pressure tube which separates the hydrogen and water flows. The pressure tube is thermally insulated from the support tube by a static gaseous hydrogen gap. The pressure tube is surrounded by concentric, aluminum, flow-divider tubes that separate the high-velocity water flow next to the pressure tube from the low-velocity flow in the main core.

After the hydrogen passes through the core, it is exhausted through the thrust nozzle. The design chamber pressure and temperature are 600 psia and 4460° R (414 N/cm^2 abs and 2478° K), respectively.

Water Flow

Water is circulated by a pump into an inlet plenum where it is distributed to three parallel-flow paths after it passes through the inlet end reflector, through the side reflector, outside the flow divider tubes in the main core, and between the flow-divider and pressure tubes to cool the pressure tubes. The water mixes at an outlet plenum and passes up through a segmented annular heat exchanger which is outside the core side reflector but inside the main pressure vessel. Heat transferred to the water by convection and generated in the water by nuclear radiation is removed in the parallel-flow heat exchanger. The water direction is reversed after it exits from the heat exchanger and flows down through the passages between the annular heat-exchanger segments where it exits from the pressure vessel and returns to the pump. The design-point water flow is 1040 pounds per second (471.1 kg/sec).

Bleed Subsystem

Bleed hydrogen flow is taken from the reactor dome and heated by centrally located reentrant fuel assemblies. The reentrant fuel assemblies are similar to the core assemblies except that they are blocked at the exit end and hydrogen is forced to flow back up the center plug passage. The heated bleed gas then passes through the reactor dome area and shield to the bleed subsystem. The bleed subsystem consists of series turbines to drive the water, first-stage (bleed), and poison-circulating pumps in that order. Each

turbine has throttle and bypass valves except for the poison-circulating turbine. The design bleed flow is 2.4 pounds per second (1.1 kg/sec).

Poison Subsystem

Reactor power can be controlled externally by varying the concentration of a neutron absorber solution flowing through small tubes extending axially into the moderator region. The concentration can be modulated by either adding a concentrated absorber or extracting it through an ion exchanger. A poison-circulating pump maintains continuous flow in the subsystem during reactor operation. A detailed description and schematic drawing of this subsystem are given in reference 7.

PHYSICAL MODEL

The system geometry and detailed component performance calculations of the preliminary reference-design system were used to derive a schematic physical model. This model formed the basis for the development of mathematical models. The resulting schematic diagrams for the hydrogen and water flow systems are shown in figures 2(a) and (b), respectively. The schematic physical model is divided into regions which correspond to the major components of the system. Several simplifications and assumptions are inferred in the figure.

Main Propellant Line and Valve

In the main propellant line (region 01), friction is assumed negligible. Heat transfer from the wall to the fluid and two-phase flow are considered. The friction factor and density are assumed constant in the main propellant valve (region 02). Heat transfer by convection from the valve to the fluid is also neglected. Thermal capacitance of the valve is lumped with the line.

Hydrogen Pumps

Performance of the bleed pump (region 03) and the topping pump (region 05) was assumed to be represented by normalized characteristics. Fluid density was assumed variable and fluid kinetic energy change is included in the pump head and enthalpy-rise char-

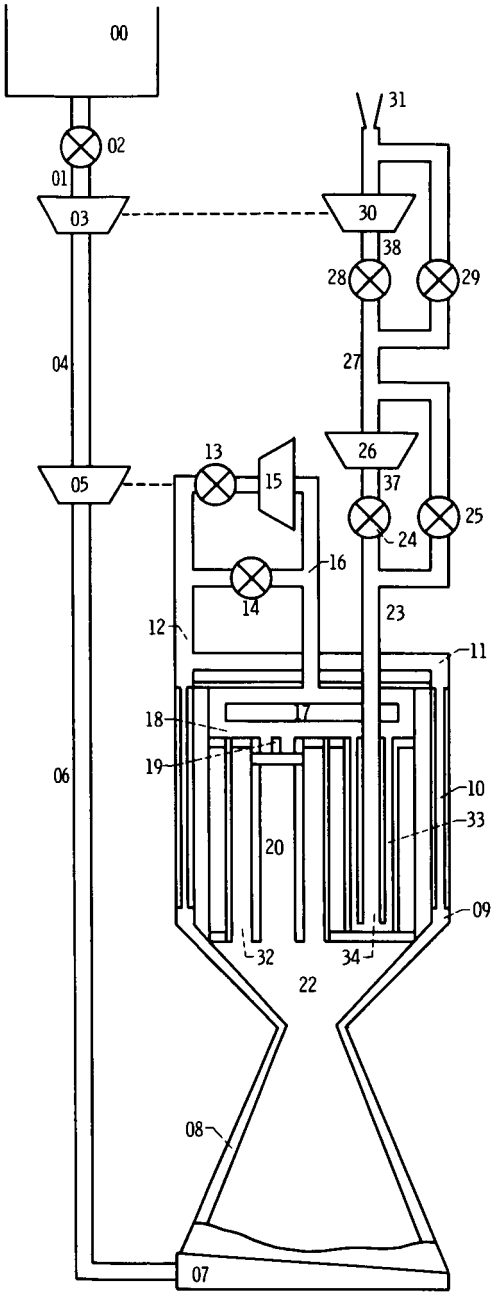

Description

00, Propellant tank
01, Piping, propellant tank to main shutoff valve
02, Main shutoff valve
03, First-stage hydrogen pump
04, Piping, first-stage hydrogen pump to second-stage hydrogen pump
05, Second-stage hydrogen pump
06, Piping, second-stage hydrogen pump to nozzle-tube-inlet manifold
07, Nozzle-tube-inlet manifold
08, Nozzle tubes
09, Heat-exchanger inlet manifold
10, Heat-exchanger tubes
11, Heat-exchanger outlet manifold
12, Piping, heat-exchanger outlet manifold to topping-turbine valves
13, Topping-turbine throttle valve
14, Topping-turbine bypass valve
15, Topping turbine
16, Piping, topping-turbine exhaust to reactor inlet
17, Shield
18, Reactor dome area
19, Inlet end reflector insert
20, Main core hydrogen flow path
22, Thrust-chamber
23, Piping, reactor bleed outlet to water-pump turbine valves
24, Water-pump turbine throttle valve
25, Water-pump turbine bypass valve
26, Water-pump turbine
27, Piping, water-pump turbine exhaust to first-stage hydrogen-pump turbine valves
28, First-stage hydrogen-pump turbine throttle valve
29, First-stage hydrogen-pump turbine bypass valve
30, First-stage hydrogen-pump turbine
31, Simulated poison pump turbine nozzle
32, Stagnant gaseous hydrogen gap
33, Reentrant fuel-assembly hydrogen flow path, first pass
34, Reentrant fuel-assembly hydrogen flow path, second pass
37, Water-pump turbine inlet plenum
38, First-stage hydrogen-pump turbine-inlet plenum

(a) Hydrogen flow system.

Figure 2. - Preliminary TWMR system model schematic drawing.

50, Water pump
51, Pump discharge line
52, Inlet water manifold
53, Inlet water plenum
54, Region between inlet end reflector and core water baffle
55, Water inside reflector
56, Core water outside of flow divider tubes
57, Annulus between pressure tube and flow divider tube (high-velocity region)
58, Outlet water plenum
59, Water in heat exchanger
60, Outlet water passage
61, Pump inlet line
62, Water in inlet end reflector

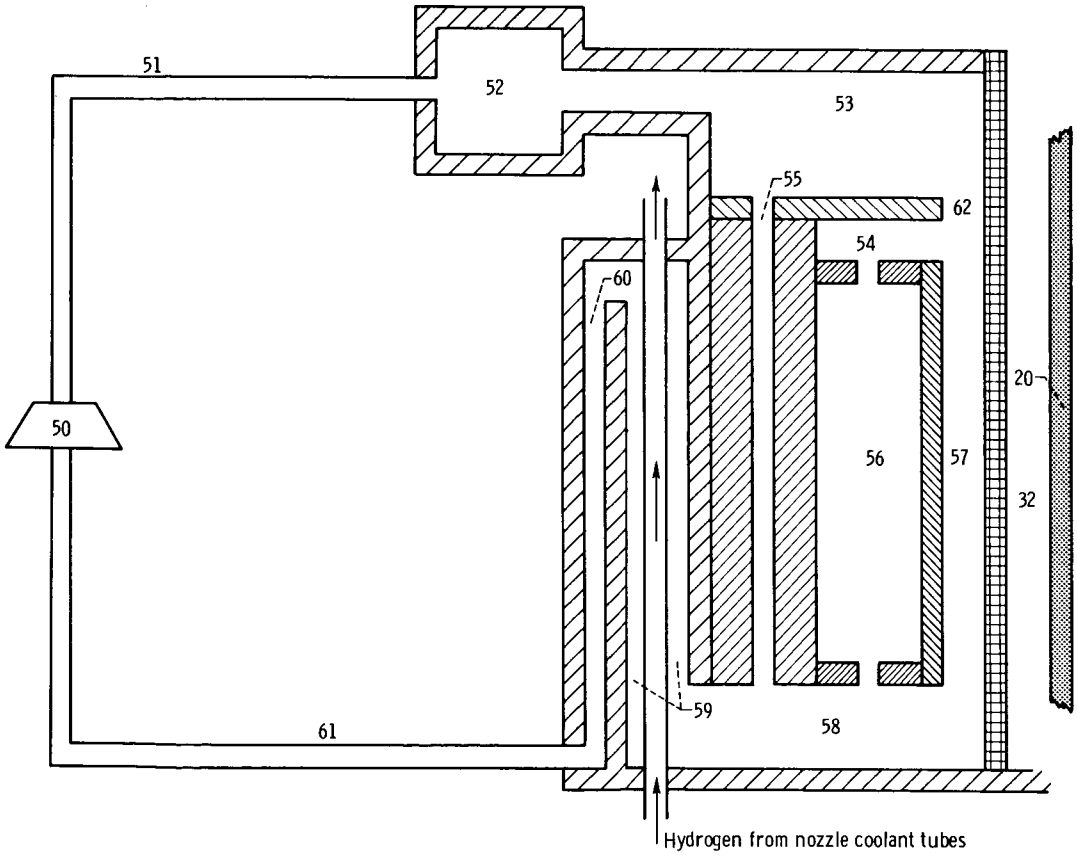

(b) Water flow system.

Figure 2. - Concluded.

acteristics. Heat transfer from the pumps to the fluid is not considered; however, their heat capacitances are lumped into their respective discharge lines (regions 04 and 06).

Feedlines

The total pressure drop in the bleed pump discharge line (region 04) is assumed negligible. Heat transfer from the walls (regions 04 and 06) is considered with no heat generation in the walls. Two-phase flow is also considered to exist. Fluid thermal capacitance in the exit plenum (region 07) is included in adjacent regions. Fluid mass capacitance is also considered in this region.

Nozzle

The parallel nozzle coolant tubes were represented by a single tube (region 08). Axial wall temperature and pressure distributions provided from the detailed component performance calculations were used directly to prevent inaccuracies in the calculation of heat-transfer rates and transient wall temperatures.

On the hot side of the coolant tubes, heat input to the wall from the hot gas was considered to occur through a series thermal resistance produced by the wall and gas film. Thermal recovery is also considered on the hot side. Heat transfer from the wall to the coolant is also through a series thermal resistance produced by the wall and coolant film. Heat transfer into the divergent section of the nozzle coolant tube wall due to radiation from the core exit face is considered. Fluid properties are evaluated at the throat of the coolant passages to check for choking. If choking occurs, the hydrogen flow is considered independent of downstream pressure.

Heat Exchanger

The multiparallel paths of the heat-exchanger segments (region 10) are assumed to be represented by a single tube. Thermal conduction of the heat-exchanger wall is not considered so that a single temperature exists at each point. All heat generated by nuclear radiation in the heat exchanger is assumed to be generated in the water and transferred through the walls to the hydrogen.

Topping-Turbine Regions

In the topping-turbine inlet (region 12), wall thermal capacitance and heat transfer to the fluid are included since the additional energy may be significant during startup operation.

Flow through the topping-turbine throttle (region 13) and bypass (region 14) valves is assumed to be governed by isentropic flow relations which allow for both choked and unchoked flow. Thermal capacitance of the valves is considered.

The topping turbine (region 15) is assumed representable by normalized functions of pressure and speed-to-temperature ratios over a range from design point to below motoring point operation. The return line (region 16) is simulated as a pipe by neglecting thermal energy relations.

Shield and Inlet End Reflector

The heat input rates within the shield (region 17) and the inlet end reflector (region 19) were determined from an assumed 15° R (8.33° K) hydrogen temperature rise across each component at the design point. Convective heat-transfer rates were derived to calculate a single wall temperature for each of the shield and inlet end reflectors.

Core

The major simplification to the system was made in the core (region 20). A single equivalent core wall, derived from detailed fuel-element calculations, was used to represent all fuel assemblies.

The axial temperature distributions of the center plug, fuel rings, and support tube walls of a centrally located core fuel element were considered equal to the wall-temperature distribution for a radial average fuel assembly. These wall temperatures were weighted according to their heat-transfer area and averaged to produce a single wall temperature for each stage of the fuel assembly. The resulting temperature distribution was assumed the same for all assemblies so that they could be represented by a single equivalent fuel assembly, as shown in figure 2(a).

The relative axial power distribution of a centrally located fuel assembly was assumed independent of power level. The total power generated in a radial average assembly was considered to be 80 percent of that in the central assembly. The hydrogen gas temperatures in the annuli of each stage of the central assembly were averaged radially

to provide a single axial fluid temperature distribution. This distribution was considered equal to the radial average gas temperature for all assemblies.

Thrust Chamber

Fluid thermal and mass capacitance were considered in the thrust chamber (region 22). The thrust nozzle was assumed choked at all times and considered isentropic. Variation of specific heat was included by having the characteristic velocity as a function of chamber exit gas temperature.

Reentrant Bleed Assemblies

The axial temperature distribution of the walls for the second pass of a typical reentrant fuel assembly (region 34) was averaged similar to the main core. Fluid temperatures were averaged to provide a single average temperature distribution for the first and second pass. Heat input to the first-pass fluid was assumed to originate from the second-pass equivalent wall. As shown in the schematic drawing (fig. 2(a)), hydrogen gas is in contact with a single equivalent fuel ring. Heat loss from the passage of the bleed gas through the core hydrogen in the reactor dome area (region 18) is considered.

Bleed-Turbine Regions

The bleed-system turbines and associated valves (regions 23 to 31) are treated similarly to the topping-turbine regions. Fluid capacitance is considered between the turbines (regions 23, 27, 38, and 39). The poison-circulating-pump turbine impedance is simulated by a choked nozzle (region 31).

Water Subsystem

Kinetic energy is not considered in the water flow loop (fig. 2(b)). Also, fluid friction is assumed constant. This assumption permits constant specific speed operation of the water pump. The assumption of incompressible flow also implies that only a single water flow needs to be calculated for the entire loop.

The inlet water manifold (region 52) and plenum (region 53) are considered plenums with perfect thermal mixing, no heat generation, and constant specific heat. Thus, ther-

mal mixing delays are provided. The region between the inlet end reflector and core water baffle (region 54) is treated similarly.

The heat rate into the reflector (region 55) is assumed to be divided equally between the beryllium reflector and the water. Convective heat-transfer relations were used to calculate an axial wall temperature. Thermal conductivity of the reflector wall is not considered. Water in the main core (region 56) was assumed to contain both thermal mixing and fluid transport delay.

In the high-velocity region (region 57), the flow-divider and pressure tubes were assumed to be at the same temperature. Heat loss from the equivalent fuel assembly (region 20) was assumed to be conducted through the stagnant hydrogen gap to the equivalent flow divider and pressure tube water and then into the high-velocity water. At the outlet water plenum (region 58), perfect thermal mixing of the three parallel water paths is assumed to occur. The heat-exchanger region (region 59) was treated to correspond to the hydrogen flow. The heat-exchanger outlet plenum is also considered a plenum with perfect thermal mixing.

Poison Subsystem

The poison subsystem was not simulated directly. Significant dynamics associated with the poison loop were represented by a transfer function technique. A poison rate command signal must pass through a transfer function before it is effective in contributing to core reactivity.

GENERAL EQUATIONS

The basis for dynamic calculation of all fluid and wall properties throughout the system are the momentum and general energy equations used with the conservation of mass and state equations. These general equations are derived from the basic partial differential equations and provide for lumped parameter representation of one-dimensional, compressible, multiphase fluid flow in a variable cross-sectional area channel. They also provide for convective heat transfer between wall and fluid, heat generation within the fluid due to friction and nuclear radiation, and wall heat generation.

The general equations are derived in reference 2 and are presented here as they apply to a general i^{th} section of the physical model. The symbols used in this report are defined in the appendix.

Energy Equation

The energy equation for an i^{th} section of fluid is

$$c_p W_i \frac{dT_i}{dt} = q_i^{cg} - \omega\left[c_p(T_i - T_{i-1}) + \frac{1}{J}\Delta e\right]$$

which relates the thermal capacitance to heat input and total heat transport.

The energy equation for a general section of wall is expressed as

$$c_p W_i^w \frac{dT_i^w}{dt} = hA_i\left(T_i^w - T_i\right) + q_i^{gw}$$

The basic Nusselt number correlation used to calculate the heat-transfer coefficient in all regions is

$$\frac{hD}{K} = 0.023\ Re^{0.8} Pr^{0.4}$$

In the feedline where the fluid phase changes, the basic Nusselt number correlation was multiplied by a factor depending on the region of the temperature-entropy diagram in which the fluid exists. For two-phase flow, the Martinelli factor is used:

$$\frac{hD}{K} = 0.023\ Re^{0.8} Pr^{0.4} \varphi_m$$

The basic Nusselt number correlation is modified for use in the nozzle tubes as

$$\frac{hD}{K} = 0.023\ Re^{0.8} Pr^{0.4}\left(1 + 0.0145\ \frac{\mu_w}{\mu_b}\ \frac{\rho_b}{\rho_w}\right)$$

where the last factor is evaluated over all regions of the temperature-entropy diagram. The Nusselt correlation is also modified for use in the top reflector, core, and reentrant tube regions by a fluid-to-wall temperature correction factor:

$$\frac{hD}{K} = 0.021\ Re^{0.8} Pr^{0.4}\left(\frac{T}{T_w}\right)^{0.55}$$

Momentum Equation

The momentum equation for an i^{th} section of fluid is given by

$$\frac{l}{gA}\frac{d\omega}{dt} + \rho_i \Delta e = (P_{i-1} - P_i) - \rho_i \left(\frac{f_i l}{D}\right) e_i$$

which relates fluid inertia to total pressure difference and fluid friction. The friction factor is defined by

$$f = f_{xc} + f_{DW}$$

where f_{xc} is a constant assigned to account for losses which are independent of Reynolds number and f_{DW} is the Darcy-Weisbach form of the friction factor given by

$$f_{DW} = 0.0032 + \frac{0.221}{Re^{0.237}}$$

Sudden contraction and expansion losses between sections are also considered for use in the momentum equation.

Continuity Equation

The continuity equation yields an equation for mass capacitance within a general section of the physical model

$$\frac{dP}{dt} = Z(\omega_{i-1} - \omega_i)$$

where Z, the compressibility factor, depends on the phase of the fluid and is based on adiabatic conditions.

For a gas:

$$Z = \frac{\gamma RT}{V}$$

For a liquid:

$$Z = \frac{B}{\rho V}$$

For mixed phase:

$$Z = \min\left(\frac{\gamma RT}{V}, \frac{\rho_g}{x\rho_e}, \frac{B}{\rho_L V}\right)$$

where ρ_g is gas density, ρ_L is density of saturated liquid, and ρ_e is equivalent density defined as

$$\rho_e = \frac{1}{\frac{x}{\rho_g} + \frac{1 - x}{\rho_L}}$$

Turbomachinery

Pump performance was represented by specific curves of

$$\frac{H_p}{N^2} = f\left(\frac{Q}{N}\right)$$

$$\frac{L_p}{N^2} = f\left(\frac{Q}{N}\right)$$

Enthalpy rise across the pumps is determined from

$$\Delta H = \frac{1}{J}\left(\frac{H_p}{\eta_p} - \Delta e\right)$$

where η_p is the pump efficiency. This representation permits fluid density dependency.

Pump stall characteristics were estimated based on existing data. The curves were extrapolated to include motoring and negative torque operation.

Turbine performance was represented by curves of

$$\frac{L_t}{P_e} = f\left(\frac{P_e}{P_i}, \frac{N}{\sqrt{T_i}}\right)$$

$$\frac{\omega_t T_i}{P_i} = f\left(\frac{P_e}{P_i}\right)$$

The torque parameter curves were extrapolated to the zero torque intercept to permit simulation of turbopump motoring. The turbine pressures were assumed to be total pressures.

Lines and Valves

Pressure drops in the lines are calculated from the momentum equation. Expansion and contraction losses between regions of the system are calculated according to

$$P_i - P_{i+1} = \rho_i(1.5\, e_{i+1} - e_i)$$

for sudden contraction and

$$P_i - P_{i+1} = \rho_i\left[\Delta e + \frac{(v_i - v_{i+1})^2}{2g}\right]$$

for sudden expansion. Standard hydrodynamic relations in the form

$$\frac{\omega\sqrt{T_i}}{P_i} = f\left(\frac{P_e}{P_i}\right)$$

were employed across all valves. In the case of gaseous flow, isentropic compressible flow relations were used to allow for choked and nonchoked conditions.

Reactor Kinetics

The equations used to describe reactor power are the kinetics equations normalized to 100-percent power including six delay groups

$$\frac{dn}{dt} = \frac{\beta(\rho_T - 1)}{\ell^*} n + \sum_{i=1}^{6} \lambda_i C_i$$

$$\frac{dC_i}{dt} = \frac{\beta_i}{\ell^*} n - \lambda_i C_i \qquad i = 1, 2, \ldots, 6$$

where

n relative neutron level

β total delay neutrons

C_i concentration of i^{th} group of delayed neutrons

β_i fraction of i^{th} group of delayed neutrons

ρ_T total reactivity, \$

λ_i decay constant of i^{th} group of delayed neutrons, sec^{-1}

The total reactivity represents the sum of the contributions due to fuel temperature, water temperature, and poison concentration.

DIGITAL-SIMULATION MODEL

A detailed digital-simulation model was developed by the direct application of the general equations to a sectionalized version of the physical model. All details of the system and components of the physical model were maintained. Appropriate averaging was done to accommodate the lumped representation. The sections used in the major regions are presented in table I. A list of the resulting equations and system constants is given in references 2 and 5 (vol. II).

A digital program was written to solve the equations and is presented in reference 5. A brief description of the features that make up the digital-simulation model and the digital-simulation model and the digital program follows.

TABLE I. - DIGITAL SIMULATION

MODEL SECTIONS[a]

Region	Section
Feed line (06)	5
Nozzle (08)	7
Heat exchanger (10)	5
Core (20)	7
Reentrant bleed tubes (34):	
First pass	1
Second pass	5
Main core water (56)	2
High-velocity water (57)	2

[a]In general, all other regions not listed were considered as one section.

Model Description

The digital-simulation model for the hydrogen flow system is basically composed of alternate impedance flow paths separated by fluid capacitance nodes. The nodes are represented by four large plenums: the heat-exchanger-exit plenum, the inlet-core plenum, the bleed-system-inlet manifold, and the plenum between the water and first-stage-pump turbines.

The continuity equation is applied to the plenums to obtain the pressure in each volume. The value of the compressibility factor in the continuity equation is determined as for capacitors in series. The momentum equation is applied between plenums to determine a single flow rate for all sections between the plenums. The inductance term in the momentum equation is obtained by summing the inductance constants for each section within the region.

Fluid inertia is included for the flow path between the propellant tank and the capacitance node at the heat-exchanger outlet. The fluid inertia for the remaining flow paths is considered negligible with respect to the fluid inertia in the combined feedline, nozzle coolant tubes, and heat exchanger. Since fluid inertia is neglected, the flow rates are obtained from algebraic solution of the momentum equation.

Fluid thermal capacitance is included only in the feedline. In all subsequent regions, the stored heat term in the energy equation is neglected.

Digital Program

A digital program was written to solve the system equations. The program consists of a main calling program and 41 subroutines. The flow diagram for the main program execution is given in figure 3. The subroutines are listed as follows:

Input-output subroutines:

INPUT	reads input data
PRNTWM	directs stored data to proper printout subroutines
H2PRT	gives printout of hydrogen temperature and pressure
TEMPWL	gives printout of wall temperatures
TUBETP	gives printout of pressure tube temperature
H2FLOW	gives printout of hydrogen flow
H2QUAL	gives printout of hydrogen qualities
TEMPWT	gives printout of water temperatures
THVPOS	gives printout of throttle-valve positions
VLVPO	gives printout of valve positions
PQNPMP	gives printout of pump volumetric flow to speed ratios
PMPTRQ	gives printout of pump torque
TRBTRQ	gives printout of turbine torque
XMODRT	gives printout of water flow, reactor power, and total reactivity
REACPT	gives printout of individual reactivity contributions of metal, water, and poison
CRTWM	directs the proper stored data to GRAPH for plotting
GRAPH	multipurpose plotting routine; plots as many as six curves on one figure
GRDEVN	ensures that grid on which curves are plotted is evenly incremented

System subroutines:

POWER	calculates reactivities and reactor power
REKIN	solves reactor kinetic equations
VALVE	determines turbine-throttle and bypass-valve positions
FLOCAL	calculates feedline flow

FEEDL	coordinates feedline calculations up to nozzle inlet
FELINE	calculates feedline pressures and temperatures, called by FEEDL
H2PUMP	calculates hydrogen pump flow, head rise, efficiency, and torque, called by FEEDL
NOZL	calculates nozzle tube pressures and temperatures
HEATX	calculates heat exchanger pressures and temperatures, hydrogen side
PLENUM	calculates pressure in plenums
TPTURB	calculates topping-turbine region flow
TRB2	calculates turbine flow, speed, and torque; includes valves
SHIELD	calculates shield pressure and temperature
REFCOR	calculates reflector and core pressures and temperatures
COR2PS	calculates reentrant fuel assembly temperatures
BLEED	calculates bleed system flows, pressures, temperatures
WATER	calculates all water loop temperatures and pressures

Hydrogen property subroutines:

HREG	determines thermodynamic region from pressure and enthalpy and calculates quality
TRCZ	calculates hydrogen temperature, density, and sonic velocity
VISC	calculates viscosity
HTC	calculates heat-transfer coefficients for all regions in system
POLY	evaluates to a sixth-degree polynomial; used by other hydrogen property subroutines
TRIDEN	evaluates hydrogen density near critical temperature

A more complete description of the program and a programmer's manual are given in reference 5.

Main program. - The main program calls and controls the subroutine sequence during the program execution. The computational sequence for one time increment is as shown in figure 3. After initialization, calculations begin at the hydrogen shutoff valve and proceed sequentially through the hydrogen system to the thrust chamber and the nozzle simulating the poison turbine. The water loop calculations are then made, hydrogen flows for the next time increment are calculated, and a new time increment is started.

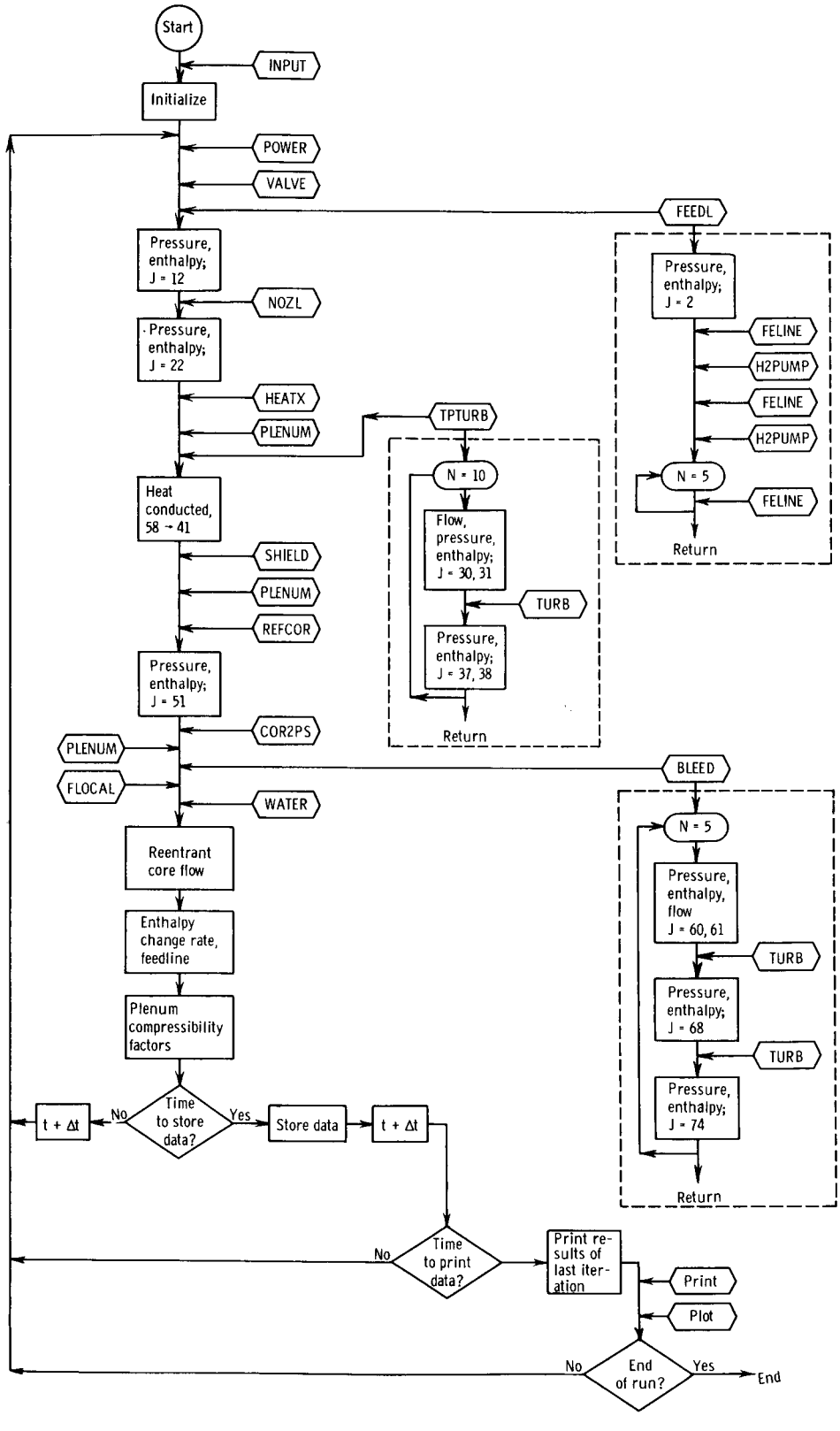

Figure 3. - Digital-simulation model program flow diagram.

The main flow of information into a time increment consists of flows, turbine speeds, wall temperatures, and pressures which were calculated during the last time increment. These quantities are used in the current time increment to generate new values. All these quantities except flows downstream of the nozzle tubes are calculated from differential equations by simple Euler integration. Though simple Euler integration is the least accurate of all numerical integration methods, the accuracy is compatible with that of the model and input data. For flows downstream of the nozzle coolant tubes, fluid inertia is neglected so that flows for the next time increment are explicitly solved by using known pressures and densities calculated in the current time increment.

Subroutines. - The subroutines can be classified into three main groups: the input-output subroutines, the system subroutines, and the hydrogen properties subroutines (see pp. 20 and 21).

The input-output subroutines are used for reading in the input data at the start of a run and for printing and plotting desired results at intervals during and/or at the end of a run. In order to have program flexibility, the region subroutines are written so that the nozzle can be subdivided into as many as 20 sections, and the feedline, heat exchanger, core, and reentrant bleed assemblies up to 10 sections by changing only input data. In this way, the number of sections need not be fixed but changed as experience indicates.

Separate subroutines were written for all the major hydrogen system regions and components and served as the building blocks for the complete program. The subroutines are used in the sequence shown on the main flow diagram during each time increment. The system subroutines are used repetitively, once during each time increment, until the run is over as determined by comparing the calculated real time with the desired time limit. This time limit is part of the input data. The results which are calculated in each time increment can be stored for output at the end of each increment or at intervals of any desired number of increments. Only the actual results that are desired for printed output are stored. The identification of the desired quantities and the printout frequency are controlled by input data.

The system subroutines essentially evaluate pressure and enthalpy at each calculational point in the hydrogen system and temperatures at each point in the water loop. In the hydrogen system, the calculated pressures and enthalpies are used at each point by the hydrogen property subroutines. The hydrogen property subroutines are common to all the system subroutines with the exception of the water loop subroutine.

Calculation of the hydrogen physical property data is accomplished by a set of polynomial equations built into the hydrogen properties subroutines. The first subroutine determines the appropriate region of a pressure-enthalpy map corresponding to the pressure and enthalpy of the hydrogen. Four regions are identified: two-phase region, subcritical pressure liquid region, subcritical pressure vapor region, and the supercritical

region. The second subroutine calculates temperature, density, and sonic velocity from the set of polynomials corresponding to the particular thermodynamic region. The third subroutine calculates heat-transfer coefficient again with polynomials. The fourth subroutine is for estimating viscosity from polynomials and is handled in a separate subroutime since it is needed only in the nozzle region.

Computing time is conserved in calculating hydrogen properties by determining if pressure or enthalpy has changed by some predetermined amount. If not, the point is assumed to be in steady state, and the subsequent subroutines are bypassed. The heat-transfer coefficient is checked similarly.

ANALOG-SIMULATION MODEL

Mathematical relations were developed for an analog-simulation model based on the general equations already discussed. A complete list of the equations is given in reference 2 and again in reference 5. This model resulted primarily from simplification and modification of the digital-simulation model. For example, all system regions were considered as one section except for two sections in the core. The primary consideration in simplifying the digital equations was to preserve critical representations and to preserve accuracy within the equipment limitations of the analog computer.

Model Description

Fluid capacitance nodes are located at the nozzle-tube-inlet manifold, the heat-exchanger-outlet manifold, the dome region, the thrust nozzle, and the bleed exit line. Approximate capacitances are located in the piping between the water and bleed turbines and at the bleed-system exit nozzle. Kinetic energy change is neglected except in the core and nozzle tubes where this change can be significant. Specific heats of walls are assumed constant. Contraction and expansion losses are lumped with friction. The friction factor is also assumed constant. Single sections are used in the feedline, nozzle tubes, heat exchanger, reentrant bleed assemblies, side reflector, and high-velocity water passage. Two sections are used in the core for both hydrogen and water.

Analog Program

The equations describing the analog-simulation model were mechanized on general-purpose analog computers. The basic system simulation mechanization required 179 op-

erational amplifiers including integrators, 105 multipliers, and 20 function generators. Circuitry was designed to separate the various subsystems to facilitate changes to the simulation model.

SIMULATION-MODEL VERIFICATION

A model verification analysis was performed on both analog- and digital-simulation models to verify steady-state and dynamic performance. An analog-digital simulation-model comparison was also made. A detailed account of the verification and comparison procedure is presented in reference 3. A summary of the procedure and results follows.

Digital-Simulation Model

Steady-state verification was made by a detailed comparison between digital results and hand calculations of the individual equations. The model was also compared with detailed component performance calculations at the 100-percent point. The comparison indicated satisfactory computation of the digital-simulation-model equations.

The dynamic verification consisted of checking the digital program outputs from all the integration equations against hand calculations. The differential equations which require integration include wall temperatures, plenum pressures, fluid flow, turbopump speeds, and water temperatures. In general, the procedure involves comparing the ratio of a change in a variable between two consecutive time increments with the excess potential against the integration gain factor. Results are given in reference 3.

Analog-Simulation Model

Steady-state verification of the analog-simulation model was obtained by comparing a detailed voltage readout with hand calculations of the equations. Errors were generally within 0.5 percent.

The analog-simulation-model dynamic characteristics were verified by checking each significant dynamic equation. The net input to each integrator was caused to vary by perturbing a valve in the system. The net input and output were recorded and reduced to numerical form. Processing these data through a digital convolution program resulted in gain and phase diagrams of the transfer function. The frequency at which the gain plot crossed zero decibels was compared with the value calculated from the equations. The

results are reported in reference 3. In each case, the frequency-response value agreed well with the value calculated from the equation.

Digital-Analog Comparison

A detailed comparison was made between the analog and digital steady-state results at 100 percent and 37 percent flow rate. The simulation-model results were also compared with the detailed component performance calculations from which the physical model was derived. This comparison is given in reference 3.

In general, the digital-simulation model, analog-simulation model, and component calculations compare closely at all levels. Some discrepancies did exist and those existing between the component calculations and the digital-simulation model were a result of variation of component inlet conditions and hydrogen properties approximations. Variations between the analog- and digital-simulation models result primarily from simpler lumped parameter representation in the analog-simulation model. The overall correlation between models was sufficient to substantiate results and conclusions.

PROCEDURE

The general approach of the research study was to use the analog-simulation model for steady-state and dynamic behavior investigations in the startup to power range to provide qualitative characteristics of the system and serve as a guide to detailed studies. To complement this information, the digital-simulation model was used to provide detailed results of transient performance particularly in the chilldown to startup region of system operation. It was also used to establish and evaluate startup programming.

COMPARATIVE SYSTEM ANALYSIS

An initial system analysis was made on the preliminary reference-design system using analog steady-state mapping and large perturbation transient techniques. The steady-state mapping defined the operating envelope under various operating conditions. The limits encountered were based on component limitations previously established. The transient studies defined permissible thrust changes during startup and shutdown and enabled a comparison of control techniques. Based on the operational problems uncovered from the analysis, modifications to the preliminary reference design were formulated to alleviate or eliminate the problems. Comparative analyses were performed on each of

the modified models to determine which modifications should be incorporated in subsequent models. The analysis of each of the models studied was designed to provide a comparison of system performance, flexibility, and system and control complexity. In this way, a final design, the reference design, was evolved on which the control analysis was performed.

Steady-State Mapping

Steady-state mapping determines static sensitivity by defining the slopes of the dependent variables with respect to the independent variables. The definition of these relations indicates which independent variables are effective control parameters with regard to static operation. In the process of defining the static gains, operational limits are encountered that limit steady-state operation. These limits usually represent material or structural limits, operation beyond which will damage or render the system inoperable. The envelope formed by these limits defines the allowable operating region of the system and indicates its relative flexibility. A narrow region usually leads to close and/or critical control requirements. Inherent static stability is demonstrated by holding all control elements fixed at various flows and reactor power without controls. The steady-state mapping results presented in this analysis were concerned with the variation of system variables rather than of valve positions.

Transient Analysis

Transient studies are used to demonstrate dynamic stability and to determine acceptable power-flow relations during system acceleration. Inherent dynamic stability is investigated by holding all system parameters constant at various flow levels without control and initiating small perturbations in various system variables.

OPERATIONAL LIMITS

Operational limits on the system are determined by component limitations which are primarily a result of material characteristics. The system operating envelope is established from the boundaries formed by the limits. The limits are determined by averaging the detailed component calculations over an interval which corresponds to a particular model section. Thus, the limit is assumed to be reached when the section value reaches the average. The limits are given for zero and indefinite dwell times to define allowable

transient limit violations. The temperature-limit - dwell-time relation is undefined for intermediate dwell times.

Nozzle Tubes

The average nozzle-tube wall temperature based on the maximum allowable throat wall temperature is 965° R (536° K) for an indefinite dwell time and 1000° R (556° K) for zero dwell time. When the average temperature of the nozzle-tube wall reaches this limit, it is assumed that the wall temperature at the coolant passage throat is at the maximum material temperature limit.

Heat Exchanger

The average heat-exchanger-exit-wall temperature is limited to not less than 492° R (273.3° K) to prevent ice formation during steady-state operation. Transient ice formation is permitted. This exit wall temperature is estimated from the average heat-exchanger-tube wall temperature and the average water temperature.

Pumps

The specific speeds of the hydrogen pumps must be maintained at a minimum of 5 percent above their respective stall value to provide a stall margin.

Core

The average wall temperature of an averaged radial core section is limited to a maximum of 4514° R (2508° K) for an indefinite dwell time and 5000° R (2778° K) for zero dwell time. This limit is the average of the wall temperature axial profile produced from the detailed core component calculations. The profile is assumed constant over the entire operating range. The average wall temperature of the inlet section of the core is also limited to a minimum of 1460° R (811° K) for an indefinite dwell time.

Pressure Tubes

The average flow-divider and pressure-tube equivalent wall temperature is limited to 719° R (399° K) for an indefinite dwell time and 735° R (408° K) for zero dwell time.

Water

The lower limit on the water is 492° R (273.3° K) for an indefinite dwell time based on the minimum allowable temperature in the heat exchanger. The upper limit on core exit water temperature is 833° R (463° K) based on 90 percent of the saturation temperature at an average water pressure of 500 psia (345 N/cm^2 abs).

Exit Bleed Gas

The exit bleed gas temperature is limited to 1860° R (1033° K). Overtemperature of the bleed gas would result in exceeding the water turbine material limit.

Model Limits

In addition to the actual engine operational limits, simulation-model limits exist which restrict the validity of the analog-simulation model. These limits are the nozzle-tube choking and nozzle two-phase flow. The model flow resistance and heat-transfer relations are not accurate under these conditions.

SYSTEM EVALUATION

System evaluation was based on a comparison of system and control simplicity, system flexibility, and system performance.

System Simplicity

System simplicity is concerned primarily with the number of components and subsystems reflecting cost, size, and reliability.

Control Simplicity

Control simplicity refers to the number of system variables which must be controlled during all phases of operation, the number of control elements required to manipulate these variables, and the resulting control system complexity required to control these variables.

System Flexibility

System flexibility is measured by the width of the operational region and the corresponding size of the operating region defined by the limit envelope. This flexibility indicates the relative ease with which the system can operate in going from chilldown, to startup, to power range operation. A narrow region would require fine, close control of the system parameters, whereas a wide region would relax these requirements.

System Performance

System performance is evaluated on the ability of the system to start up and shut down rapidly without violating component limits, the capability of rapid thrust transients in the power range, the ability to produce wide steady-state thrust variation at maximum specific impulse, and the ability to hold design thrust and specific impulse within close tolerances. In addition, the system must possess inherent static and dynamic stability of thrust and power over the operating region without closed-loop control.

COMPARATIVE SYSTEM ANALYSIS

The following discussion presents the results of the comparative system analysis for the preliminary reference design and several modifications. Each system is described, analyzed, and finally compared to produce a reference-design system for further study.

PRELIMINARY REFERENCE-DESIGN CONFIGURATION

The preliminary reference-design configuration is as described in the section DESCRIPTION OF PRELIMINARY REFERENCE DESIGN. Both analog- and digital-simulation models were used in the analysis.

Preliminary Control Analysis

The preliminary reference-design system is characterized by a high degree of control flexibility, as indicated by its six control elements. These control elements can be associated with five primary system variables: topping-turbine bypass valve (TTBV) with total hydrogen flow, water-turbine throttle valves (WTTV) with water flow, water-turbine bypass valve (WTBV) with bleed hydrogen flow, bleed-turbine throttle valve (BTTV) with turbopump power split, and poison concentration with reactor power. The bleed-turbine bypass valve (BTBV) is not associated with any primary system variable and can be considered redundant. A control system composed of closed loops around each of the primary system variables would result in the most flexible but most complex system. It is advantageous to simplify the control system to minimize interaction between the loops and to avoid a complex control network.

Possible interaction was investigated by integrating a control configuration, where each primary variable was controlled with its related control element, into the analog simulation. The WTBV and BTBV were mechanically linked to operate as a unit. The first attempt at operating this scheme showed that severe interaction existed between the three bleed-subsystem-valve control loops. Severe interaction also occurred with the BTBV linked to the BTTV, and again with the BTBV held fixed. Interaction ceased when either the bleed flow (WTBV) or turbopump power split (BTTV) control was inactive.

Steady-State Mapping

The general procedure employed in conducting steady-state mapping was to change the system variables from a nominal operating point until a system limit was encountered. Nominal operating points were established at 100-, 60-, and 37-percent total hydrogen flow by adjusting poison reactivity to obtain maximum reactor power governed by either maximum chamber temperature or turbopump stall. Poison reactivity was then held fixed at that reactor power level. The BTTV was adjusted to obtain equal stall margins; that is, each pump operated at an equal percentage from its respective stall line. Bleed hydrogen flow was set at 2.6 percent of the total hydrogen flow with the WTBV. The WTTV was adjusted to provide the water flow specified for each particular nominal operating point, that is, proportional with hydrogen flow. By holding total hydrogen flow constant through a closed-loop proportional-plus-integral control around the TTBV, excursions were made from the nominal operating point by changing only one bleed subsystem variable at a time, the others being held fixed. In this way, functional relations between the control element and its associated primary system variable, its sensitivity, and limitations were determined.

Water flow variation. - The WTTV was used to vary water flow about each of its nominal point values until operational limits were met. Bleed hydrogen to total hydrogen flow ratio was held fixed by closed-loop control around the WTBV and the turbopump power split ratio was varied on closed-loop control around the BTTV to hold equal stall margins on both turbopumps.

The effect of water flow variations on heat-exchanger and pressure-tube-wall temperatures is shown in figure 4. The component temperature is given as a function of water flow with total hydrogen flow and maximum, nominal, and minimum water flow as parameters. A separate map is shown for heat-exchanger-exit-wall temperature and the pressure-tube-wall temperature.

Maximum water flow is limited by the WTTV size and available bleed gas energy and occurs when the WTTV is wide open. The minimum water flow is limited by the pressure-tube-wall temperature limit. Both maps show that the allowable range of water flow variation increases as total hydrogen flow decreases. Also, and most important, both the heat-exchanger and pressure-tube-wall temperatures move away from their respective limits as water flow is increased at constant hydrogen flow. Increasing water flow increases the heat-transfer coefficient on both the heat-exchanger and pressure

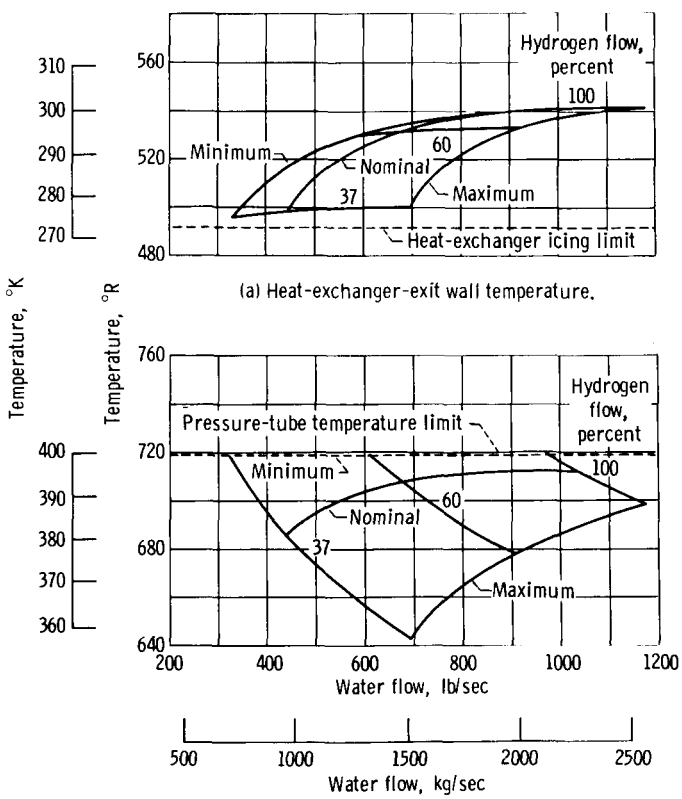

(a) Heat-exchanger-exit wall temperature.

(b) Pressure-tube wall temperature.

Figure 4. - Variation of water loop component temperatures with water flow.

tubes so that the same quantity of heat can be transferred with lower differential temperatures. This effect is stronger in the pressure tubes so that a wider variation in wall temperature occurs compared with that in the heat exchanger.

Therefore, operating at an increased water flow would produce a wider margin from both heat-exchanger-icing and pressure-tube overtemperature. It also provides a faster thermal response of the water system. Fixing the WTTV at its maximum value would result in the maximum water flow and produce the widest margin. With the value fixed, no control action would be required thus simplfying the control system.

Turbopump power-split variation. - The original concept for controlling series turbopumps was to maintain a constant topping- to bleed-pump power-split ratio. Since the total hydrogen flow is common to both pumps, this implies controlling pump speeds to produce a constant pump pressure rise ratio. To investigate the implication of this concept, power-split-ratio variations were made about each nominal point by varying the BTTV until operational limits were met. Water flow and bleed- to total-hydrogen ratio were held fixed with closed-loop controls. The results are shown in figure 5. In this figure the normalized flow parameter of the bleed pump is plotted against that of the topping pump with percent total hydrogen flow as a parameter. The flow parameters of both pumps were normalized on a scale so that both stall points occurred at a value of 54.2. Stall and motoring limits are also shown and form an envelope which defines the operating region of the pumps. The stall limits shown are actual stall; subsequent references to stall limit in the report refer to the stall margin limit described in the section OPERATIONAL LIMITS.

Since the pump stall margins were equalized at the nominal points, these points lie on a 45^{o} line through the origin. Diversion from this line indicates a stall margin mis-

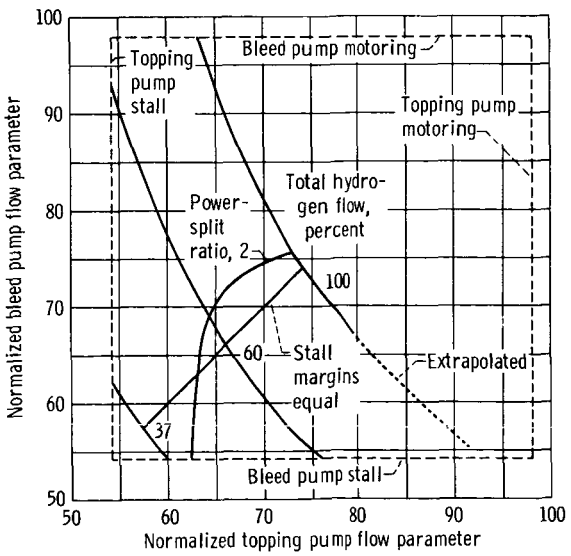

Figure 5. - Variation of pump power split ratio.

match. As percent total hydrogen flow is reduced along the matched stall line, the sensitivity to stall increases as indicated by the narrowing field.

At 100-percent flow, the bleed pump reaches a motoring condition before the topping pump reaches stall as the BTTV is closed. This indicates that the system can operate as an all-topping cycle near the 100-percent design point. At lower flow levels, the topping pump encounters stall before the bleed pump motors. As the BTTV is opened, the topping turbine reaches the TTBV wide open position limit as it approaches motoring. This is caused by the total hydrogen flow control on the TTBV trying to maintain a constant value. Extrapolating the 100-percent flow curve beyond this limit indicates that continued loading of the bleed pump would probably result in stall before the topping pump motored.

A curve of a constant topping- to bleed-pump power-split ratio of 2 is also shown. The data for this curve were taken from the Lewis study. At 100-percent flow, the topping pump is closer to its stall point. As flow is reduced, the margins tend to remain constant. Below about 50-percent, the imbalance swings sharply toward bleed pump stall. The power-split ratio of 2 becomes independent of topping pump loading.

Matching pump stall margins appears to be a better criteria by which to control the pump compared with pump power-split ratio. By maintaining equal stall margins, the system stall sensitivity is optimized. Also, the fact that the stall margin field expands as flow is increased indicates that the stall margins could be equalized at a low total hydrogen flow and the BTTV held fixed at that point. The results of this technique are discussed in reference 4. No control action would then be required, and the control system would be further simplified.

Bleed hydrogen flow variation. - Bleed hydrogen flow variations were not investigated directly in the contractual study. However, it was noted throughout all steady-state mapping operations that the WTBV remained choked over the entire operating range investigated and the WTTV remained choked over a major portion of the range. It was reasoned, therefore, that if the sum of the areas of the WTTV and WTBV were held constant at all operating points, the bleed flow would be dependent only on the bleed hydrogen inlet pressure and temperature. This could be accomplished by mechanically linking the valves to form a water-turbine flow-splitter valve (WTSV) so that their respective areas are complementary, thus providing additional control system simplification.

Since the bleed subsystem inlet pressure is essentially equal to the chamber pressure and the corresponding temperature is closely proportional to chamber temperature, not only will the bleed hydrogen flow remain constant at any position of the combination throttle-bypass valve, but will be a fixed ratio of the total hydrogen flow. Since the data on water flow variation indicate that a fixed maximum area for the WTTV is required, a fixed WTBV is also implied (fixed WTSV).

The variation of bleed hydrogen flow with fixed bleed subsystem valves is shown in

table II. The data were taken from the Lewis steady-state mapping study reported in reference 1. Bleed to total hydrogen flow ratio and water-pump-turbine-inlet gas temperature is listed for three total hydrogen flows and reference-design-point values. The reference-design points are at 100-, 60-, and 37-percent total hydrogen flow at maximum design chamber temperature. The bleed subsystem valves are fixed at each of these points to provide a water flow proportional to the hydrogen flow, a fixed bleed to total hydrogen flow ratio of 2.6 percent, and a topping to bleed-pump headrise ratio of 2. The 2.6-percent bleed- to total-hydrogen flow ratio value is determined from the minimum bleed flow required to cool the reentrant bleed-tube fuel elements. However, this minimum provides a wide margin from fuel-element overtemperature so that the gas temperature entering the water-pump turbine is actually the governing limit.

Table II indicates that with the bleed subsystem valves fixed at each reference-design point, the bleed- to total-hydrogen flow ratio increases as total hydrogen flow decreases. A corresponding decrease in water-pump-turbine-inlet gas temperature occurs. As the bleed subsystem valves are set to lower reference-design points, the range of bleed to total hydrogen flow and water-turbine-inlet gas temperature increases. However, the allowable range decreases since the water-pump-turbine-inlet gas-temperature limit is met at progressively lower total hydrogen flow. Thus, the valves are restricted to being fixed at high reference-design points. If the valves were fixed at the 100-percent reference-design values, the increasing bleed to total hydrogen flow and corresponding decrease in water-pump-turbine-inlet gas temperature would ensure safe operation as

TABLE II. - VARIATION OF BLEED- TO TOTAL-HYDROGEN FLOW RATIO WITH WATER-TURBINE-INLET GAS TEMPERATURE

Reference-design point valve settings	Total hydrogen flow, percent	Bleed- to total-hydrogen flow ratio, percent	Water-turbine-inlet gas temperature	
			^{o}R	^{o}K
100	100	2.59	1827	1015
	60	2.78	1729	961
	40	2.89	1690	939
60	100	2.31	2030	1128
	60	2.59	1905	1058
	40	2.77	1764	980
37	100	1.90	2400	1333
	60	2.30	2041	1134
	40	2.57	1874	1041
	37	2.58	1864	1036

total hydrogen flow is decreased over the entire range. This compromises bleed subsystem turbine performance somewhat because the turbines are forced to operate at lower inlet gas temperatures; however, no control on the bleed- to total-hydrogen ratio would be necessary, and the control system would be further simplified.

Operating envelope. - Based on the results and conclusions drawn from the bleed subsystem variation mapping, the entire system was remapped. In mapping the system, a closed-loop control was placed around the TTBV to control total hydrogen flow. Poison reactivity was used to vary reactor power level until operational limits were met. The WTTV and WTBV were held fixed at their 100-percent design-point values to provide a maximum water flow and a fixed bleed to total hydrogen flow ratio. Turbopump stall margins were equalized with a closed-loop control around the bleed-turbine flow-splitter valve (BTSV), a combination BTTV and BTBV.

A hydrogen flow control was required to maintain stability. Without flow control, the system was marginally stable. Small perturbations would produce low frequency and lightly damped oscillations in hydrogen flow. The low system damping is, for the most part, a result of the head-flow characteristics of the topping turbopump and the topping section of the hydrogen flow system. The marginally stable condition agrees with the results of reference 1, although no qualification as to the degree of stability is given in that reference.

The results of the steady-state mapping of the preliminary reference design is shown in figure 6. In this figure, percent of design power is plotted as a function of percent de-

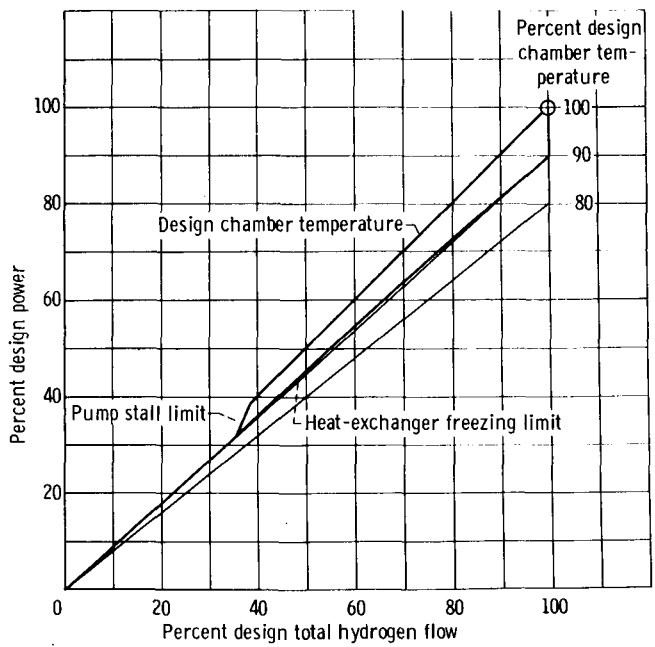

Figure 6. - Preliminary reference-design-system operating envelope. Operating conditions: poison reactivity variable; water turbine valves fixed at 100-percent design point; bleed turbine valves combined as flow splitter valve; pump stall margins matched.

sign total hydrogen flow with percent design chamber temperature as a parameter. The operating envelope is formed by system component limits.

The upper limit on reactor power is governed by design chamber temperature and pump stall. The nozzle-coolant-wall-temperature limit lies on a line of constant chamber temperature 1 percent above the design value; that is, if chamber temperature were increased 1 percent at any hydrogen flow level, the nozzle-coolant-wall temperature would be at its limit. Actually, it is not realistic to have a design point on or near a limit. In this case, chamber temperature is an imposed limit; the actual limit is core-wall temperature which lies above the chamber-temperature limit. However, the nozzle-coolant-wall temperature is met first. The pump-stall limit is for optimized operation with both pump stall margins equal. Under this condition, the stall limit is least restrictive; that is, it would occur at a higher power level than if the power-split ratio of 2 were adhered to. The lower limit on reactor power is governed by heat-exchanger water freezing. This limit coincides approximately with a chamber temperature of 90 percent of design.

Because of intersecting pump-stall and heat-exchanger-icing limits, steady-state operation below about 36-percent hydrogen flow and 32-percent reactor power is not feasible. Although this does not necessarily preclude startup, it does present a difficult obstacle. Startup may be possible, however, because transient operation through the region below the intersection may be significantly different from steady-state operation. Also of significance on the map is the narrow corridor in which the system must be operated. Undoubtedly, close control of independent system variables would be required to reach the design point. The results of the independent mapping done in this study corroborates the results of the Lewis study reported in reference 1.

Transient Performance

Transient operation of the preliminary reference design was concentrated mainly on chilldown and startup in order to determine if the problem of intersecting stall and freezing limits was restrictive. However, transient operation in the power range was also studied.

Chilldown. - Through use of the digital-simulation model, several chilldown transients were conducted to investigate the effects of varying water temperature and fuel-element temperature initial conditions, and the effect of main propellant-valve opening rate. A summary of the results is given in the following paragraphs. Detailed results of the chilldown study are given in reference 3.

Chilldown runs of 5-seconds duration were made at zero reactor power level and fixed system valve positions. The TTTV and BTTV were closed and the TTBV and BTBV

open to 100 percent to effect a motoring condition. The WTTV and WTBV were held fixed at their 100 percent design-point value.

The primary objective of varying initial water temperature was to determine its effect on heat-exchanger icing. All sections of water and walls in contact with the water were initialized successively at 530°, 610°, and 720° R (294°, 339°, and 400° K). The runs indicated that by using a 720° R (400° K) initial water temperature, heat-exchanger icing could be avoided for a 5-second-duration chilldown. At this initial water temperature, the pressure tube temperature is at its limit. Lower initial water temperatures resulted in icing in the heat exchanger prior to 5 seconds.

Initial fuel-element temperature determines the initial system impedance and is therefore reflected in pump-stall performance. This effect was investigated by initializing all sections of the core and reentrant fuel assemblies successively at 530°, 720°, and 1000° R (294°, 400°, and 556° K). The water temperatures and all walls in contact with the water were initially at 720° R (400° K). The results showed that increasing the initial fuel-element temperature decreased the maximum hydrogen flow. Although stall was approached, stall of neither pump occurred.

The general trend is for hydrogen flow to increase for the first few seconds of the chilldown, level off temporarily, and then increase again. The effect on the heat-exchanger-wall temperatures is quite noticeable. The wall temperatures remain about 30° R (17° K) above freezing mostly because of the increased regenerative heat transfer in the thrust nozzle.

Variation of the main propellant-valve (MPV) opening rate affects mainly hydrogen flow. As the valve opening rate is decreased, nozzle-coolant-tube choking occurs for a shorter period of time. A 5-second MPV opening rate eliminated choking completely. During the first 5 seconds, heat-exchanger minimum wall temperatures increased as the valve opening rate increased. The runs also indicated that the combination of high initial water temperature and slow valve opening rate considerably limits the cooling rate of the core because the hydrogen leaving the heat exchanger and entering the core is hotter under these conditions.

Startup transient performance. - The analog-simulation model was used to initiate startup transients from a point in time during chilldown. The initial conditions correspond closely to the final conditions produced after 5 seconds of chilldown on the digital-simulation model. In each of the starts made, control and valve programming were varied to define the range over which each parameter would produce a satisfactory startup. The water in the core was assumed to be preheated to 680° R (378° K) to help prevent immediate freezing and yet not produce an immediate pressure-tube overtemperature.

A typical startup from initial chilldown to the nominal 37-percent point is shown in figure 7. The transient was made by ramping reactor power through an ideal control

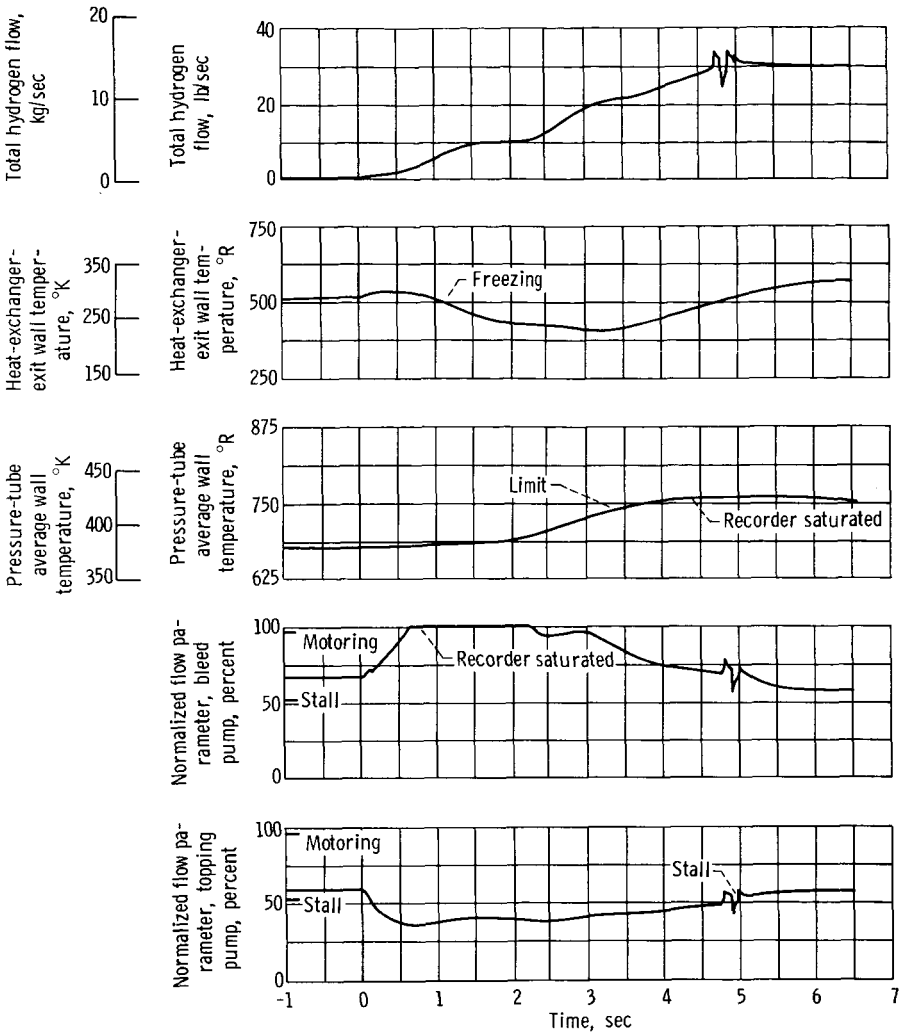

Figure 7. - Thrust transient of preliminary reference-design configuration.

around poison reactivity, total hydrogen flow through closed-loop control on the TTBV, and the BTTV to their nominal 37-percent-point values in 5 seconds. The topping pump went into deep stall while the bleed pump went to motoring. The pressure-tube-wall temperature exceeded its 719° R (399° K) limit. The heat-exchanger-exit-wall temperature went below freezing for 3. 5 seconds. The start was unsatisfactory since stall, freezing, and pressure-tube-temperature limits were encountered. The remainder of the study was aimed at alleviating these conditions.

Results of this study showed that startup could not be achieved without encountering pump stall even though pump-stall margins were equalized. Heat-exchanger icing at one extreme and excess pressure-tube temperature at the other imposed startup limitations. There was an indication, however, that a satisfactory start transient might be achieved by preheating the water to 700° R (389° K), incorporating a controllable TTTV, and

properly programming the TTTV. The region of satisfactory transient operation would be narrow and control of independent system variables critical.

System Modifications

The problems associated with the preliminary reference-design system center around heat-exchanger icing and pump stall. These problems were essentially the same as those uncovered in the Lewis study reported in reference 1.

Independent control of water temperature in the heat exchanger would essentially eliminate or at least alleviate the icing problem. Since hydrogen flow through the heat exchanger has a strong influence on bulk water temperature, a controllable hydrogen bypass flow around the heat exchanger would provide independent water temperature control.

Three potential design modifications were considered: (1) hydrogen bypass around the heat exchanger, (2) hydrogen bypass around the nozzle coolant tubes and heat exchanger, and (3) a combination heat-exchanger - topping-turbine bypass. The merits of each are discussed in the following sections. A schematic diagram showing these modifications is presented in figure 8.

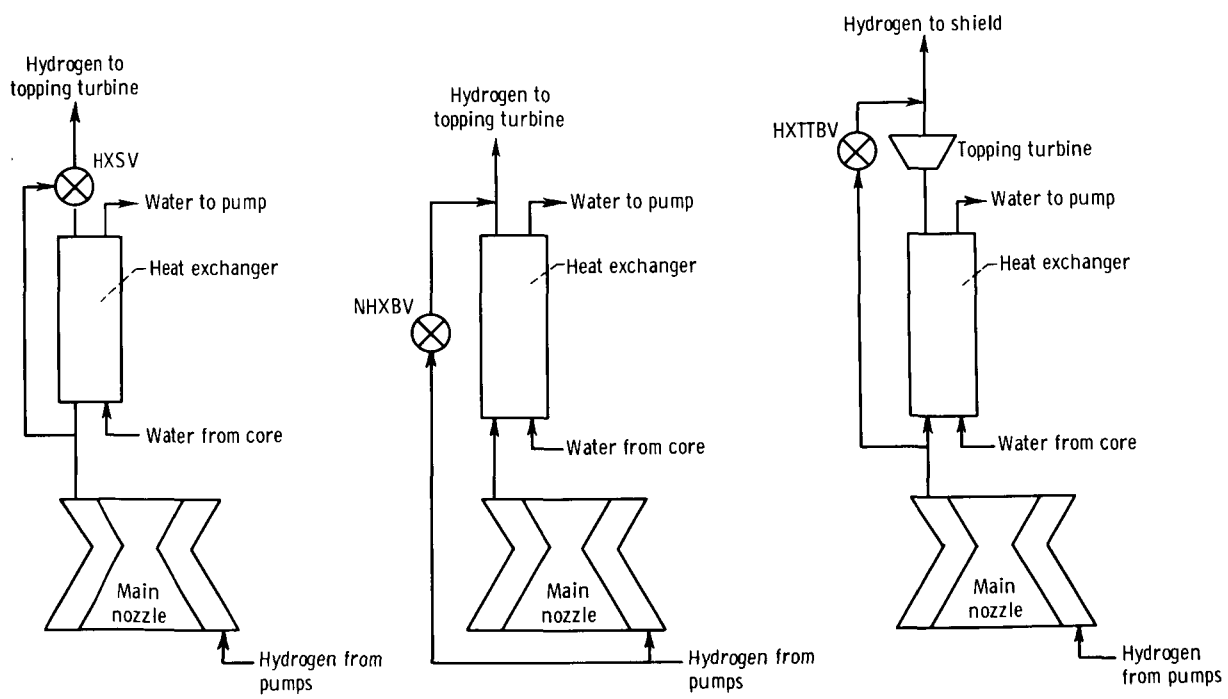

(a) Heat-exchanger bypass with flow splitter valve.

(b) Nozzle - heat-exchanger bypass.

(c) Combination heat-exchanger - topping-turbine bypass.

Figure 8. - Schematic diagram of split-feed configurations with alternate bypass schemes.

The heat-exchanger-bypass configuration represents the most direct solution to eliminating or avoiding heat-exchanger icing. However, since the pressure drop across the heat exchanger is relatively small, a large valve would be required to provide a large hydrogen bypass flow. This could be overcome by using a flow-splitter valve downstream of the heat exchanger. This configuration, however, could impose a flow distribution problem on the nozzle-coolant discharge plenum.

The second configuration considered, the nozzle-heat-exchanger bypass, could provide a large bypass flow with a small valve since the pressure drop across the nozzle coolant tubes is quite high. It also provides a low impedance path for most of the hydrogen flow so that pump loading would be lessened somewhat. The main advantage of this bypass scheme is that it can be implemented without major mechanical redesign to the reactor. Disadvantages include a possible minimum nozzle-coolant-flow requirement and a potential hydrogen mixing problem at the topping-turbine-inlet manifold.

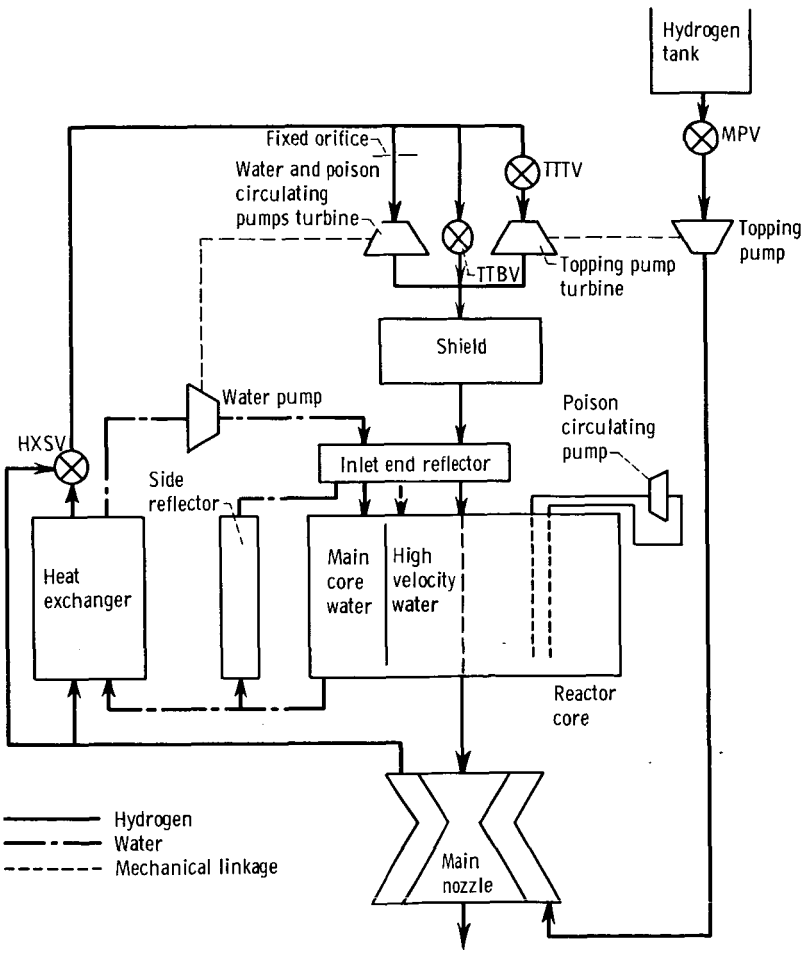

Figure 9. - Schematic diagram of topping cycle configuration with flow-splitter heat-exchanger bypass.

The third configuration incorporates a bypass from the nozzle discharge manifold to the core inlet in parallel with the topping turbine. Although this bypass configuration does not require an additional valve, and in fact, replaces the topping-turbine bypass valve (thus not increasing system complexity) system flexibility is lost because of the resulting interrelation between control of total hydrogen flow and heat-exchanger-bypass fraction.

As stated previously, one of the problems associated with the preliminary reference design was pump stall due to the complexity of series pumps. In this respect, elimination of the bleed system in favor of an all-topping cycle appears to offer a major improvement in system simplicity, reliability, and ease of operation. However, its growth potential is limited. A schematic diagram of this system is shown in figure 9. A single hydrogen pump is driven with a topping turbine. An auxiliary turbine in parallel, as shown, or a power takeoff from the topping turbine would be required to power the water and poison pumps.

The performance of each of these four configurations is discussed in the following sections. Detailed results and discussion are given in reference 4.

HEAT-EXCHANGER-BYPASS CONFIGURATION

The heat-exchanger-bypass configuration uses a flow-splitter valve (HXSV) downstream of the heat exchanger to provide a positive restriction to heat-exchanger hydrogen flow.

Steady-State Performance

The same control scheme used for the preliminary reference design, except for reactor power control, was used to map the heat-exchanger-bypass configuration in steady state to determine the extent of increased operating latitude. Only the TTBV and HXSV were manipulated. Poison concentration was held fixed at the value required to maintain 100-percent design-point conditions without bypass flow. The results are shown in figure 10. Percent design reactor power is plotted as a function of percent design total hydrogen flow. In this case, the upper limit to reactor power is governed by design chamber temperature and pump-stall limits. Again, the nozzle-tube-overtemperature limit lies on a line of constant chamber temperature 1 percent higher than design. The lower boundary on reactor power is no longer heat-exchanger icing, as in the preliminary reference design, but pressure-tube overtemperature and, in a small region, the topping-turbine-power limit.

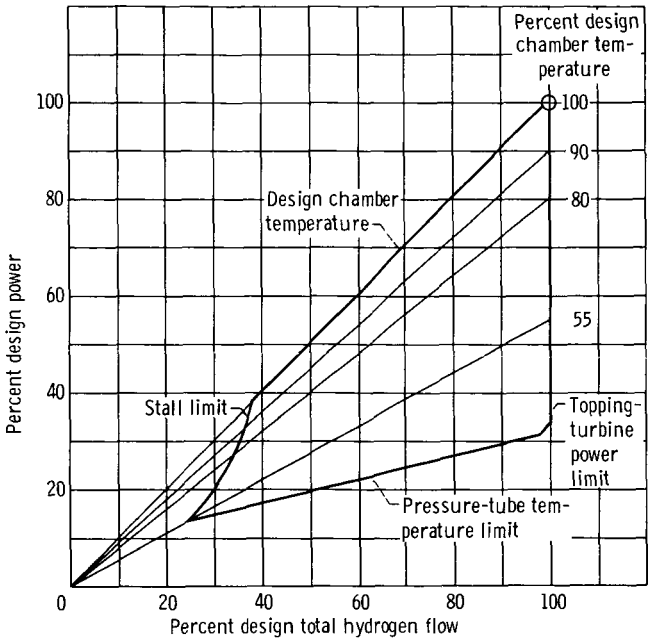

Figure 10. - Operating envelope of heat-exchanger-bypass configuration. Operating conditions: poison reactivity fixed at 100-percent design-point value; water pump turbine valves fixed at 100-percent design point; bleed turbine valves combined as flow-splitter valve.

The effect of bypassing hydrogen around the heat exchanger is to increase the bulk water temperature. Eventually, the pressure-tube-temperature limit is reached. This temperature limit could be increased by changing the material of the pressure tubes; however, neutronic considerations in the core could prohibit this. Other possible alternatives would be to increase the heat-exchanger effectiveness by increasing its length or using a counterflow technique. Although these alternatives tend to produce water freezing, they are feasible since the margin from heat-exchanger icing is larger than the pressure-tube-temperature margin.

As stated earlier, poison reactivity was held fixed throughout the steady-state mapping. With poison reactivity fixed, an increase in heat-exchanger hydrogen bypass flow produces an increase in water temperature. This temperature increase, in turn, produces a decrease in core reactivity through the negative water temperature reactivity and in reactor power. The map shows that not only does heat-exchanger bypass eliminate icing, but is also an effective means for reactor power control. Control of this configuration can be effected by manipulation of only the TTBV (to control hydrogen flow) and HXSV (to control reactor power) with no loss in system flexibility. Poison control could then be relegated to gross changes in reactor power. This differs from the preliminary reference design in which poison reactivity was used to control reactor power.

Steady-state operation below about 24-percent hydrogen flow and 13-percent reactor power is not possible because of intersecting stall and pressure-tube-temperature limits.

However, this operating point is substantially below the lowest steady-state operating point of the preliminary reference design.

Transient Performance

Transient tests were conducted on this configuration with the BTTV and BTBV set to match hydrogen pump-stall margins at 35-percent total hydrogen flow and reactor power. These valves were held fixed during the transients. All other bleed subsystem valves were fixed at their 100-percent design-point positions. Total hydrogen flow was controlled through a closed-loop control around the TTBV. Poison reactivity was held fixed so that reactor power varied as a function of HXSV position. A hydrogen flow increase transient from 40 to 100 percent of design value produced by ramping the flow demand in 1 second with the HXSV held fixed to produce an initial hydrogen heat-exchanger-bypass flow of 16 percent did not encounter any system limit except for the pressure-tube temperature. Hydrogen flow increased much faster than reactor power. Although a leading hydrogen flow tends to produce a freezing condition in the heat exchanger, the bypass flow effect reduced this tendency.

A hydrogen flow decrease transient from 100 to 40 percent produced results similar to the preliminary reference-design configuration. A typical transient is presented in figure 11 where system variables are shown as functions of time. This transient was made by ramping the hydrogen flow reference from 100 to 40 percent in 8 seconds and stepping the heat-exchanger-bypass flow fraction from 25 to 50 percent in anticipation of an overtemperature condition. The pressure-tube temperature was initially over its limit because of the initial heat-exchanger bypass.

The thrust chamber and nozzle-coolant-tube temperatures went over their respective limits. The pressure-tube temperature increased approximately 35° R (19.4° K) over and above its initial overtemperature. Both pumps approached but did not enter stall. Hydrogen flow decreased faster than reactor power; thus, overtemperature could be expected. Subsequent transients showed that by increasing the bypass-flow-fraction step to 70 percent overtemperatures could be eliminated. This larger step in bypass flow fraction effectively increased the negative reactivity of the water and produced a faster reactor power reduction.

From these transients, it was concluded that the heat-exchanger-bypass configuration is capable of reasonably fast flow modulations between 40- and 100-percent flow through control of only hydrogen flow and the heat-exchanger-bypass flow fraction with all-bleed subsystem valves and poison reactivity held fixed. The pressure-tube-temperature problem indicates that the heat exchanger effectiveness must be optimized to provide suitable margins from heat exchanger icing and pressure tube overtemperature during heat-exchanger-bypass operation.

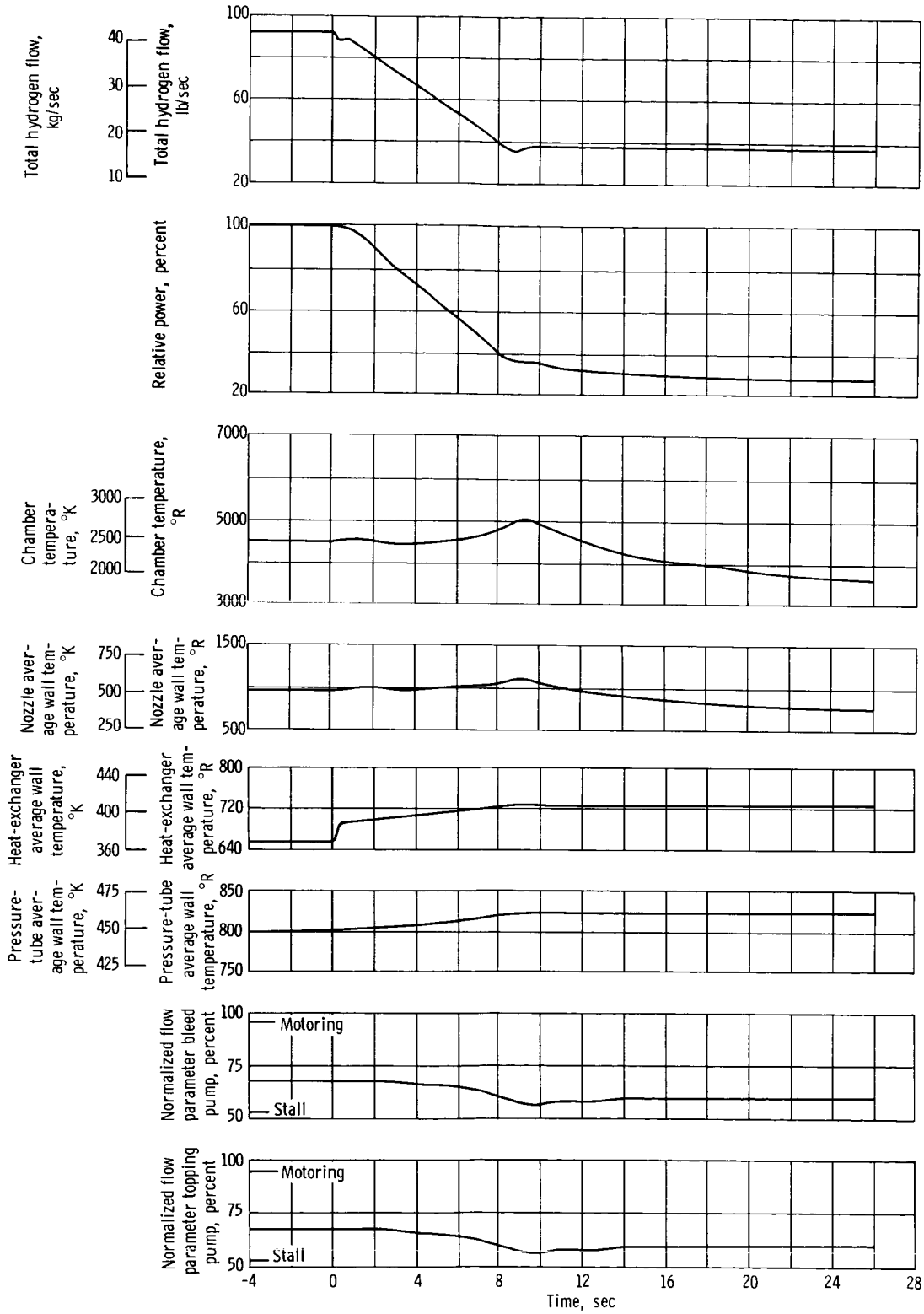

Figure 11. - Flow decrease transient of heat-exchanger-bypass configuration.

NOZZLE-HEAT-EXCHANGER-BYPASS CONFIGURATION

The nozzle-heat-exchanger hydrogen-bypass configuration (NHXBV) eliminates the need for a large heat-exchanger hydrogen-bypass valve because of the large pressure drop in the nozzle coolant passages, as discussed in the section System Modifications.

Steady-State Performance

Steady-state performance of the nozzle-heat-exchanger-bypass configuration was mapped holding poison reactivity constant at the 100-percent design-point value obtained with zero heat-exchanger-bypass flow. The only controlling elements were the TTBV and NHXBV. The operating envelope is shown in figure 12. The lower boundary of reactor power is formed by both pressure-tube overtemperature and maximum NHXBV opening at approximately 40 percent of design chamber temperature. The pressure-tube-temperature limit has approximately the same limiting effect as in the previous configuration. However, the NHXBV flow capacity limits operation even before toppping-turbine power becomes insufficient because of the valve size used and the maximum pressure differential obtainable across the nozzle coolant tubes. If, as in the previous configuration, a flow-splitter valve had been used, the bypass limit would be removed and replaced by the pressure-tube-temperature and topping-turbine-power limits.

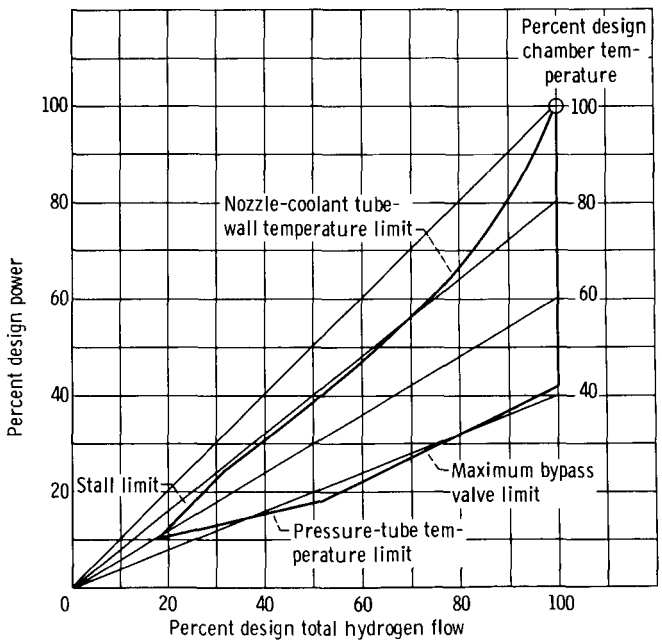

Figure 12. - Operating envelope of nozzle - heat-exchanger-bypass configuration. Operating conditions: poison reactivity fixed at 100-percent design point; water turbine valves mixed at 100-percent design-point positions; bleed turbine valves combined as flow-splitter valve; pump stall margins matched.

The stall limit is significantly lower than that for the preliminary reference design, particularly as bypass flow is increased. The large heat-exchanger-bypass flow is not subject to high nozzle-coolant-tube impedance. Therefore, the overall system operating impedance is lowered, and a lower stall limit results. The stall and pressure-tube-temperature limits intersect, but at a lower hydrogen flow and reactor power level than for the preliminary reference design primarily because of the lower stall limit.

The most significant aspect of the map is the upper operating envelope limit. The upper limit of reactor power is determined by a minimum hydrogen bypass flow governed by the nozzle-coolant-tube-temperature limit. Only 80 percent of design chamber temperature is obtainable up to about 70-percent hydrogen flow. A lower bypass flow fraction (higher nozzle-heat-exchanger flow) at each hydrogen flow level would cause the nozzle-tube-temperature limit to be exceeded. This is caused by the steady-state effect of heat-exchanger-bypass flow on reactor power through the bulk water temperature. For higher bypass flow fractions (lower nozzle-heat-exchanger flow), the reduction in power caused by increased water temperature more than offsets the heating effect of decreased nozzle coolant flow on the nozzle tubes. The nozzle-tube-temperature limit could be avoided by changing poison reactivity.

Another interesting result is that the 100-percent design value of poison reactivity is the only value that allows operation at the design point. A lower poison reactivity will not allow design chamber temperature even at zero heat-exchanger bypass. A higher poison reactivity will also not allow design chamber temperature. For if a higher poison reactivity is introduced, heat-exchanger bypass must be increased to prevent reactor power from exceeding its design value; however, a nozzle-coolant-tube overtemperature would result. Therefore, operation at the design point is not possible with other than design-point poison reactivity.

Transient Performance

Transient tests were conducted on this configuration to evaluate both flow and reactor power transients over the operating range. Poison reactivity was held fixed to provide design chamber temperature at 100-percent hydrogen flow with zero nozzle-heat-exchanger bypass. Reactor power varied as a function of the bypass flow fraction and inherent feedback reactivities. The WTTV and WTBV were fixed at their 100-percent design values. The BTTV and BTBV were also fixed at a position which matched the pump-stall margins at 40-percent hydrogen flow at design chamber temperature. A control loop around the TTBV was used to control total hydrogen flow.

Reactor power transients were conducted at 100- and 40-percent flow primarily to evaluate nozzle-coolant-tube-wall-temperature transients. The transient at 100-percent

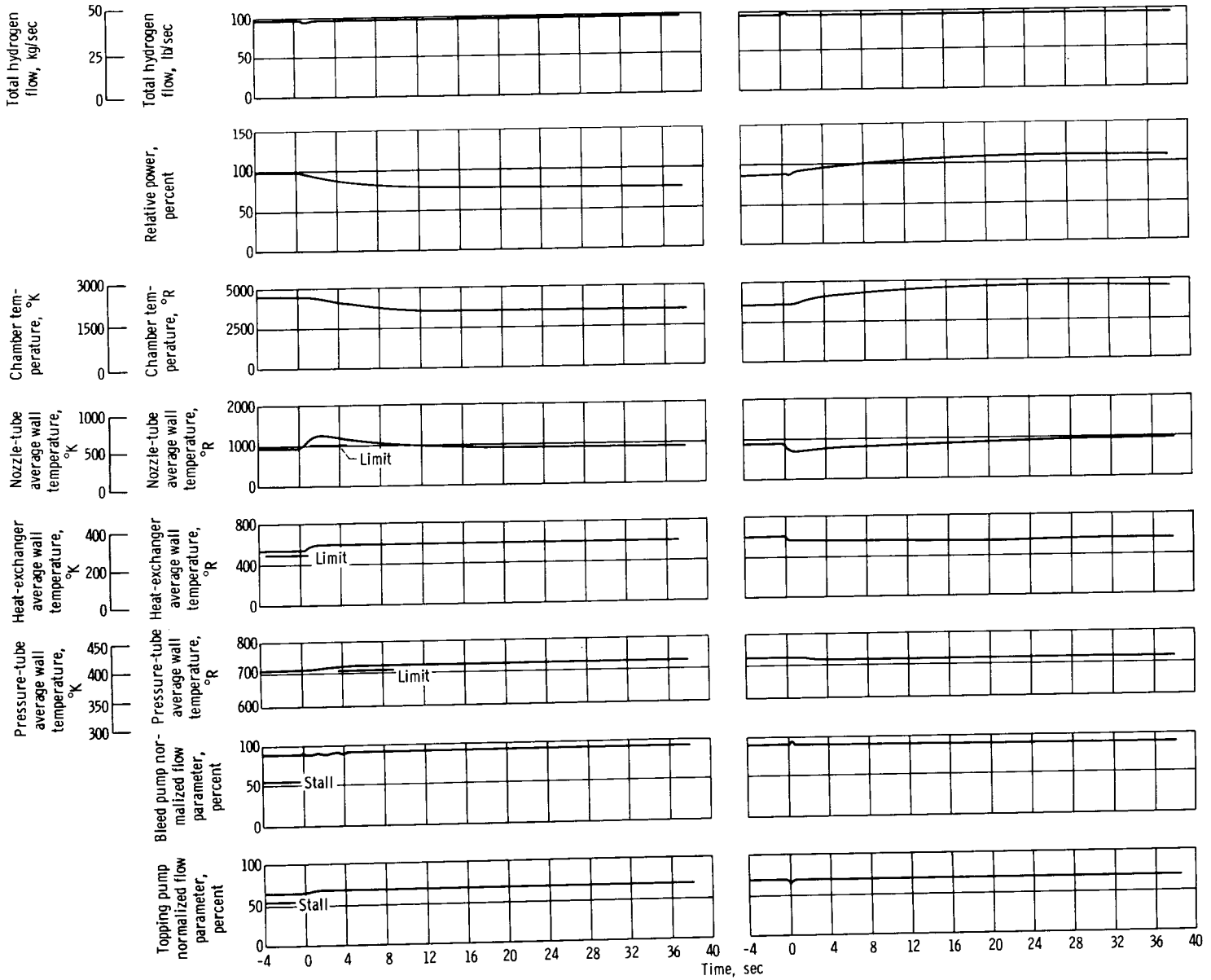

(a) Bypass valve opened.

(b) Bypass valve closed.

Figure 13. - Reactor power transient performance of nozzle - heat-exchanger-bypass configuration.

flow is shown in figure 13 where system variables are given as functions of time. The transient was made by ramping the NHXBV to a 20-percent open area position in 1 second resulting in a heat-exchanger-bypass flow fraction of 34.5 percent. The reactor power dropped to 79 percent while the average nozzle-tube temperature reached a peak of about 1200° R (667° K). The initial value was 950° R (528° K) and the final steady-state value was 875° R (486° K). Thus, even though the steady-state value was below the nozzle-coolant-tube-temperature limit of 965° R (536° K), the transient produced by changing the NHXBV with fixed poison reactivity results in rapid nozzle-coolant-tube-wall-temperature increases. Reactor power reacts slowly to changes in heat-exchanger-bypass flow since the slow dynamic effect of water temperature is in series between them. On the other hand, the response of nozzle-coolant-tube temperature to bypass flow is much faster.

After steady-state conditions were reached, the NHXBV was stepped closed, raising the reactor power to its initial value. No nozzle-tube overtemperature occurred during the reactor power increase transient. Similar results were observed in the power transient at 40-percent hydrogen flow.

Flow transients were conducted between 40- and 100-percent hydrogen flow with constant NHXBV positions. In the flow increase transient from 40 to 100 percent, initial reactor power was set at the maximum value permitted without exceeding the nozzle-coolant-tube-wall-temperature limit through use of the NHXBV. The reference total hydrogen flow was ramped from 40 to 100 percent in 1 second. No system limits were encountered during the transient. Because of the relatively high resulting bypass flow, reactor power and chamber temperature increased to final values of only about 80 percent of design.

A flow decrease transient was made from 100 to 40 percent of total hydrogen flow. The initial conditions were the same as the final conditions of the flow increase transient. In this case, the total hydrogen flow demand was ramped from 100 to 40 percent in 5.5 seconds. The results are shown in the time traces of figure 14. The nozzle-tube temperature peaked at 450° R (250° K) overtemperature and remained over temperature for 20 seconds. The chamber temperature and bleed-pump stall limits were approached but not reached.

In general, it may be concluded that a reactor power decrease transient produced by NHXBV control with constant poison reactivity will result in rapid nozzle-coolant-tube overtemperature because of the reduced coolant flow. Changing poison reactivity to decrease reactor power would not have caused this condition. Flow increase transients can be accomplished quite rapidly without changing poison concentration. Flow decreases, however, will require poison control to prevent overtemperatures in the nozzle-coolant-tube wall.

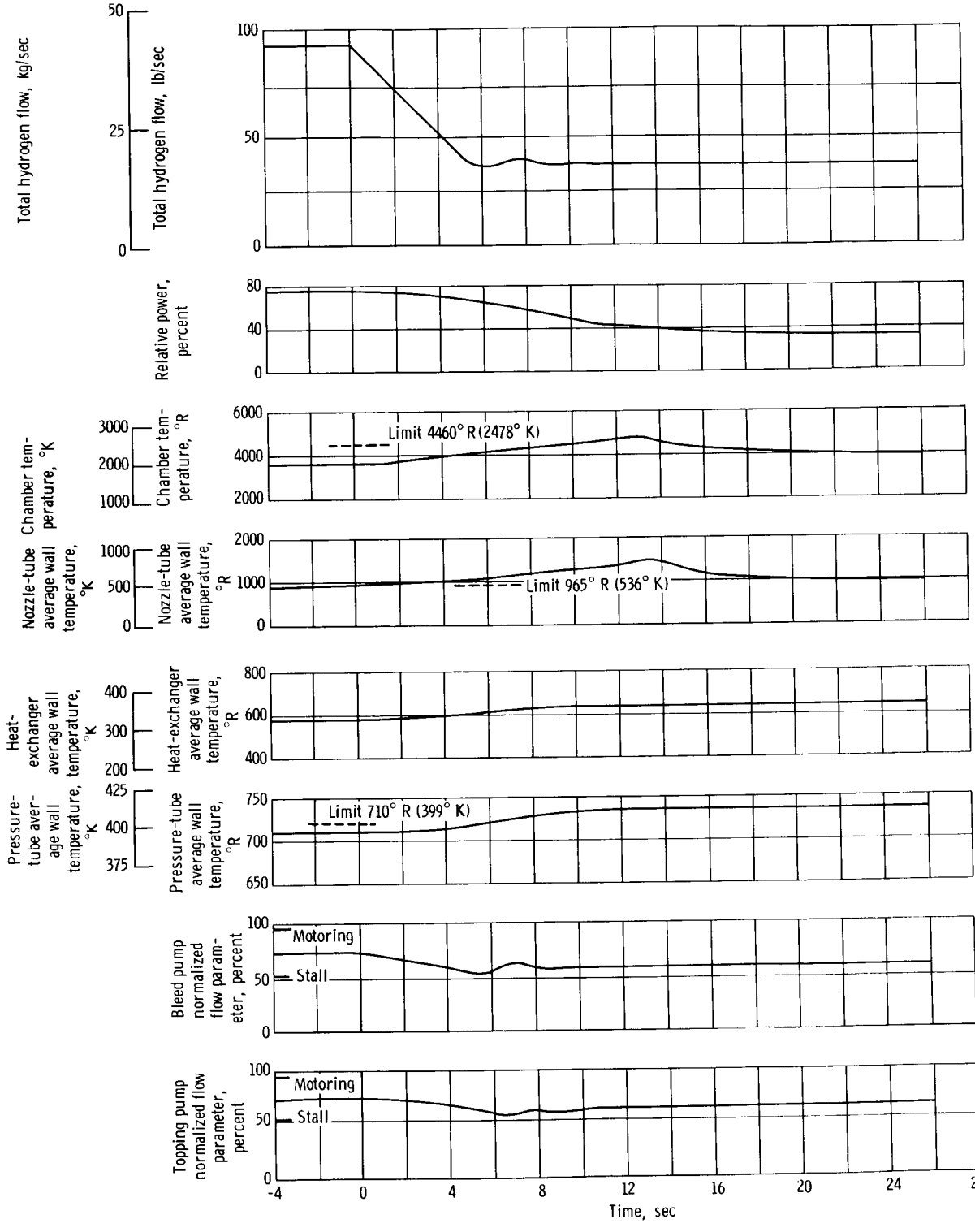

Figure 14. - Flow decrease transient of nozzle - heat-exchanger-bypass configuration.

Heat-Exchanger - Topping-Turbine-Bypass Configuration

The heat-exchanger - topping-turbine-bypass configuration was not evaluated by using the simulation models. Estimates of general performance were made based on the results of the other configurations.

A prominent characteristic of this configuration is that total hydrogen flow and bulk water temperature are uniquely related because the bypass flow is common to both the heat exchanger and topping-turbine bypasses. However, the necessary relation between these flows required for proper operation of the system does exist; that is, a low bypass flow will produce both a high total hydrogen flow and reactor power. A high bypass flow will produce the opposite effect. The rate of change of reactor power with respect to a change in total hydrogen flow, which results from bypass changes, will determine whether water freezing or component overtemperature is a problem. Results of the other configurations indicate that the rate would tend to produce freezing. Therefore, poison control would be necessary to maintain a maximum chamber temperature.

A certain amount of bypass is required for the topping turbine at the design point to provide a control margin. Since the heat exchanger will also experience this bypass, the water temperature will be higher and produce a more negative reactivity. To operate at the design point then, the contribution of poison reactivity to the net reactivity must be increased. Alternatives include changing core criticality or increasing heat-exchanger effectiveness.

In summary, the heat-exchanger - topping-turbine configuration could probably be operated satisfactorily over the required flow range with a poison control system. There appears, however, to be no advantage to this configuration over the heat-exchanger-bypass configuration especially since flexibility is considerably reduced and control complexity increased.

TOPPING-CYCLE CONFIGURATION

Although the preliminary reference-design configuration is capable of all-topping operation, an independent topping-cycle design study was made using a new multistage axial-flow hydrogen pump driven by a one-stage impulse turbine. The water turbopump was the same as for the preliminary reference-design configuration. Pump and turbine performance curves were developed and a preliminary component matching study conducted to determine main-stage operating conditions. The reactor was the same as that used for the preliminary reference design except that the bleed reentrant fuel elements were eliminated. A heat-exchanger flow-splitter valve (HXSV) was used based on the results of the split-feed configurations. A detailed account of the analysis is presented in reference 4.

With this configuration, only three system control elements were required: the TTBV controlled hydrogen flow; the HXSV, the bypass fraction; and poison, the reactor power level or chamber temperature. With the parallel topping and water pump turbines, the TTBV valve acts as a bypass for the water-pump turbine also. An orifice replaced the WTTV used in the split-feed configurations.

Steady-State Performance

To obtain the steady-state operating map, the poison reactivity was held fixed at the value required to attain 100-percent design hydrogen flow and reactor power with a 25-percent bypass fraction. The water-pump turbine was throttled by an orifice fixed to provide 1140 pounds per second (517 kg/sec) water flow at the 100-percent design point. Hydrogen flow was held fixed by a closed-loop control around the TTBV. Reactor power was changed by varying the heat-exchanger-bypass fraction with the HXSV. The results of the mapping are presented in figure 15.

The upper limit on reactor power is governed by design chamber temperature (nozzle-tube-temperature limit is 1 percent higher) above 17 percent flow and by stall below that flow. The lower limit on reactor power was determined by the topping-turbine power limit which occurred at about the same level as for the other configurations. Because of the different pump design, stall occurred at a lower level.

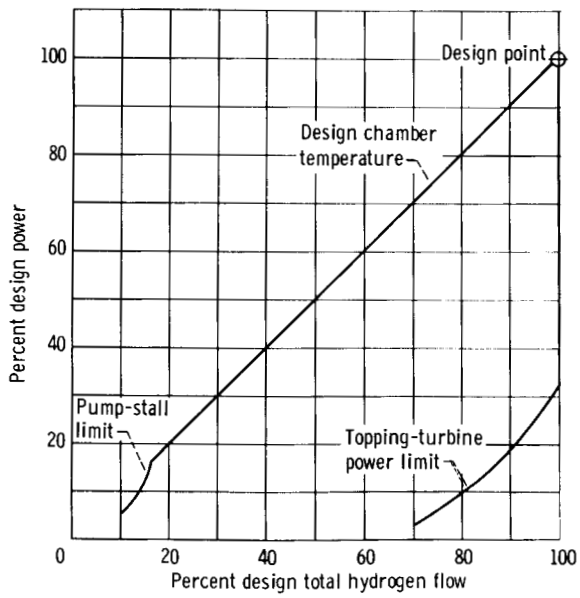

Figure 15. - Operating envelope of topping-cycle configuration with heat-exchanger bypass. Operating conditions: poison reactivity fixed at value corresponding to 25-percent bypass at 100-percent design point; water turbine throttled with fixed orifice.

Two effects noticed in the mapping but not shown here are of interest. To maintain a constant chamber temperature, only about 7 percent variation in heat-exchanger bypass was required. Also, water flow was essentially proportional to the hydrogen flow as in the preliminary reference design with a variable WTTV. This relation differs considerably from the split-feed designs with fixed WTTV where water flow is proportional to hydrogen flow to a power greater than 1. The difference is attributed to the different turbine and valving arrangements.

It must be pointed out here that the split-feed and topping-cycle designs do not represent comparable systems. The components in the split-feed configurations were not designed for full topping-cycle operation. For instance, the pressure-tube-temperature limit was exceeded for all points within the envelope because of the combination of poison concentration and bypass fraction used at the design point. The topping-cycle design only serves to show that such a system can be as flexible as a split-feed configuration and yet be considerably simpler.

Transient Performance

Flow transients were conducted between 40- and 100-percent flow through manipulation of the flow reference on the closed-loop control around the TTBV. During the transients, poison reactivity was held fixed so that reactor power level varied as a function of heat-exchanger-hydrogen-bypass fraction.

Flow increase transients from 40- to 100-percent flow showed that, as in the split-feed configurations, hydrogen flow responded faster than reactor power. Thus, no system limits were encountered except for the pressure-tube limit, as explained in the section Steady-State Performance.

The results of a flow decrease transient from 100- to 40-percent flow are shown in figure 16. Initially, hydrogen flow, chamber temperature, and reactor power were at 100 percent. Poison reactivity was held fixed, and the HXSV was open to 33.4 percent of its maximum area. The hydrogen flow reference was ramped from 100 to 40 percent in 8 seconds. When the flow ramp was initiated, the HXSV was stepped open to 77.5 percent of its maximum area in order to obtain an initial reactor power reduction and in anticipation of a chamber overtemperature condition, as experienced by the split-feed configurations. The figure shows that this technique was effective since no chamber overtemperature was encountered. At initiation of the ramp, a small perturbation in hydrogen flow, caused by the momentary increase of system flow resistance of high flow through the HXSV, resulted in a momentary increase in nozzle-coolant-tube-wall and chamber temperatures. The pressure-tube-temperature limit was again exceeded.

As in the case of the split-feed configurations without poison reactivity control, fast

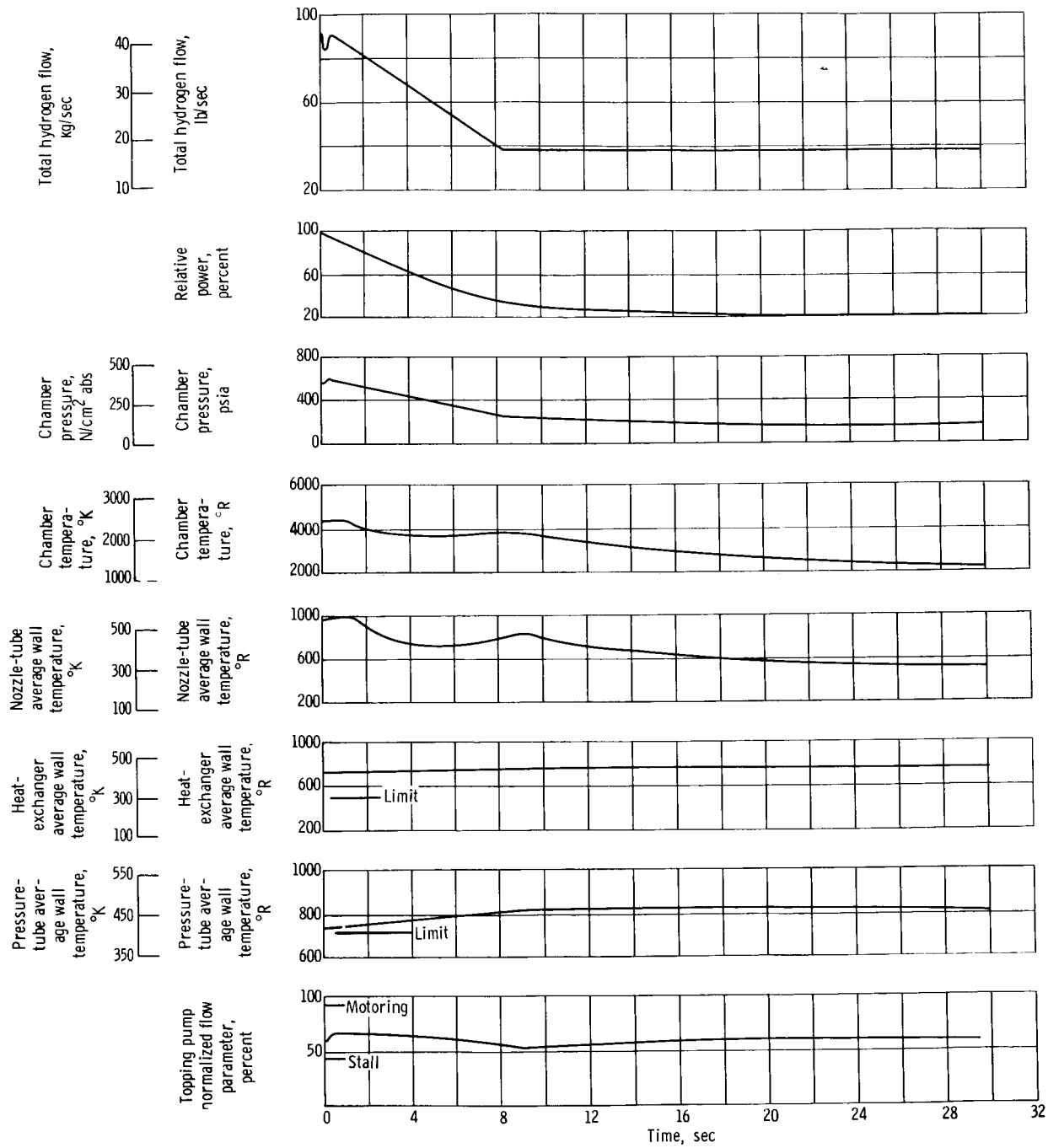

Figure 16. - Flow decrease transient of topping-cycle configuration.

hydrogen flow decrease transients produce overtemperature conditions because of the inability of reactor power to decrease rapidly enough to prevent overtemperatures during a rapid hydrogen flow reduction. The use of poison to change reactivity can probably increase the rate of flow reduction by effecting a faster change in reactor power.

CONCLUSIONS AND RECOMMENDATIONS

A comparison of the qualitative results was made based on system simplicity, system flexibility, control simplicity, and performance. The comparison is discussed, and some recommendations are made.

System Simplicity

The topping-cycle configuration is the simplest system investigated because the bleed hydrogen reentrant tubes and associated bleed subsystem is absent. The split-feed configurations using variations of heat-exchanger bypass are all comparable to each other with respect to complexity. They are, however, more complex than the preliminary reference design since they each require an additional valve (NHSBV or HXSV).

System Flexibility

All configurations are superior to the preliminary reference design in flexibility. This superiority is easily seen in comparing the size of the operating envelopes. The heat-exchanger - topping-turbine-bypass configuration has the least advantage of the bypass designs because independent control of bypass flow and total hydrogen flow is not possible. The nozzle-heat-exchanger-bypass configuration is restricted to zero bypass at the 100-percent design point because of the nozzle-coolant-tube-overtemperature limit. The heat-exchanger-bypass and topping-cycle configurations have the most flexibility as reflected in their large operating envelopes.

Control Simplicity

The preliminary reference design would undoubtedly require a fine controllable poison system as would the nozzle-heat-exchanger and heat-exchanger topping-turbine-bypass configurations. The other two designs can control chamber temperature at the

design point and perform hydrogen flow modulation without fine poison control. The topping-cycle design is simpler in that no bleed system control or programming is required.

System Performance

With respect to system performance, the nozzle-heat-exchanger and heat-exchanger - topping-turbine-bypass configurations will probably require a larger chamber temperature tolerance at the design point using the on-off poison control. The heat-exchanger-bypass and topping-cycle configurations can probably hold closer tolerances through control of the heat-exchanger bypass. Also, more rapid hydrogen flow transients can probably be accomplished with these designs because of the larger range capability of poison control. Rapid hydrogen flow transients can be made possible through heat-exchanger-bypass flow control to guard against water-loop-temperature limits. The topping-cycle configuration has the widest hydrogen flow capability at maximum chamber temperature.

Conclusions

Based on the system evaluation presented, the topping cycle is superior to the other configurations. While the all-topping cycle is simple and efficient at the particular reactor power and chamber temperature conditions used in this study, it has poor uprating potential, since, for a given reactor, an all-topping cycle is chamber-pressure limited. Also, higher pump heads would require heavier thrust nozzles. Because of the superior chamber pressure uprating potential of the split-feed cycle, the heat-exchanger-bypass configuration was selected for further study.

Two design changes within the heat-exchanger-bypass configuration were also indicated. Performance of the heat-exchanger-bypass configuration results in operation close to the pressure-tube-temperature limit. Because a material change in the core is probably not permissible because of neutronic considerations, lengthening the heat exchanger is required to decrease the water temperature and provide a larger margin to the the pressure-tube-temperature limit. The results also indicated that the water flow should be increased to as high a value as possible within the capability of the water turbopump and bleed hydrogen flow designs. With these changes the pressure-tube temperature would be further reduced and the water-loop thermal response would be improved.

REFERENCE-DESIGN CONFIGURATION

Based on the comparative analysis of the preliminary reference design and its modified configurations, the heat-exchanger-bypass configuration was chosen for futher analysis. This configuration with the recommended design changes was designated the reference design. The design changes incorporated were a 12-percent increase in heat-exchanger length and an increase in water flow from 1040 to 1200 pounds per second (472 to 544 kg/sec). The system was remapped for steady-state performance and a transient chilldown optimization made.

Design Changes

Steady-state mapping was performed to determine the heat-exchanger length required to lower the water temperature and to determine a suitable design-point heat-exchanger-bypass flow fraction.

Effect of heat-exchanger length. - The effect of increased heat-exchanger length and water flow on water temperature, was investigated at the 100-percent design point for zero heat-exchanger bypass. Runs were made at a 1040 pounds per second (472 kg/sec) water flow with no increase in heat exchanger length, and at 1200 pounds per second (544 kg/sec) water flow with 11-, 12-, and 13-percent increases in heat-exchanger length. The exit-heat-exchanger-wall temperatures were 540°, 501°, 498°, and 494° R (300°, 278°, 277°, and 274° K), respectively. A length increase of 12 percent was chosen to decrease the water-loop temperatures as much as possible but with a reasonable margin from freezing.

Effect of heat-exchanger-bypass flow. - The effect of heat-exchanger-bypass flow on heat-exchanger and pressure-tube-wall temperatures is shown in figure 17. The data were obtained at 100-percent design chamber temperature for 100- and 41-percent total hydrogen flows with water flows of 1200 and 785 pounds per second (544 and 356 kg/sec), respectively. The difference between each component temperature and its limit is given as a function of heat-exchanger hydrogen bypass flow.

The heat-exchanger-temperature margin increases and the pressure-tube-temperature margin decreases with increasing heat-exchanger-bypass flow. The temperature margins are greater for the 41-percent than for the 100-percent level. This greater margin is a result primarily of the fact that water flow decreases proportionally less than reactor power as total hydrogen flow is reduced. Because of this, the difference between the maximum and minimum temperatures in the water system decreases, and larger temperature margins result.

The optimum bypass fraction at 100-percent total hydrogen flow level occurs at

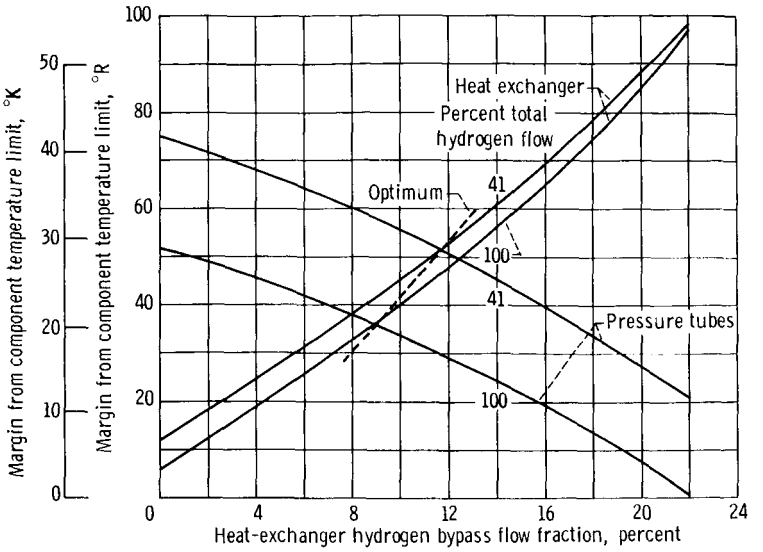

Figure 17. - Effect of heat-exchanger bypass flow on heat-exchanger and pressure-tube temperatures.

9 percent and increases to 11.7 percent at the 41-percent hydrogen level. Since larger heat-exchanger-bypass fractions are required at lower power levels, the pressure-tube temperature will generally increase. Therefore, a nominal heat-exchanger bypass at the design point should be chosen below the optimum to give the pressure-tube temperature a larger initial margin. A bypass fraction of 8 percent was chosen as a basis for further steady-state mapping. This value will also provide a control margin at the design point.

Steady-State Performance

Before the reference design was mapped with the design changes to determine its operating region, a control takeover (CTO) point was established at approximately 30-percent total hydrogen flow and 12-percent design reactor power, which corresponds to a chamber pressure of 112.5 psia (77.6 N/cm^2 abs) and a chamber temperature of 1750° R (972° K). The CTO point is defined as the point above which primary control loops are closed and required to follow a demand signal. Choice of the CTO point was based on a minimum hydrogen flow and reactor power level at fixed poison reactivity which provides a sufficient margin between pump-stall and pressure-tube-temperature limits. Minimum hydrogen flow is also considered with respect to thermal response of chamber temperature instrumentation.

At the CTO point, the pump-stall margins were matched and the resulting BTTV and BTBV positions were held fixed. The WTTV and WTBV positions were set at the design point to produce a water flow of 1200 pounds per second (544 kg/sec) and a bleed- to total-

hydrogen flow ratio of 2.6 percent. Poison reactivity was fixed at a value which gave 100-percent chamber temperature at 100-percent total hydrogen flow with 8-percent heat-exchanger bypass. Reactor power was regulated by the HXSV. The resulting operating envelope of the reference design is shown in figure 18 where percent reactor power is plotted against percent total hydrogen flow.

The upper boundary of the operating region is governed by design chamber temperature from 100- to 42-percent total hydrogen flow. The nozzle-coolant-tube-temperature limit is reached, as in the heat-exchanger-bypass configuration, when the chamber temperature is increased 1 percent. Below 42-percent flow, pump stall determines the upper limit on reactor power.

From 100- to 78-percent flow, the lower limit on reactor power is governed by insufficient topping-turbine power. This boundary occurs at a higher level than it does for the heat-exchanger-bypass configuration (p. 42) because of a higher topping-pump loading, and consequently, a higher topping-turbine loading, in the reference-design configuration. The balance of the lower boundary, from 78- to 26-percent hydrogen flow, is governed by the pressure-tube-temperature limit. Reactor power cannot be further reduced by increasing the heat-exchanger hydrogen bypass flow.

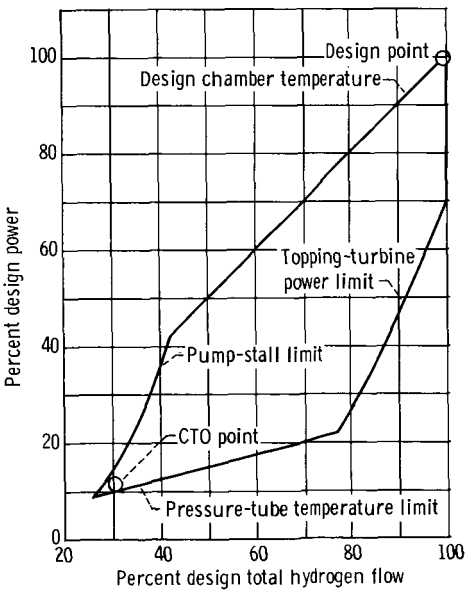

Figure 18. - Operating envelope of reference-design configuration. Operating conditions: poison reactivity fixed at 100 percent design value; WTTV and WTBV fixed at design-point values to provide water flow of 1200 pounds per second (544 kg/sec); BTTV and BTBV fixed to match stall margins at CTO point; heat-exchanger length increased 12 percent; 8 percent heat-exchanger hydrogen bypass at design point.

The stall and pressure-tube-temperature limits intersect at 26-percent hydrogen flow and 9-percent reactor power. Below this hydrogen flow, poison reactivity must be varied to prevent system limits from being exceeded. Additional mapping results for the reference-design configuration are presented in reference 5.

Transient Performance

The transient performance of the reference design in the power range of operation is similar to that of the heat-exchanger-bypass configuration (p. 42) except for the water temperatures. The different water temperatures are the result of the heat-exchanger length and water flow design changes that were included in the reference design.

Initial startup studies, which include chilldown and bootstrap, were performed by using the digital-simulation model to develop a procedure which would bring the system from zero hydrogen flow and source reactor power level condition to the CTO point without encountering system operational limits. The CTO point was at 12-percent reactor power and 30-percent total hydrogen flow. The valve positions corresponding to this operating point, as obtained from the analog model steady-state mapping, are as follows: TTTV, 100 percent; TTBV, 57.5 percent; HXSV, 78.7 percent; BTTV, 46.2 percent. The startup studies included effects of initial conditions, initial bootstrap programming, and optimization of valve and reactor power programming.

Effects of initial conditions. - The first step in making the chilldown runs was to obtain a set of initial conditions for various heat-exchanger-bypass flow fractions and system temperatures. Initial total hydrogen flow was set at 0.5 pound per second (0.23 kg/sec) by the MPV. The pump speeds and water flow were also held at 10 rpm and 100 pounds per second (45.4 kg/sec), respectively. To ensure that the initial temperatures would stay constant, their corresponding wall thermal capacitances were increased by 10^{12}, only for the initial condition runs. Initial conditions were obtained for the heat-exchanger-bypass fractions, water temperatures, and core temperatures given in table III. In each case, the heat-exchanger, pressure-tube, and side-reflector wall temperatures were assumed equal to the water temperature.

Starting with the initial conditions produced, 5- to 20-second-duration chilldown runs were made. All valves with the exception of the MPV were held in fixed positions; the TTTV and BTTV were closed, and the WTTV was wide open. The MPV was programmed open in 1 second. The opening rate of the MPV was simulated as a function of time cubed. Runs were made at different fixed reactor power levels including 0, 0.1, and 1 percent. Results of all the runs are also summarized in table III using conditions at the end of 5 seconds as a basis for comparison. A comparison of the runs shows that initial water temperature has the largest effect on the heat-exchanger-wall temperature. Increased

TABLE III. - SUMMARY OF DIGITAL-MODEL CHILLDOWN RUNS

Heat-exchanger bypass, percent	Initial conditions					Conditions at end of 5 sec											
	Water temperature		Core-wall temperature		Power, percent	Feedline flow		Power, percent	Poison reactivity, $	Core-wall temperature				Heat-exchanger wall temperature			
						lb/sec	kg/sec			Minimum		Average		Minimum		Average	
	°R	°K	°R	°K						°R	°K	°R	°K	°R	°K	°R	°K
[a]50	530	294	530	294	0.01	4.81	2.18	0.01	-3.85	331.8	184.3	443.0	246.1	491.7	273.2	498.5	276.9
[a]75	530	294	530	294	.01	5.37	2.44	.01	-3.89	282.5	156.9	409.2	227.3	510.6	283.7	513.8	285.4
[a]75	610	339	610	339	.01	5.23	2.37	.01	-3.38	294.6	163.7	418.9	232.7	592.9	329.4	596.3	331.3
[a]75	680	378	680	378	.01	5.13	2.33	.01	-2.44	303.2	168.4	424.9	236.1	662.4	334.7	666.3	370.2
[a]75	530	294	530	294	.1	5.27	2.39	.1	-3.82	297.8	165.4	455.0	252.8	511.1	283.9	514.2	285.7
[a]75	530	294	530	294	1.0	4.29	1.95	1.0	-3.14	486.4	270.2	933.0	518.3	515.8	286.6	518.2	287.9
[a]90	530	294	530	294	.01	5.82	2.64	.01	-3.93	239.4	133.0	375.4	208.6	521.4	289.7	522.8	290.4
[a]90	700	389	1000	556	.1	3.58	1.62	.17	-1.12	568.5	315.8	897.0	498.3	693.7	385.4	695.1	386.2
[a]90	700	389	1610	894	.1	3.26	1.48	.18	-.80	731.2	406.2	1295.0	719.4	701.6	389.8	702.6	390.3
[a]90	600	333	1000	556	.1	4.02	1.82	.45	-3.00	547.0	303.9	890.0	494.4	585.5	325.3	588.2	326.8
[b]90	600	333	1000	556	.1	4.00	1.81	.45	-3.00	552.0	306.7	976.0	542.2	585.6	325.3	587.0	326.1
[c]90	600	333	1000	556	.1	2.94	1.33	.45	-2.85	713.0	396.1	1050.0	583.3	584.8	324.9	587.0	326.1

[a]Main propellant valve programmed to open in 1 sec.
[b]Main propellant valve programmed to open in 5 sec.
[c]Main propellant valve programmed to open in 50 sec.

initial water temperature produces higher wall temperatures. The effects of initial reactor power and heat-exchanger-bypass fraction are also apparent but to a lesser degree. The effect of initial reactor power on core-wall temperatures is also quite evident. As the initial power level is raised, the core wall responds accordingly. Consideration of the core-wall temperatures shows the extreme cooling effect of the cold hydrogen, particularly on the first section of the core. Temperatures in this section range from about 720° to 240° R (400° to 133° K) and are as much as 1200° R (667° K) below the minimum allowable fuel-element temperature. The last three runs listed show a comparison of various MPV opening rates which were investigated to alleviate the low-core-temperature problem. The data indicate only a slight advantage in extending chilldown at slow rates.

Initial bootstrap. - The chilldown runs were extended to simulate bootstrap operation. The primary purpose of this portion of the study was to investigate general reactor power and valve programming which would bring the system to a CTO condition. A successful program is one in which pump stall, heat-exchanger icing, and low core temperatures do not occur. Bootstrap runs were made with the TTTV, BTTV, and reactor power programmed at different rates to reach the CTO point.

Results of this series of runs led to the conclusions that a TTTV is necessary to prevent topping pump stall during initial bootstrap; the bleed subsystem valves could be preset; the pumps should be prechilled to lessen the probability of pump stall; reactor power should be increased with the TTTV opening to prevent heat-exchanger icing; icing in the heat exchanger would be no problem with 90-percent heat-exchanger-bypass flow; and a core-wall temperature of less than 1000° R (556° K) was required to prevent pump stall during initial bootstrap.

Programming optimization. - As a result of the chilldown-bootstrap studies, the following ground rules were established for optimization of valve and reactor power programming: core-wall temperatures were initialized at 1000° R (556° K); core-wall temperatures are to be maintained as high as possible during startup to the CTO point; and light pump stall for short durations is acceptable.

To find the best valve programming to the CTO point that satisfied the ground rules, a series of three startup runs was made where the core walls were fictitiously held constant at 1000° R (556° K) to eliminate finding a reactor power program to keep this temperature. The startup procedure for the runs was to open the MPV, wait for chilldown, and program open the turbine-throttle valves. The BTTV was programmed to open to 15, 33, and 50 percent for the three runs to cover a range of pump-power-split ratios. If the pumps were not in stall at the end of the throttle-valve programming, the TTBV was programmed to its CTO point value. For all three runs, reactor power was ramped at 0.1 percent per second and the HXSV was held fixed. The results of these runs are discussed in reference 5.

On the basis of these runs, the startup procedure from initiation of chilldown to the CTO point was as follows:

(1) Initialize reactor power at 0.1 percent.

(2) Preset HXSV to 78.7 percent open.

(3) Initialize TTTV and BTTV at zero percent, TTBV at 100 percent open.

(4) Open MPV and increase reactor power at approximately 0.13 decade per second and permit 5 seconds of chilldown.

(5) After chilldown, open TTV at 20 percent per second to 100 percent open, open BTTV at 9.24 percent per second to 46.2 percent open, and continue reactor power increase at 0.13 decade per second to 2.0 percent reactor power.

(6) When throttle valves are open, close the TTBV to 57.5 percent and continue reactor power increase at 0.06 decade per second.

After approximately 25 seconds, the system should be at or near the CTO point.

REFERENCE-DESIGN CONTROL SYSTEM

A control analysis was performed on the reference-design configuration. The selected control system is described and its operation discussed. An alternate control system is also presented. An evaluation of the control system is made over a typical operational cycle. References are given for a control system specification and design.

CONTROL ANALYSIS

System control schemes were formulated for the reference design. Open-loop dynamic analysis and closed-loop response of the primary controls were evaluated, and a control scheme selection was made. A thorough treatment of this analysis is given in reference 5.

Control Philosophy

After the performance of the reference design was evaluated, control schemes were formulated to begin conceptual design of a complete control system. These schemes consist of primary controls used to control thrust through chamber pressure control and specific impulse through chamber temperature control, and auxiliary controls used to protect system components and augment the primary controls. Each scheme uses the topping-turbine-bypass valve to control chamber pressure. Chamber temperature is controlled by manipulation of the HXSV or the poison reactivity, or a combination of the two, with or without a reactor power control loop. Water temperature is controlled within limits by the control element not used to control chamber temperature. A control system for matching pump-stall margins by manipulation of the BTSV was also considered.

Control Scheme Evaluation

The evaluation of the control schemes was conducted in three steps. First, open-loop transfer functions were obtained relating the independent control elements to system variables. Second, controller networks were synthesized. Finally, closed-loop controls were evaluated under both isolated and interacting conditions.

Open-loop response. - Response testing was conducted through use of the analog-simulation model. Open-loop transient responses of chamber pressure, chamber temperature, reactor power, and bulk water temperature to small steps of TTBV position, HXSV position, and poison reactivity were obtained at 100- and 59-percent total hydrogen flows at 100-percent chamber temperature, and the CTO point at 30-percent total hydrogen flow at 39-percent chamber temperature. Transient data were recorded, and the frequency response of each transfer-function combination was calculated by use of a digital-convolution program. Transfer functions were calculated to approximate the frequency response for use in root locus synthesis.

Control system synthesis. - Proportional-plus-integral controllers were used to

keep controller complexity to a minimum; root locus plots were made of the characteristic equation for a range of controller gains and break frequencies. From the root locus plots, a set of parameters was chosen for each primary control scheme based on desired damping ratios and response time for the dominant transient mode.

Closed-loop evaluation. - Having obtained initial design parameters for the chamber pressure and chamber temperature controllers, a closed-loop analysis of the primary control system was conducted on the analog-simulation model. Nine modifications of the basic temperature control schemes were also studied in an attempt to improve closed-loop dynamics or broaden engine operating capability. Several schemes were eliminated at this point. Acceptable schemes were tested around the CTO point to investigate nonlinear effects. Closed-loop evaluations were made at three operating conditions: the design point, 59-percent hydrogen flow at 100-percent chamber temperature, and the CTO point at 30-percent hydrogen flow and 39-percent chamber temperature.

Control Scheme Selection

Based on the foregoing closed-loop analysis, primary controls were selected. These controls were combined with auxiliary controls and formed the basis for the complete reference-design control system. An alternate set of controls was also selected. A brief description is given here. A more complete description of the selected and alternate control systems is presented in subsequent sections.

Primary control. - The primary control scheme chosen consisted of a control of the TTBV to control chamber pressure and a control of the HXSV to control chamber temperature without an internal reactor power control loop. To obtain satisfactory response over a wide range, the initially chosen parameters of the chamber pressure controller were modified, and the gain of the chamber temperature control was made a function of the chamber pressure.

Auxiliary control. - Auxiliary controls were designed to protect system components in the water loop, to provide poison reactivity augmentation of the chamber temperature primary control during wide thrust transients, and to control reactor power during the start transient below the CTO point. The poison reactivity augmentation consists of relatively fast insertion or withdrawal rates when the chamber temperature error reaches a prescribed level.

Alternate control. - An alternate control system was conceptually designed for use if unforeseen difficulties should arise with the selected system. The chamber pressure control loop is the same as in the selected system. Chamber temperature, however, is controlled by poison reactivity insertion or withdrawal rather than by varying heat-exchanger-bypass flow. To obtain close temperature control with on-off poison valves,

the system contains a pulse width modulation feature. With this feature, the length of time during which a valve is open, and thus the average poison insertion and removal rate, is proportional to the temperature error signal. The same control loop controls reactor power during startup. Water temperature is controlled with the HXSV.

SELECTED CONTROL SYSTEM

The control system selected from the control analysis is described and its operation explained in detail.

Description

The major components of the control system consist of system sensors, control

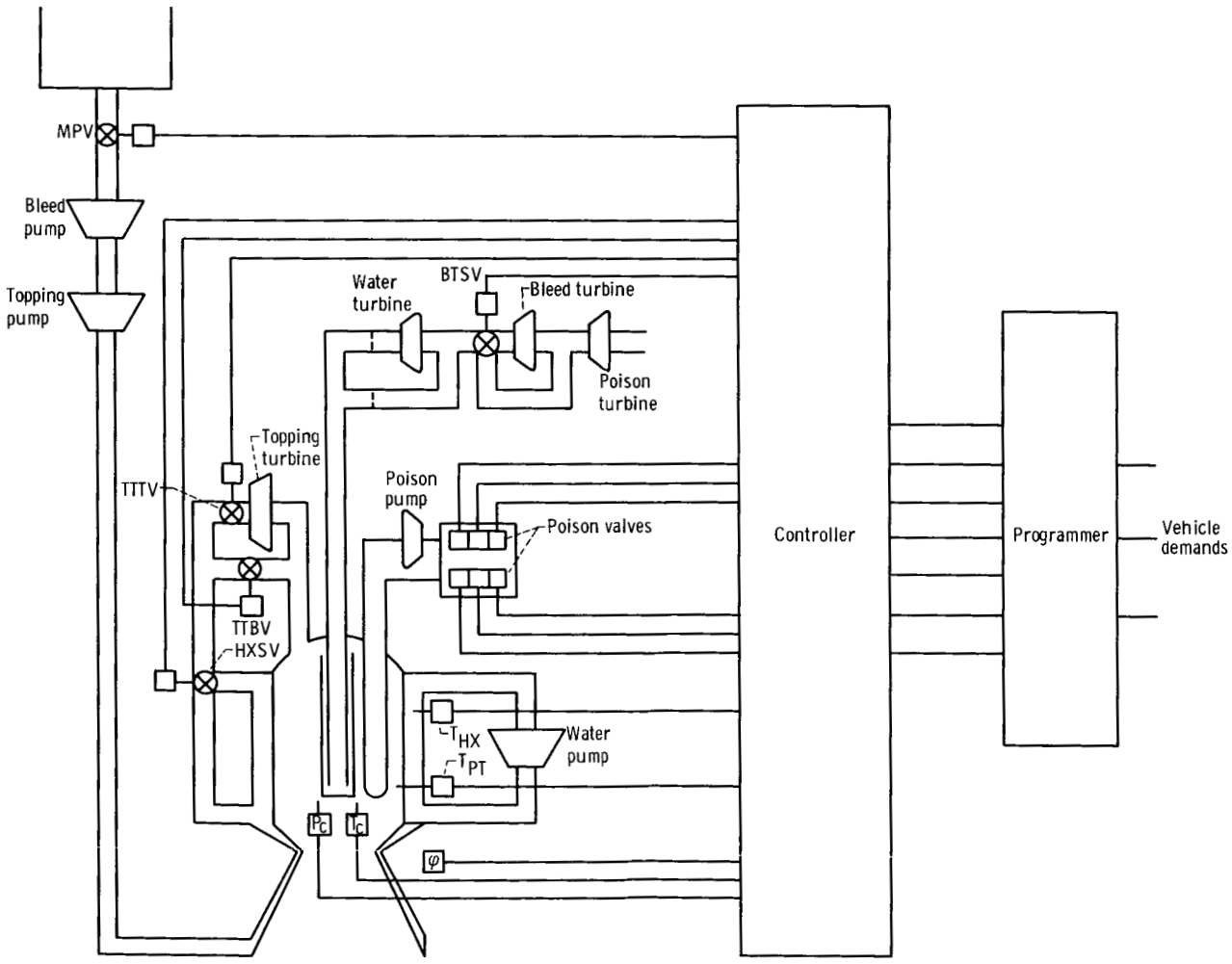

Figure 19. - Reference-design configuration and control system. Heat-exchanger-wall temperature, T_{HX}; pressure-tube-wall temperature, T_{PT}; neutron flux, φ; chamber pressure, P_c; chamber temperature, T_c.

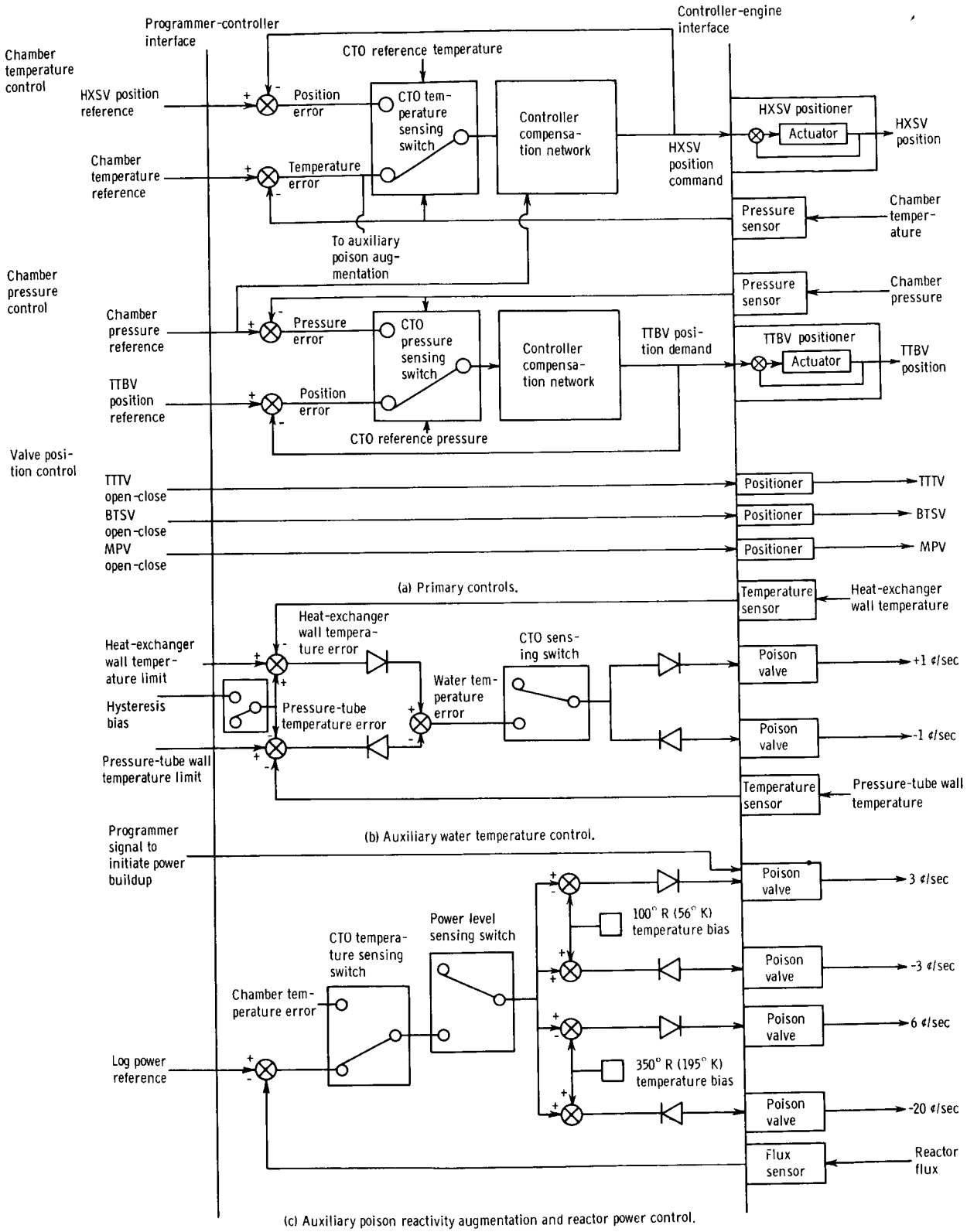

Figure 20. - Selected control system schematic drawing. (All switches are shown in prestartup positions.)

valves, a controller, and a control programmer. The control valves depend on output signals from the controller for their operation, and the sensors provide feedback signals to the controller. The system controller incorporates the compensation networks and switches of the primary controls which control chamber pressure and temperature and auxiliary controls which protect system components and augment the primary controls. The control programmer provides reference and logic signals which program the various control functions based on vehicle command signals. A reference-design system and control system schematic is presented in figure 19 to show the interrelation of the control system components. A schematic drawing of the control system controller and its interfaces is shown in figure 20.

Primary Controls

The primary controls provide closed-loop control of chamber pressure and temperature. These controls are active during system operation between the CTO and design levels. Below the CTO point, the control loops are open and the position of the HXSV and TTBV are determined by position reference signals from the control system programmer. A schematic diagram of the primary controls used with the control system is shown in figure 20(a).

Chamber pressure control. - Chamber pressure control is effected through action of the TTBV on topping-turbine power which in turn determines total hydrogen weight flow. The TTBV receives a position reference signal from the system controller. A valve position loop and servoactuator components provide valve positioning. Controller feedback is provided by a chamber pressure sensor. Below the CTO point, the CTO pressure sensing switch is in the TTBV position control position. A TTBV position reference signal is compared with the position demand signal. Any existing error is passed through the controller compensation network which varies the position demand signal to null the error. Operation of the CTO pressure sensing switch occurs when the chamber pressure sensor signal received by the control system programmer exceeds the CTO reference level. At this time, the input to the compensation network is zero, and the output of the compensation network is the desired position demand signal. Thus, a zero input signal exists at the compensation network of the valve positioner and abrupt valve motion is avoided. Above the CTO pressure, the chamber pressure control loop is closed and follows a chamber pressure reference signal generated in the control programmer.

Chamber temperature control. - Chamber temperature control is accomplished through action of the HXSV on the heat-exchanger hydrogen bypass flow. A wide-open position of this valve corresponds to 100-percent bypass flow. The HXSV receives a position reference signal from the system controller and, through its position loop and

servoactuator components, provides a valve position. Feedback in this loop is provided by a temperature sensor in the thrust chamber. The chamber temperature control operates similar to the chamber pressure control. The control becomes active above the CTO temperature. A smooth transition between the open and closed control modes as in the chamber pressure control is provided. The controller gain is a function of chamber pressure to permit the temperature control to adapt to the nonlinearity of the system.

Auxiliary Controls

The auxiliary controls are used in the control system to protect components within the water system, to provide poison reactivity augmentation of the chamber temperature control during power range transients, and to provide reactor power control during the start transient below the CTO point. A schematic diagram of the auxiliary controls is shown in figures 20(b) and (c).

Water temperature control. - Components within the water system are protected from over-limits by an auxiliary water temperature control used in conjunction with the poison system. Six poison control valves provide poison insertion or extraction rates which produce initial reactivity changes. These valves receive logic signals to either open or close. The water temperature control prevents the aluminum pressure-tube-wall temperature from exceeding 719° R (399° K) and the heat-exchanger-exit-wall temperature from falling below 492° R (273° K). The control is inactive below the CTO point and the poison valves remain closed. A CTO sensing switch, which is actuated when both CTO temperature and pressure are reached, makes the control active between the CTO and design levels. Although the control is active during thrust transients as well as in steady-state operation, its performance is relatively insignificant during the transients.

On reaching a particular operating level, the final position of the HXSV is not predictable exactly and therefore the resulting bulk water temperature is also not predictable. An optimum bulk water temperature or centered value at the design point provides a margin of approximately 38° R (21° K) between both the aluminum pressure-tube-wall temperature and its limit of 719° R (399° K) and the heat-exchanger-exit-wall temperature of 492° R (273° K). The HXSV position which approximates this condition is 15 percent open. The auxiliary water temperature control functions to find this centered bulk water temperature at all conditions above the CTO point. The auxiliary water temperature control schematic is shown in figure 20(b).

Error signals are produced by the heat-exchanger-exit and pressure-tube-wall-temperature signals and their respective limit bias. These analog signals are passed through diodes and summed. The resultant water temperature error is then channeled through the CTO sensing switch to diodes which provide logic signals to the poison valves.

If the water temperature error is positive, the 1-cent-per-second poison valve is opened, and the -1-cent-per-second poison valve is closed. If the error is negative, the valves reverse their position. Control action is continued until the error is removed. To avoid error oscillations about either limit, logic is incorporated in the control which introduces a hysteresis bias through a switch whenever a finite water temperature error exists. Should a temperature limit be exceeded, corrective action to adjust bulk water temperature will continue beyond the point where the error is just removed. At this point, even though neither the heat-exchanger-exit or pressure-tube-wall-temperature limits are exceeded, the water temperature error will be finite and will energize the poison valves until the margin from the heat-exchanger-wall temperature equals the margin from the pressure-tube-wall temperature. When this occurs, bulk water temperature is centered.

The HXSV can be closed without exceeding the heat-exchanger-exit-wall-temperature limit. Should this occur, the chamber temperature control loop will lose control. As a precaution against this loss of control, logic is provided which will introduce the hysteresis bias when a HXSV closed signal is received. This will recenter the bulk water temperature and permit the HXSV to return to its approximate 15 percent open nominal value.

Poison augmentation control. - During a start transient from the CTO to the design point, the primary chamber temperature control is too slow to enable the chamber temperature to follow its reference closely and large chamber temperature errors result. The errors increase in magnitude during the transient. The poison augmentation control functions to prevent these large errors through use of the poison system. The introduction of reactivity by reducing poison concentration during the start transient has the effect of increasing power rapidly which tends to reduce the temperature error. The converse is true for shutdown transients. A schematic diagram of this control is shown in figure 20(c).

The control is active between the CTO and design levels. The chamber temperature error generated in the primary control is passed through a CTO temperature sensing switch and a reactor power level sensing switch to four comparitors. The signal is compared with positive and negative values of two bias levels, $\pm 100^{\circ}$ R (55.6° K) and $\pm 350^{\circ}$ R (194° K). The output of each comparitor is fed to analog-to-digital converters, which transform the analog signal into open-close logic signals. These signals actuate four poison valves at initial reactivity changes of 3, -3, 6, and -20 cents per second. When the chamber temperature error is between 0 and $\pm 100^{\circ}$ R (55.6° K), no valve action occurs; between 100° and 350° R (55.6° and 194° K) the 3-cent-per-second valve is open; signals greater than 350° R (194° K), both 3- and 6-cent-per-second valves are open to give a reactivity increase of 9 cents per second.

During transients in which negative chamber temperature errors are generated, such as a shutdown transient, the poison augmentation control functions similarly. For a chamber temperature error below -100° R (55.6° K), an initial reactivity change of

-3 cents per second is introduced; for errors above -350° R (194° K), -23 cents per second is introduced.

Reactor power control below control takeover point. - The primary chamber temperature control, which uses reactor power as its means to control chamber temperature, is active between the CTO and design-point levels. Below the CTO, reactor power control is required for the dry core power buildup and chilldown-bootstrap phases. However, it is not possible or practical to use the chamber pressure control loop during these phases. The auxiliary reactor power control functions to fulfill these control requirements by controlling reactor power directly with poison reactivity. A schematic diagram of the control, which is a part of the auxiliary poison reactivity augmentation control, is shown in figure 20(c).

The objective of the auxiliary control during the dry core power buildup is to bring the reactor power from approximately 10^{-12} (source level) to 0.05-percent design power and hold that power level until chilldown starts. The buildup is initiated by a control programmer logic signal which opens the 3-cent-per-second poison reactivity valve. When a power level of approximately 0.05 percent is attained, the programmer logic signal is removed and the power sensing switch closes to provide closed-loop power level control. Log power is used as the control parameter in the closed-loop control. A log power reference signal is generated in the control programmer and compared with a log power sensor signal. The resulting error passes through the CTO temperature and power level sensing switches and into the poison control valve network which operates to null out the existing error. All poison valves remain closed if the magnitude of the error is within the 0.0267-decade deadband. A log power error between 0.0933 and 0.0267 decade in magnitude will actuate the ±3-cent-per-second valves depending on the error direction. An error larger than 0.0933 decade will actuate the 6- and -20-cent-per-second valves, again, depending on the error direction.

During the chilldown-bootstrap operational phase, the closed-loop power control provides a power increase according to a log power reference signal generated within the control system programmer. In this phase, valve and power programming is critical since hydrogen flow and reactor power must increase in such a way as to (1) avoid pump stall by matching the pump stall margins, and (2) maintain relatively high core-wall temperatures to avoid tungsten embrittlement and bring the system to the CTO point in a short time period.

When the CTO temperature is reached, the CTO temperature sensing switch closes and the primary chamber temperature control becomes active, as discussed in a previous section, Chamber temperature control.

Programmed valves. - In addition to the primary control-loop valve programming below the CTO point, other valves are used in startup and shutdown sequences. These are shown at the bottom of figure 20(a). The MPV receives a logic signal from the sys-

tem programmer to open or close at a predesignated rate. The TTTV varies topping-turbine power and the BTSV varies power to the first-stage hydrogen pump turbine during startup and shutdown transients below the CTO point. Both valves receive logic signals from the system programmer to open or close at preset rates.

ALTERNATE CONTROL SYSTEM

An alternate control system was conceptually designed as a technical backup system to the selected system. The system is described and its functions discussed.

Primary Controls

The primary controls use poison reactivity rate as the basic independent variable to control chamber temperature instead of the HXSV as in the selected control system. A schematic diagram of the system is shown in figures 21(a) and (b).

Chamber pressure control. - The chamber pressure control loop shown in figure 21(a) is similar to that of the selected control system. It provides for both closed-loop control of chamber pressure and open-loop TTBV positioning.

Chamber temperature and power level control. - The chamber temperature control shown schematically in figure 21(b) uses pulse width modulation (PWM) of three poison reactivity rate valves to make the average poison rate proportional to the chamber temperature error. Thus, close quasi-continuous control of chamber temperature is provided within a small deadband. The same control loop controls reactor power level below the CTO point.

Above the CTO point, a chamber temperature error, generated from feedback and controller reference signals, passes through the power level and CTO temperature sensing switch. It is compared with positive, negative, and biased signals of a fixed maximum amplitude triangular wave generator. The output of the comparitors are logic signals used to operate three poison rate valves, ±9 and -15 cents per second. For a positive chamber temperature error, the 9-cent-per-second valve is open whenever the triangular wave amplitude is below the error and closed for the remainder of the duty cycle. This corrective action reduces the time duration that the triangular wave amplitude is less than the chamber temperature error, thereby reducing the open duration time for the 9-cent-per-second valve and decreasing the average poison rate. The -9-cent-per-second valve behaves similarly for negative chamber temperature errors. If this error is negative and greater than the maximum triangular wave amplitude, the -9-cent-per-second valve is open continuously and the -15-cent-per-second valve opens when the bi-

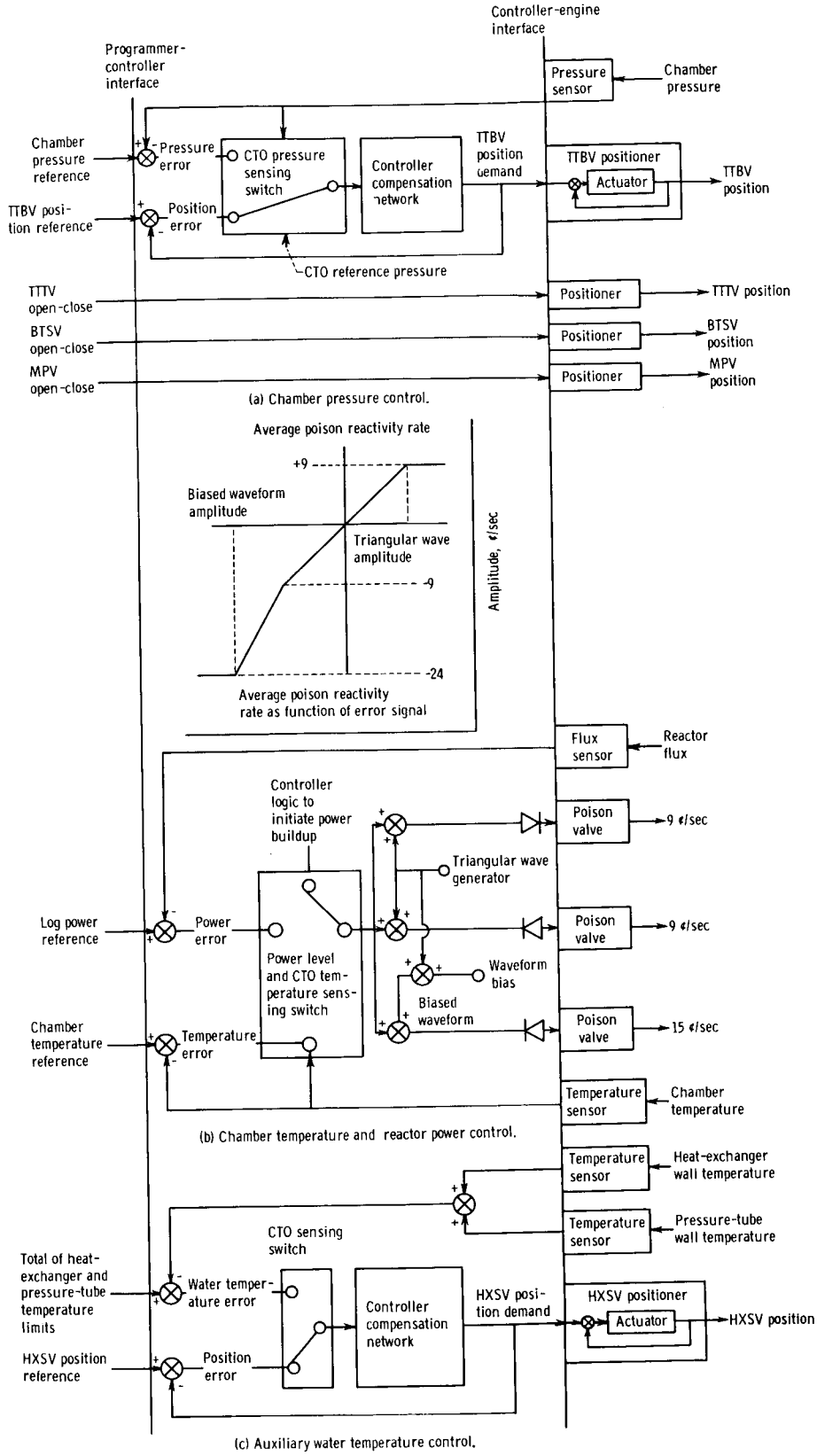

Figure 21. - Alternate control system schematic.

ased waveform is less than the chamber temperature error magnitude, thus providing -24 cents per second of reactivity. The resulting average poison rate as a function of chamber temperature error is shown in the block next to the chamber temperature control schematic.

Below the CTO point, the chamber temperature control loop becomes a reactor power control. In this mode, it functions similarly to the reactor power control of the selected control system. From source level to approximately 0.05-percent design power, an external signal from the control programmer is used to actuate the poison valves. When 0.05-percent power is reached, the power level and CTO temperature sensing switch switches to closed-loop power control. The control loop then follows a programmed power reference to a CTO point where the chamber temperature control-loop becomes active.

Auxiliary Controls

Auxiliary controls for the alternate control system include only a water temperature control loop. The reactor power level control in this system is part of the chamber temperature control.

The water temperature is controlled with a closed loop around the HXSV. Open loop position control is also provided. A schematic diagram of the control is shown in figure 21(c).

Signals from sensors measuring the heat-exchanger-exit and aluminum pressure-tube-wall temperatures are summed and compared with the sum of the wall-temperature limits. Above the CTO point, the error passes through the CTO sensing switch to a proportional-plus-integral controller which sends a valve position reference signal to the HXSV positioner. The controller output continues to integrate as long as an input error exists. In steady state, with zero error, the midpoint of the sensed wall temperatures equals that of their respective limits. Thus, the temperatures differ from their limits by equal amounts thereby maintaining a centered water temperature as in the selected control system.

Below the CTO point, an open loop HXSV positioning control is active. The resulting closed loop causes the valve position signal to follow the input reference signal generated in the control programmer. Also, MPV, TTTV, and BTSV position control is provided for startup and shutdown programming.

COMPARISON OF SELECTED AND ALTERNATE CONTROL SYSTEMS

The difference between the selected and alternate control systems lies in the basic control philosophy applied to each system. The two control elements, HXSV and poison, provide the means for controlling water and chamber temperatures simultaneously through the heat-exchanger-bypass flow and reactor power. The HXSV is capable of continuous variation while the poison system is inherently discontinuous. Also, water and chamber temperature react slowly to changes in HXSV position, while these same dependent variables are affected quite rapidly with poison variation. These control-element characteristics form the basis of two control philosophies, continuity and response, used in the selected and alternate systems.

The selected system uses the continuous feature of the HXSV to provide close, exact control of chamber temperature with poison augmentation to improve the response. The inherently discontinuous action of poison insertion or extraction controls water temperature which can vary safely within a deadband. On the other hand, the alternate control system uses the high response characteristic of poison to control chamber temperature which requires rapid response. The PWM feature compensates for discontinuity by providing for quasi-continuous control. The lower response control element HXSV is used to control water temperature whose time response is less important.

Reliability is the chief factor leading to the choice of an HXSV primary and poison augmentation control for chamber temperature. As for the alternate control system, its chief advantage is the possibility of closer reactor power control during startup and closer chamber temperature control during startup, thrust transients, and shutdown. The ideal characteristics of the PWM may be difficult to achieve and would result in a small chamber temperature deadband or oscillation. The chief disadvantage is the continual poison valve actuation. Also, because of the separation of HXSV and poison control functions, the control system appears more susceptible to system failures.

EVALUATION

The selected control system was evaluated over a major portion of the system operational cycle on the analog-simulation model and over the complete cycle on the digital-simulation model. The operational cycle is described and results of the evaluation on both models presented.

Operational Cycle

Briefly, the operational cycle consists of a dry core power buildup, a chilldown bootstrap phase to the CTO point, a thrust transient to the design point, thrust modulations between 100 and 50 percent at maximum specific impulse (chamber temperature), and a shutdown transient. Aftercooling is not included. The cycle is controlled by command signals generated within the control system programmer. These signals produce primary and auxiliary control action which in turn generate operational results. A schematic diagram of control system and programmer including all primary controls, auxiliary controls, and logic elements along with a description of the programmer sequence during a typical operational cycle is presented in reference 5.

Analog-Model Evaluation

A major portion of the control system was evaluated on the analog model over most of the system operating range. The system was brought to the CTO point by ramping the

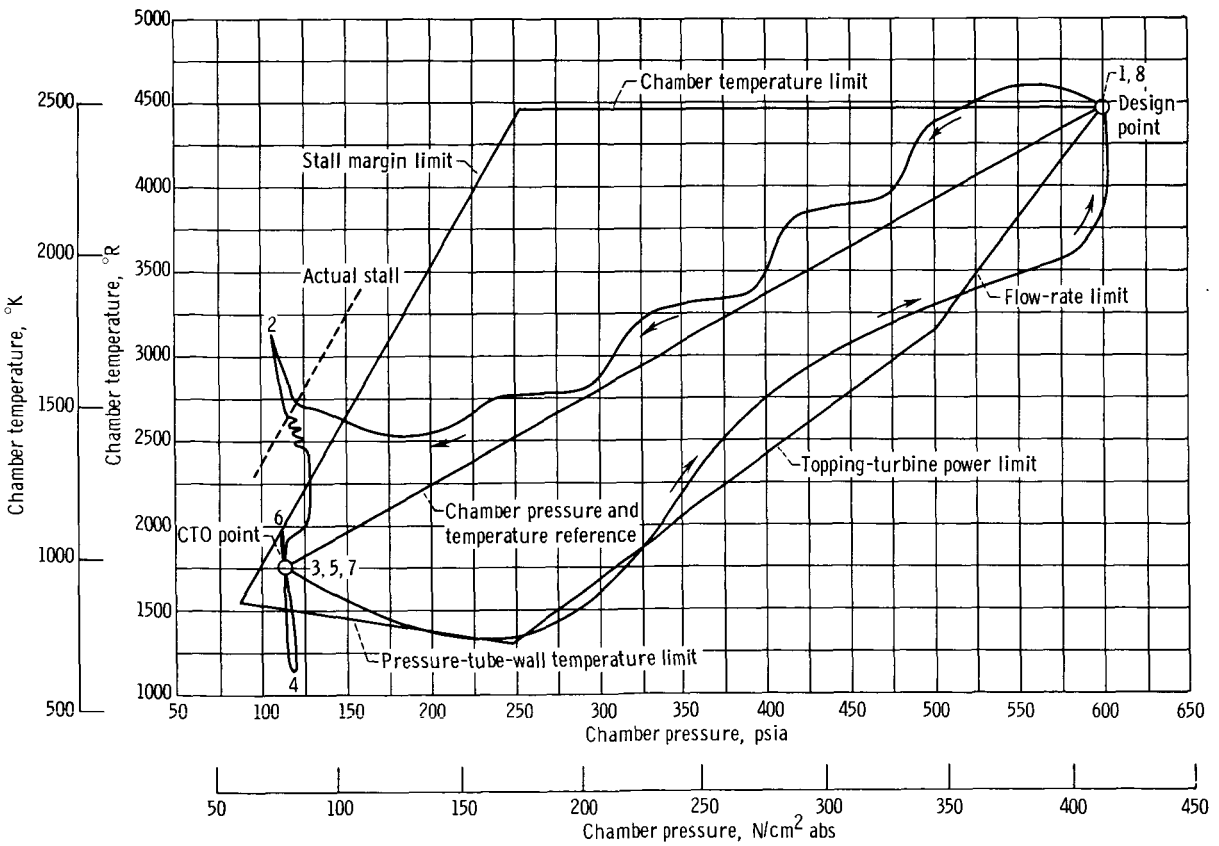

Figure 22. - Transient performance of reference design without poison reactivity augmentation.

TTBV and the poison reactivity. The primary controls took over automatically. The chamber pressure and temperature reference signals were ramped to their design point values. At the design point, a reactivity ramp caused by fuel depletion, and two reactivity steps were simulated to demonstrate the action of the auxiliary controls. The chamber pressure reference was reduced to 50 percent and then increased back to 100 percent with the chamber temperature reference held constant. Finally, the chamber pressure and temperature references were ramped to their CTO values. The control system performance was satisfactory over all the system operating cycle that was evaluated. The transients produced in this study are described in detail in reference 5.

Effect of poison augmentation. - To evaluate the effectiveness of poison augmentation, transients between the CTO and design point were run on the analog model with only the primary and poison augmentation controls active. The results of these transients are shown in figures 22 and 23, which show plots of chamber temperature as a function of chamber pressure. The system operating envelope is also shown. The envelope applies only to steady-state relations, whereas the pressure-temperature locus is a transient relation.

In one transient, the poison reactivity was held constant while neither the poison

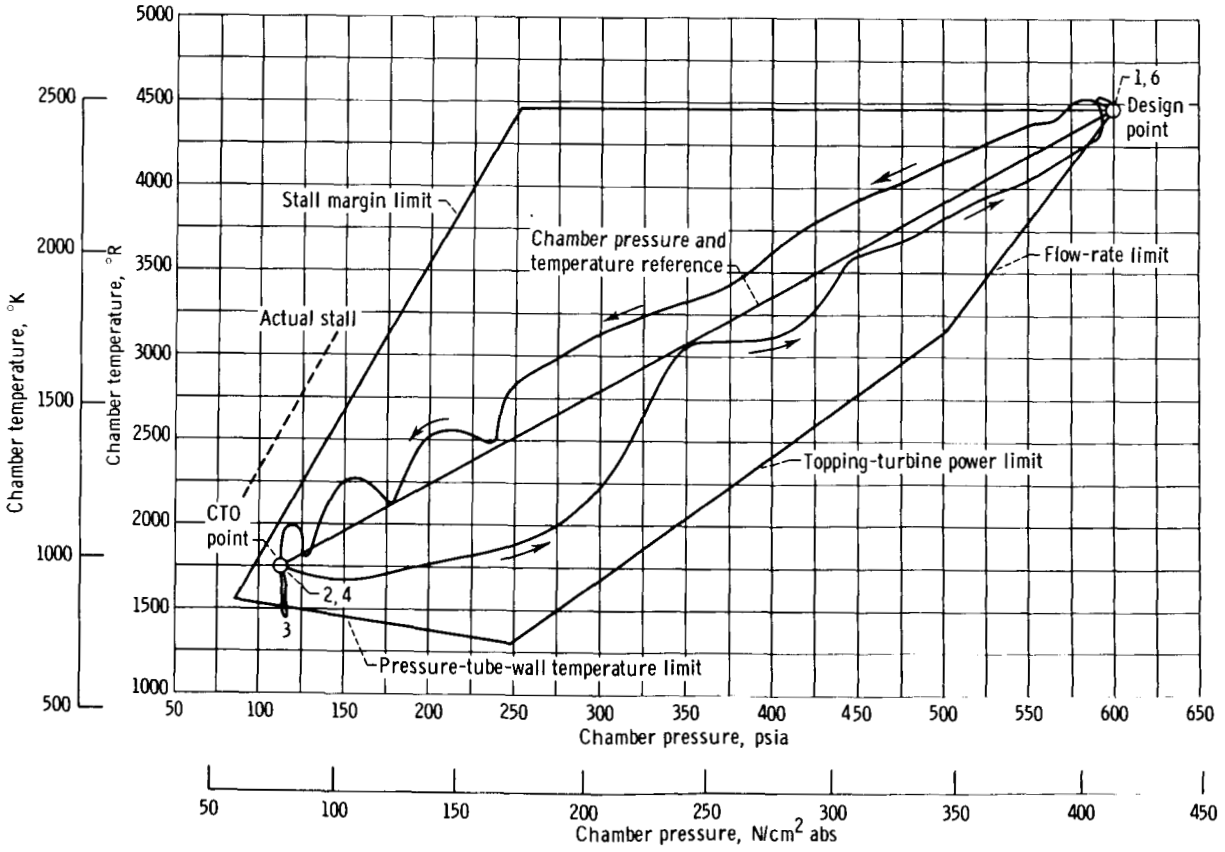

Figure 23. - Transient performance of reference design with poison reactivity augmentation.

augmentation in the chamber temperature control nor the water temperature control was active. The chamber pressure and temperature reference signals were ramped from their 100 percent to CTO values in 30 seconds. The resulting transient went from point 1 to point 7 in figure 22. The chamber temperature was above its reference for the entire ramp. Both pumps went into stall at point 2 and remained there for 7 seconds. After coming out of stall, the system followed the circuitous path through points 3, 4, 5, 6, and finally terminated at point 7, the CTO point. At point 4, the pressure-tube-wall temperature reached a peak of 732° R (407° K) and was above its limit for 37 seconds.

After steady-state conditions were achieved at the CTO point, the reference signals were ramped to their 100-percent values in 15 seconds. The path from point 7 to 8 resulted. The chamber temperature lagged far behind its reference. The hydrogen flow peaked at 100 pounds per second (45.4 kg/sec) at a chamber temperature of 3600° R (2000° K). The time traces, not shown, indicated that the heat-exchanger-exit-wall temperature barely reached the freezing point and remained there for approximately 12 seconds. Also, they showed that the HXSV went fully closed about halfway through the transient indicating that chamber pressure control was lost. The HXSV began to open 14 seconds after the ramp ended.

In the next transient, the poison augmentation in the chamber temperature control loop was active, but the water temperature control remained inactive. As in the previous run, the chamber pressure and temperature were ramped from 100 percent to CTO values in 30 seconds, and back up in 15 seconds. The result is shown in figure 23.

The decrease transient followed the path from point 1 to 2 and circled through point 3 to point 4, the CTO point. The increase transient followed the path through points 4 to 6. No system limits were exceeded on either transient. Because of the poison augmentation, the chamber temperature lagged its reference much less than in the unaugmented transient.

These transients clearly demonstrate the need for poison augmentation in the chamber temperature control loop.

Malfunction analysis. - A malfunction analysis of the engine and control systems was performed using the analog model. The analysis included valve failures which result in full open or closed positions and control signal loss from sensors. The effects of additional failures were deduced from the simulated failures. Corrective or preventative action was recommended and the resulting performance evaluated.

The results of recommended corrective or preventative actions are categorized according to (1) performance not significantly affected, (2) performance degraded, and (3) safe emergency shutdown. Included in the second category are loss of precise chamber pressure or temperature control and reduced operating point. The third item includes interruption of the startup sequence or a premature shutdown, both without significant damage to the system. Effects on mission are not covered.

The recommended action for each failure requires the use of additional equipment not considered in the control system and programmer. This additional equipment includes sensors for valve position limits and control signal loss. In some cases, recommendations include system design changes. In comparing alternate corrective actions, complexity of the required additional components was considered. The detailed descriptions of the malfunctions, corrective or preventative actions, and resulting performance are described in reference 5.

One of the most significant results of the malfunction analysis resulted from the BTTV fail-close simulation. The effect of such a failure at 100-percent design conditions is shown in figure 24, which presents several system variables as functions of time. The BTTV was stepped closed from a steady-state condition. After a mild transient, the TTBV closed to about 1 percent of its maximum area and the topping pump assumed the full system load at the 100-percent design point. Even under this condition, the topping

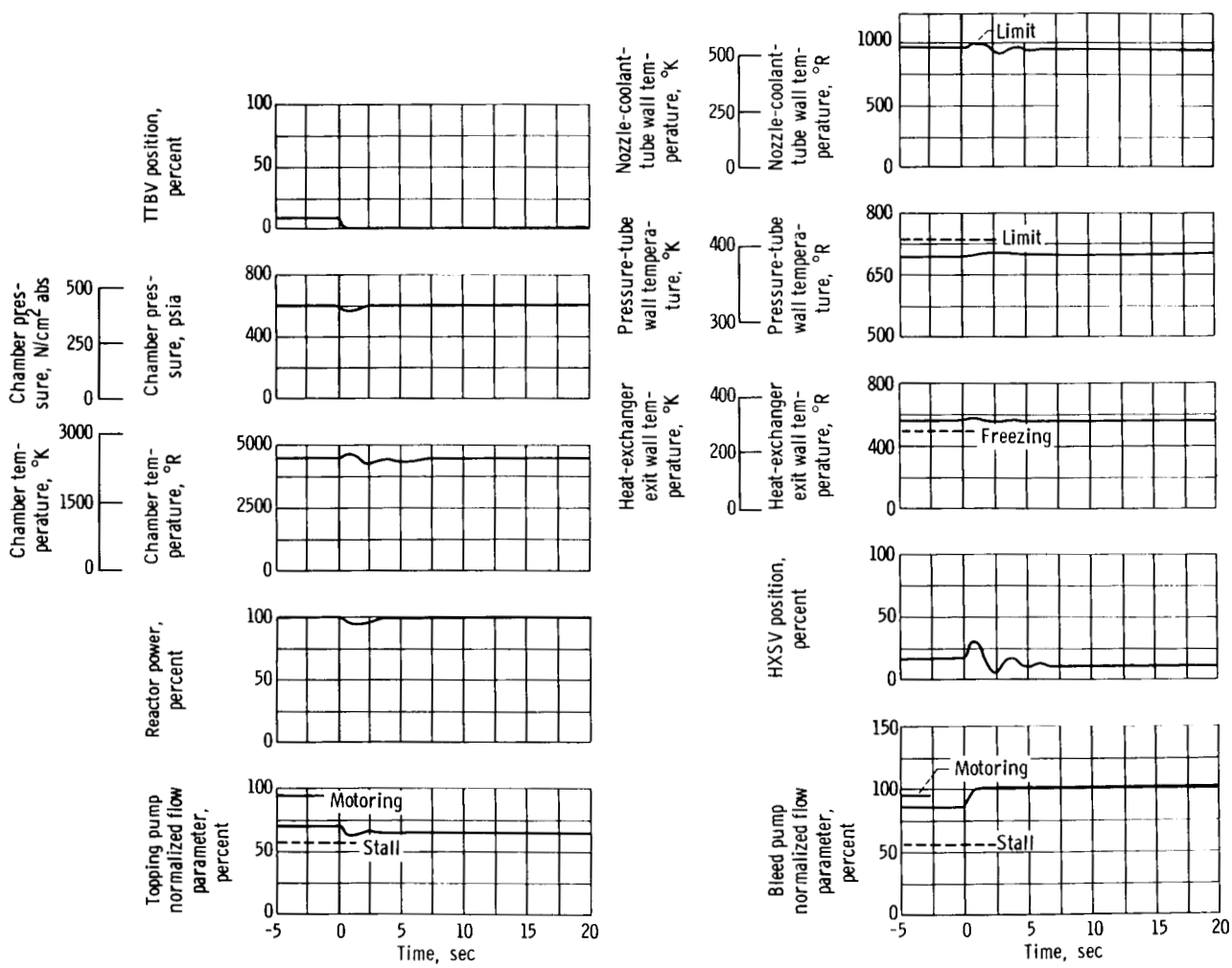

Figure 24. - Transient performance of reference design to BTTV fail-close signal.

pump had an adequate stall margin. No limits were exceeded during or after the transient. The final steady-state conditions attained with a propellant tank pressure of 35 psia (24 N/cm^2 abs) indicated a pressure drop of 5 psi (3.5 N/cm^2) across the MPV, a drop of 17 psi (11.7 N/cm^2) across the motoring bleed pump, and a static pressure of 13 psia (9 N/cm^2 abs) at the inlet to the topping pump. Since the saturation pressure of liquid hydrogen at 40° R (22° K) is 24 psia (16.5 N/cm^2 abs), the topping pump would actually have been cavitating. With this condition, the chamber pressure and temperature reference signals would have to be reduced to bring the system to an operating level that the topping pump could maintain without cavitation.

If the topping and bleed pumps were reversed in order, that is, topping pump first and bleed pump second, the inlet to the topping pump would not be subjected to the large static pressure drop produced by the motoring bleed pump. With this change, the topping pump would not cavitate (if appropriate design changes were assumed made to the topping pump) and could carry the entire system load at the 100-percent design point without corrective action; however, the control margin would be narrow. This aspect of series pump operation exemplifies the inherent reliability (redundancy) in such a system.

From this analysis, it was concluded that the order of the hydrogen pumps should be reversed to provide full design-point capability in the event of a BTTV and/or TTBV close-failure.

Digital-Model Evaluation

A simulation of the complete control system was incorporated in the digital-simulation model as a separate subroutine. The subroutine included all primary, auxiliary, and logic control functions of the control system and programmer.

Performance evaluation tests were conducted on the complete simulation model covering the entire operational cycle. The cycle segments included chilldown and initial bootstrap, continuation of bootstrap to CTO, thrust buildup from CTO to design point, chamber pressure transients at design chamber temperature, shutdown from design point to CTO, and scram from CTO. A digital computer run was made for each segment using the final conditions of the previous segment for the initial conditions of the following segment. In this way, a continuous operational cycle was obtained. Detailed results of each segment run are given in reference 5. A summary of the complete operational cycle is given in the following sections.

A summary of digital-model results of a complete start cycle consisting of 5 seconds of chilldown, 20 to 25 seconds of bootstrap to the CTO point, and 15 seconds of thrust buildup to the design point is presented in figure 25. Reactor power level, chamber pres-

sure, and chamber temperature are given as functions of time. Also shown is the major control system sequencing and valve programming associated with the start cycle.

Chilldown and initial bootstrap. - The start of this segment corresponds to zero time. At this time, the MPV receives a signal to open. The HXSV is positioned at 78.7 percent open, the TTBV at 100 percent open, and the BTTV and TTTV closed from programmer reference signals. Reactor power level is initially at 0.1 percent and on closed-loop control.

The MPV was programmed open in 1 second and the log-power reference was increased from log 0.1 percent to log 2 percent in 10 seconds. At 5 seconds elapsed time, the TTBV and BTTV were ramped open to 100 and 46.2 percent, respectively, in 5 seconds. The resulting transient is shown in figure 25(a).

The reactor power level followed the reference level closely for most of the transient verifying that the power control was able to produce the desired power transient. Chamber temperature remained above 1000° R (556° K) throughout the transient indicating that the core-exit-wall temperature was at least that temperature. The topping pump stalled slightly at 9 seconds indicating that this segment of the startup was near optimum as regards pump stall and core-wall temperatures.

Continuation of bootstrap to control takeover point. - During this segment, the log-power reference was ramped from log 2 percent to log 12 percent in 15 seconds and the TTBV was ramped closed at 4.25 percent per second. Both rates continued until the chamber temperature and pressure controls became active at the CTO point. This portion of the transient is shown in figure 25(b).

Power level followed its reference close during the run. The topping pump, which was in light stall at the end of the last segment and the beginning of this run, came out of stall at 10.3 seconds and was not encountered by either pump for the remainder of the startup.

The primary controls became active shortly after the power reference reached 12 percent. The chamber pressure reached 112.5 psia (77.6 N/cm^2 abs) at 25.2 seconds. At this point, the chamber pressure control was activated. Chamber temperature reached it CTO value of 1750° R (972° K) at 28.2 seconds at which time the reactor power control became inactive and the chamber temperature, poison augmentation, and water temperature controls became active.

Thrust buildup from control takeover to design point. - The chamber pressure reference signal was ramped from 112.5 to 600 psia (77.6 to 413.7 N/cm^2 abs) and the chamber temperature reference ramped from 1750° to 4460° R (972° to 2478° K) in 15 seconds. The results of this portion are shown in figure 25(c).

The chamber pressure followed its reference closely producing errors of 15 psia (10.3 N/cm^2 abs) or less for the most part. The chamber temperature lagged its refer-

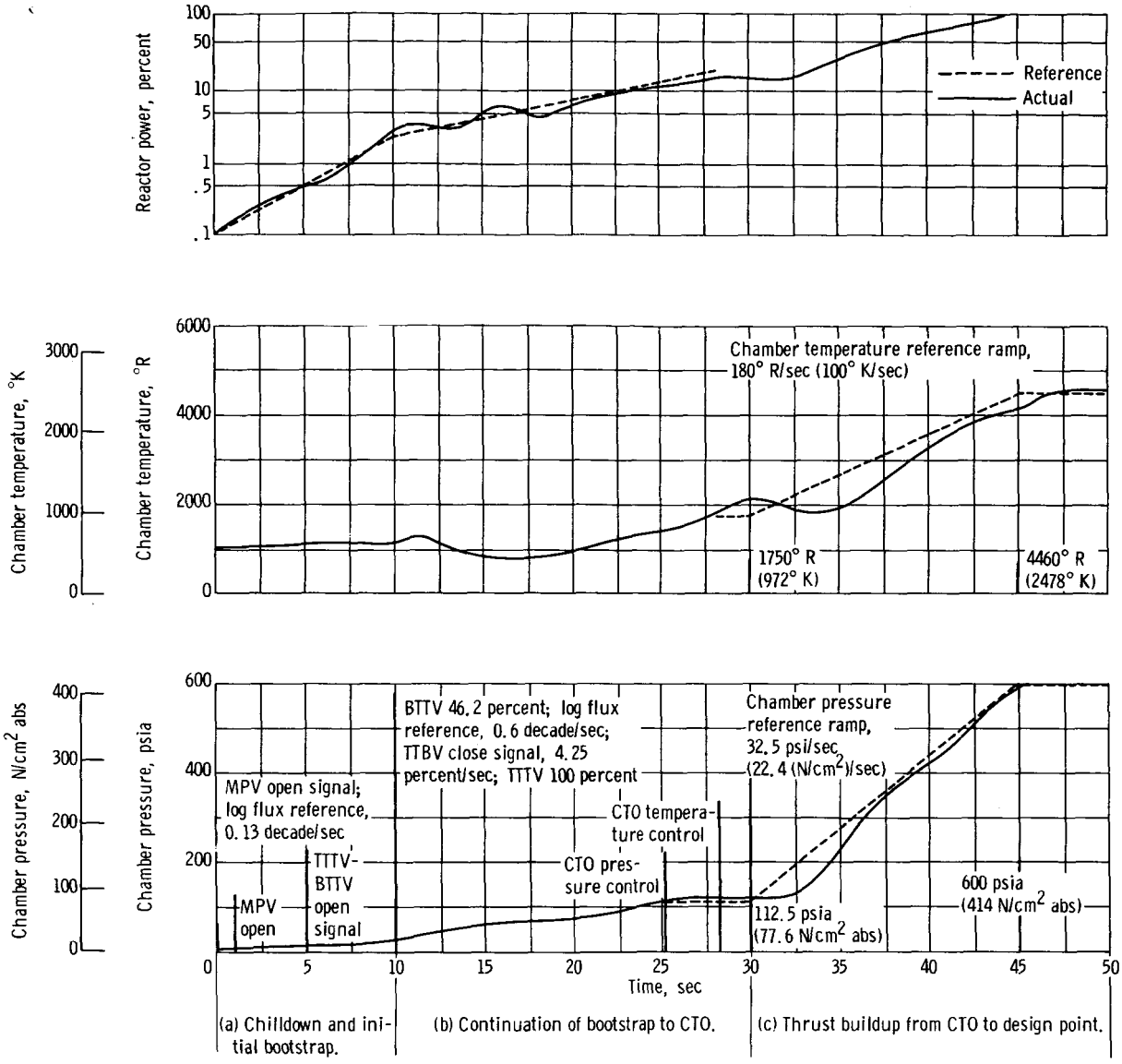

Figure 25. - Digital-model evaluation of reference-design control system over typical operational cycle.

ence by 700° R (389° K) at the start and thus triggered the poison augmentation control. The chamber temperatures responded rapidly and reduced the error to about 250° R (139° K). At the end of the transient, a 100° R (56° K) overshoot occurred.

Although not shown in the figure, the HXSV went fully closed and produced momentary icing in the heat exchanger. The full closed HXSV signal activated the water temperature control loop which, in turn, initiated water temperature centering. The water temperature centered, and the control was deactivated.

Chamber pressure transient at maximum chamber temperature. - The chamber pressure reference was ramped from 100 to 50 percent in 15 seconds, held constant for 5 seconds, and then ramped back to 100 percent in 15 seconds. The chamber temperature

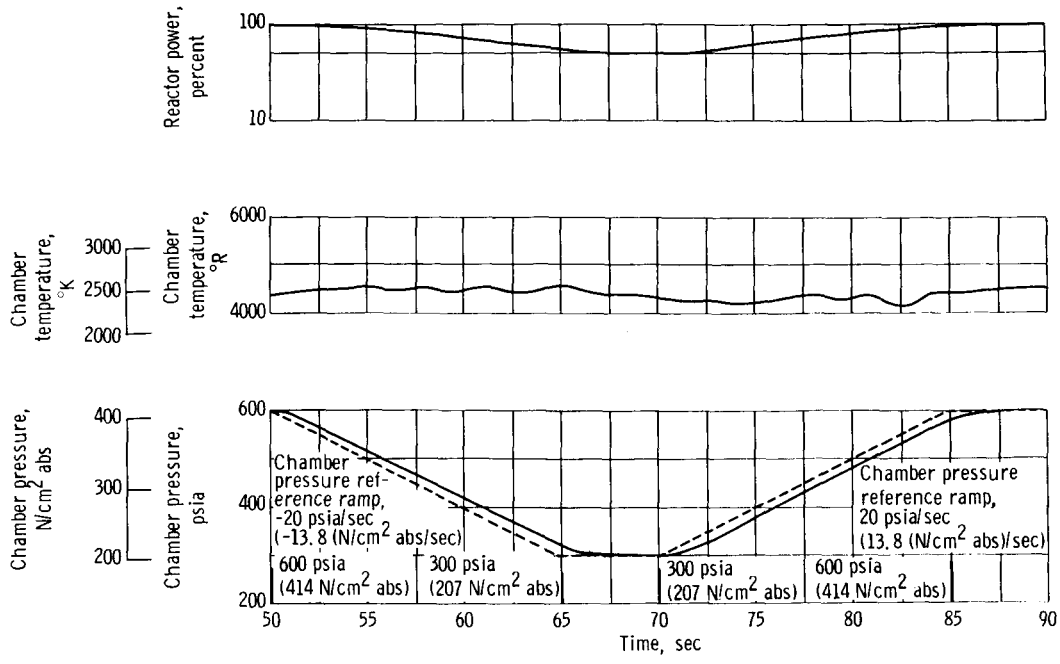

(d) Chamber pressure (thrust) transient at maximum chamber temperature.

Figure 25. - Continued.

reference was held fixed at 100 percent design. The transient simulated a thrust variation at maximum specific impulse. The results are shown in figure 25(d).

During the decrease transient, chamber temperature tended to increase above its reference value and triggered the poison augmentation control which, in turn, produced chamber temperature oscillations. Neither pump stalled, and no system limits were exceeded. During the first part of the thrust increase, the poison augmentation control was also activated. At the end of the reference ramp, chamber temperature overshot its reference by less than 100° R (56° K). No system limits were exceeded.

Shutdown from design point to control takeover point. - The chamber pressure and temperature reference signals were ramped down to their CTO values in 30 seconds. Results for this segment are shown in figure 25(e).

As in the power increase transient, chamber pressure followed its reference closely. Chamber temperature lagged its reference in excess of 100° R (56° K) so that the poison augmentation control was activated. Near the end of the reference ramp, the aluminum pressure-tube-wall temperature exceeded its limit and the water temperature control was triggered to recenter water temperature.

Scram from control takeover point. - At the end of the chamber pressure and temperature shutdown ramps, a scram (emergency shutdown) signal was immediately initiated by stepping the chamber temperature reference to zero. This action ensured that maximum negative poison reactivity would be injected into the reactor. After 5 seconds, the chamber pressure reference was stepped to zero to open the TTBV fully and thus re-

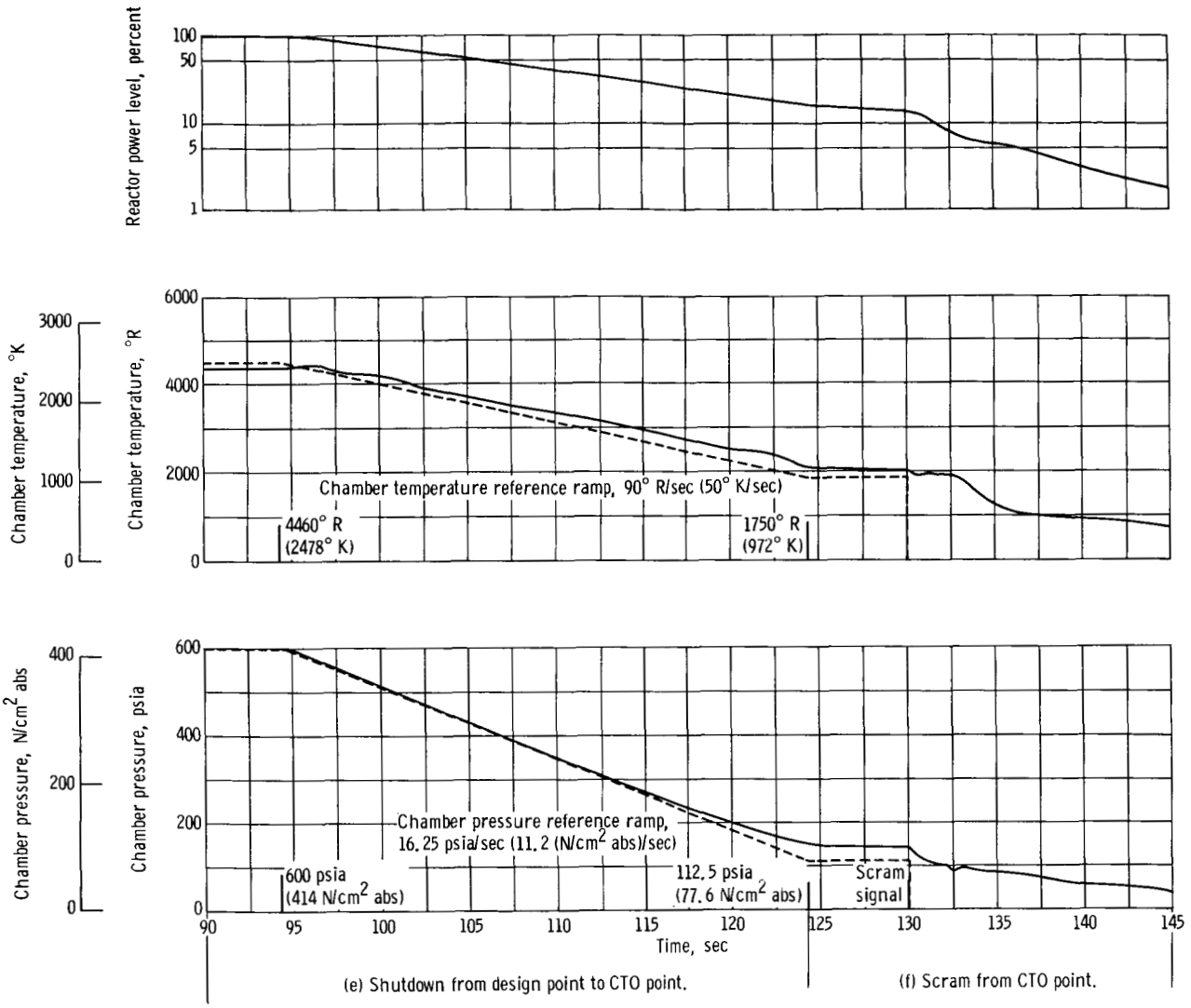

Figure 25. - Concluded.

duce power to the topping turbine. Results for the scram segment are shown in figure 25(f).

The power level dropped to 2.3 percent after 15 seconds (t = 145 sec) from the initiation of the scram signal. Both pumps stalled briefly about 2.5 seconds (t = 132.5 sec) into the scram but recovered immediately. Additional information, not shown, indicated that the TTBV was wide open and the total hydrogen flow was about 20 pounds per second (9.1 kg/sec). Also, the core wall reached low temperatures indicating that the TTTV and BTTV should have also been closed to drop the flow faster and thereby maintain

higher core wall temperatures. After this segment, afterheat controls would need to be activated; however, such controls were not a part of the overall study.

SPECIFICATION

A specification was written to cover performance requirements of all valves and sensing elements within the control system and programmer. Valve response requirements, slew rate, flow resistance, type of input signal, and fail-safe mode are included in the specifications. Also included are sensor response requirements, accuracy, operating range, and the desired output signal form. For the most part, the control system valve and sensor requirements are within the present state of the art of development. Exceptions to this are the log-power sensor and the chamber temperature sensor. A complete account of the control system specification is given in reference 5.

APPLICATION OF CONTROL SYSTEM DESIGN

The control analysis, conceptual design, and evaluation of the control system was intentionally kept general so that the results would be amenable to a wide range of control design techniques. To demonstrate this feature, an all-pneumatic, pure fluid control design approach was taken.

An incentive for the use of all-pneumatic, pure fluid components in a control system design stems primarily from the high reliability potential under the adverse environmental conditions of nuclear rockets. Fluidic controls are most appealing when the severe environmental problems of temperature and radiation are encountered.

The control functions and logic elements which constitute the control system, as conceptually designed and described in this report, were implemented with fluidic components. The fluidic control system was then combined with the reference-design system and a functional sequence generated for a complete operational cycle.

A detailed description of the fluidic control system and its function, fluidic components used in the implementation, and the functional sequencing used in the operational cycle are given in reference 5 along with schematic diagrams of the complete system.

CONCLUDING REMARKS

This study has shown that the tungsten water-moderated nuclear rocket system requires heat exchanger hydrogen bypass to prevent icing at low reactor power and hydro-

gen flow levels. Operation without this capability restricts steady-state operation to a narrow corridor which would undoubtedly require close system control. Although bypass eliminates icing, it aggravates the critical pressure tube overtemperature problem. These two opposing characteristics indicate that the heat exchanger effectiveness should be optimized with respect to water flow and length to provide suitable margins from icing and pressure tube overtemperature. Preheating the water prevents icing during chilldown but aggravates pump stall.

The preliminary reference design (and those which use the split-feed cycle) is characterized by a high degree of control flexibility. The results of steady-state mapping studies show that this flexibility is not required to maintain high system operation flexibility. Because of this, it is possible to simplify the control system by eliminating bleed subsystem valve controls and thus minimize loop interaction and avoid complex control networks. Only hydrogen flow and reactor power control is needed to control the system.

Based on the comparative system analysis, the topping cycle configuration is superior to the other configurations with respect to system and control flexibility, simplicity, and performance. Although this cycle is simple and efficient at the particular chamber pressure and reactor power levels used in this study, it has poor uprating potential. Because of the superior uprating potential of the split-feed cycle, the heat exchanger configuration was selected for further study.

An important characteristic of the heat exchanger bypass feature discovered in this study is that it is an effective means of reactor power control. Thus, the choice between this feature and poison reactivity control creates a conflict in the basic control philosophy: whether chamber temperature control should be based on the high response and discontinuous character of the poison system, or the slower response but accurate continuous character of the water temperature control.

The conflict is resolved in this study by selecting the continuous features of the heat-exchanger flow-splitter valve to provide continuous control of chamber temperature with poison augmentation to improve response. The poison system controls water temperature which can safely vary within a deadband. The operation of this control system was demonstrated satisfactorily over a typical operating cycle. Also, it was shown that poison augmentation does improve control response.

On the other hand, the alternate control system uses the high response characteristic of poison to control chamber temperature through a pulse width modulation feature. The pulse width modulation compensates for discontinuity by providing quasi-continuous control. The application of discontinuous control theory is yet required to determine the effectiveness of this promising technique. The lower response heat-exchanger flow-splitter valve is used to control water temperature whose response requirement is less important. The final choice of a control system would depend on the specific requirements of a mission.

Overall, this study has shown the value of simulation in system and control analysis. In the course of performing the study, an analytical technique or process was developed which could be applied to other systems. The parallel analog-digital simulation technique was particularly effective. The speed and simplicity of analog simulation delineated problem areas and produced gross results; the accuracy and broad range capability of digital simulation provided detailed information in specific areas and enabled wide range evaluation of system performance.

Lewis Research Center,
National Aeronautics and Space Administration,
Cleveland, Ohio, August 24, 1967,
122-29-01-09-22.

APPENDIX - SYMBOLS

A	area, $in.^2$; m^2
B	bulk modulus, lb force/$in.^2$; N/cm^2
BTBV	bleed-turbine bypass valve
BTSV	bleed-turbine splitter valve
BTTV	bleed-turbine throttle valve
C_i	concentration of i^{th} group of delayed neutrons
c_p	specific heat at constant pressure, Btu/(lb)(^oR); J/(kg)(^oK)
c_v	specific heat at constant volume, Btu/(lb)(^oR); J/(kg)(^oK)
D	diameter, in.; m
e	specific kinetic energy, in.; m
f	friction factor
H	head, ft; m
HXBV	heat-exchanger bypass valve
HXSV	heat-exchanger flow-splitter valve
h	heat-transfer coefficient, Btu/($in.^2$)(sec)(^oR); J/(m^2)(sec)(^oK)
J	Joule's equivalent, 778.2 ft-lb force/Btu; in.-m/J
K	thermal conductivity, Btu/(in.)(^oR)(sec); J/(m)(^oK)(sec)
L	torque, ft-lb force; N-m
l	length, in.; m
MPV	main propellant shutoff valve
N	rotational speed, rpm
NHXBV	nozzle-heat-exchanger bypass valve
n	relative neutron level
P	pressure, psi; N/cm^2
Pr	Prandtl number, $c_p\mu/k$
Q	volumetric flow, ft^3/sec; m^3/sec
q	heat rate, Btu/sec; J/sec
R	gas constant, ft/^oR; J/^oK
Re	Reynolds number
T	temperature, ^oR; ^oK
TTBV	topping-turbine bypass valve
TTTV	topping-turbine throttle valve
V	volume, ft^3; m^3
v	velocity, ft/sec; m/sec
W	mass, lb; kg mass
WTBV	water-turbine bypass valve
WTTV	water-turbine throttle valve
x	fluid quality, percent
Z	compressibility factor
β	total delayed neutrons
β_i	fraction of i^{th} group of delayed neutrons
γ	ratio of specific heats, c_p/c_v
λ_i	decay constant of i^{th} group of delayed neutrons, sec^{-1}

μ absolute viscosity, lb mass/(ft)(sec); kg mass/(m)(sec)

ρ density, lb mass/ft^3; kg mass/m^3

ρ_T total reactivity, $

φ_m Martinelli factor

ω mass flow rate, lb mass/sec; kg mass/sec

Subscripts:

b bulk

e exit, equivalent

g gas

i inlet

L liquid

p pump

t turbine

w wall

Superscripts:

c convected

g generated

w wall

REFERENCES

1. Cavicchi, Richard H.: Mapping a Tungsten-Reactor Rocket Engine as a Guide to Operation and Control. NASA TN D-3840, 1967.

2. Marcy, R.; Cannon, W.; Bulgier, L.; and Harper, B.: Feed System Analysis: Tungsten-Water Moderated Reactor. Rep. No. R-6124 (NASA CR-54270), Rocketdyne Div., North American Aviation, Inc., Mar. 31, 1965.

3. Marcy, R.; Cannon, W.; and Bulgier, L.: Feed System Analysis: Tungsten-Water Moderated Reactor. Rep. No. R-6338 (NASA CR-54438), Rocketdyne Div., North American Aviation, Inc., Oct. 15, 1965.

4. Marcy, R.; Cannon, W.; and Bulgier, L.: Engine System Analysis: Tungsten-Water Moderated Reactor. Rep. No. R-6504 (NASA CR-54931), Rocketdyne Div., North American Aviation, Inc., July 31, 1966.

5. Marcy, R.; Cannon, W.; and Bulgier, L.: Engine System Analysis for TWMR Nuclear Rocket. Vol. 1 and 2. Rep. No. R-6797 (NASA CR-72120), Rocketdyne Div., North American Aviation, Inc., Nov. 15, 1966.

6. Ribble, Guy H., Jr.: Feasibility Study of a Tungsten Water-Moderated Nuclear Rocket. VI. Feed System and Rotating Machinery. NASA TM X-1425, estimated publication, approximately Dec. 1967.

7. Eanes, W. F., comp.: Analysis of Reference System. Task I: Feasibility of a Chemical Poison Loop System. Rep. No. WCAP-2690 (NASA CR-54291), Westinghouse Electric Corp., Feb. 1965.